Welding GAP Control Using Infrared Sensing

Final Report
Office of Naval Research
Grant No. NAVY-N00014-97-1063

Author:
Bryan A. Chin, PH.D.
Materials Research and Education Center
Auburn University
Auburn, Alabama

Submitted:
July 20, 2001

TABLE OF CONTENTS

PREFACE

TECHNICAL CONTENT

REPORT DOCUMENTATION PAGE

Form Approved
OMB NO. 0704-0188

1. AGENCY USE ONLY (Leave Blank)	2. REPORT DATE	3. REPORT TYPE AND DATES COVERED
	16 JULY 01	Final 9/98 - 5/01

4. TITLE AND SUBTITLE
Welding GAP Control Using Infrared Sensing

5. FUNDING NUMBERS
NAVY-N00014-97-1063

6. AUTHOR(S)
Bryan A. Chin

7. PERFORMING ORGANIZATION NAME(S) AND ADDRESS(ES)
Materials Engineering 101 Ross Hall
Auburn University, AL 36849

8. PERFORMING ORGANIZATION REPORT NUMBER
1063F

9. SPONSORING / MONITORING AGENCY NAME(S) AND ADDRESS(ES)
Office of Naval Research
Program Officer George R. Yoder ONR 332
Ballston Centre Tower One
800 North Quincy Street / Arlington, VA 22217-5660

10. SPONSORING / MONITORING AGENCY REPORT NUMBER

11. SUPPLEMENTARY NOTES

12 a. DISTRIBUTION / AVAILABILITY STATEMENT
Approved for public release; distribution unlimited.

12 b. DISTRIBUTION CODE

13. ABSTRACT (Maximum 200 words)

The objective of the research was to develop real-time infrared sensing techniques to monitor and control the Submerged Arc Welding (SAW) process utilized by the US Navy in shipbuilding. Infrared sensors were used to measure the front side surface temperature distribution of the sections being welded. Since the thermal profile in the vicinity of the weld is dramatically affected by weld perturbations, it is possible to identify the changes in thermal distributions and use this information to monitor and control weld gaps. The sensors thus provide in-situ non-destructive weld quality information that will improve both quality and productivity, resulting in a decrease in fabrication costs. Detailed heat and mass transfer modeling was conducted to predict the thermal distributions and matched with actual experimental measurements to improve our understanding and capability to model the welding process.

14. SUBJECT TERMS
WELDING, INFRARED SENSOR, SUBMERGED ARC, CONTROL

15. NUMBER OF PAGES

16. PRICE CODE

17. SECURITY CLASSIFICATION OR REPORT	18. SECURITY CLASSIFICATION ON THIS PAGE	19. SECURITY CLASSIFICATION OF ABSTRACT	20. LIMITATION OF ABSTRACT
UNCLASSIFIED	UNCLASSIFIED	UNCLASSIFIED	UL

REFERENCES

LIST OF FIGURES AND TABLES

4.0 INFRARED SENSOR DEVELOPMENT

4.0 INFRARED SENSOR DEVELOPMENT

5.0 THERMAL DISTRIBUTION

6.0 EXPERIMENTS

6.0 EXPERIMENTS

1.0 INTRODUCTION

1.1 Weld Types

The need for better, cheaper and more reliable products has necessitated new and improved manufacturing processes. Most or all manufactured products contain joints, and the quality of the product often depends on the quality of the joints. Mechanical fastening through the use of rivets, nuts and bolts were the joining methods available in the 19th century. But during the past century, welding/joining science and technology have progressed significantly, making it an essential and important part of virtually every manufacturing industry. Welding/joining technology has improved what we manufacture by reducing weight, production time and cost. It has improved reliability, increased product life and made possible the construction of giant structures with great ease. Notable improvements have been made in the fields of welding processes, consumables and welding metallurgy due to the development of new alloys for severe service conditions and the need for increased productivity.

A weld can be defined as the localized coalescence of two surfaces, such that the properties of the joint are substantially similar to the properties of the base materials being joined. The coalescence can be achieved through the application of heat; with or without pressure, or by pressure alone; and with or without filler metal. The American Welding Society[1] identifies over 17 commercially used metals joining processes. These processes can be typically grouped into six categories: [1] arc welding; [2] resistance welding; [3] oxyfuel gas welding; [4] solid state welding; [5] high energy density welding; and [6] brazing and soldering. Seven processes are classified under arc welding, and these together account for the greatest amount of welding and filler metal deposited commercially.

The term "arc welding" applies to a large and diversified group of welding processes that use an electric arc as the source of heat to melt and join metals. The arc is struck between the workpiece and an electrode, either one of which is manually or mechanically moved along the joint. A welding arc is a sustained high-current, low-voltage electrical discharge through highly conducting plasma that produces high thermal energy. The arc occurs when electrons are emitted from the surface of the negative pole (cathode) and flow across the region of hot electrically discharged plasma to the positive pole (anode). The electrode is either a consumable wire or rod, or a non-consumable carbon or tungsten rod, which serves to carry the current and sustain the electric arc between its tip and the workpiece. The major arc welding processes[2] are shielded metal arc welding (SMAW), gas-tungsten arc welding (GTAW), gas-metal arc welding (GMAW), flux-cored arc welding (FCAW), plasma arc welding (PAW), submerged arc welding (SAW), electroslag welding (ESW) and eletrogas welding (EGW).

Resistance welding is used extensively to join sheet metal, a process that does not required filler metal. Spot welding, seam welding, projection welding and flash-butt welding are variations of this process.

Oxyfuel gas welding, which uses bare wire as filler metal, is used for small repair and maintenance welding. It is not widely used because of the inferior quality of weld produced.

Solid-state welding includes diffusion bonding, friction welding, hot- and cold-pressure welding, explosive welding, and ultrasonic welding. Common to these processes is that they can be done without melting or filler metal. The two surfaces are brought into intimate contact, and the joint between similar or dissimilar materials is achieved through the application of heat and/or pressure.

The high-energy density processes include electron-beam and laser-beam welding. In the electron-beam welding process, the joint is bombarded by a highly accelerated and focused beam of electrons, resulting in the instant conversion of kinetic energy into thermal energy. This causes the melting and penetrating of the welding-seam interfaces to form the joint.

In the case of laser-beam welding, a high-density coherent light beam is used for creating the thermal energy required for welding.

In brazing and soldering processes[2], the base materials are not melted to form the joint. The surfaces to be joined are heated to the brazing or soldering temperature, thereby melting the filler metal that flows into the joint gaps due to capillary forces and forming the joint on cooling. Heating can be achieved through the use of oxy-fuel torch, electric induction or resistance, inert or reducing atmosphere furnace, or vacuum furnace. For soldering, the filler metal melting temperature is below 840°F; for brazing, it is above 840°F, but below the solidus of the base materials being joined. Brazing and soldering make it possible to join dissimilar materials that cannot be joined by traditional fusion welding processes due to metallurgical incompatibilities of the base materials. They are sometimes the only methods applicable for producing large number of very small joints in one operation for components such as automobile radiators, heat exchangers and electronic circuits. Brazing and soldering processes produce significantly less distortion and while creating cosmetically neater joints.

Apart from the above processes, new processes such as friction stir welding and transient liquid phase (TLP) bonding have recently been developed to join alloys that are otherwise difficult to weld using other conventional processes.

1.2 Effects of Weld Parameters and Conditions

The quality of the joint is determined by the geometrical (e.g., bead width, profile, penetration depth, weld defects) and metallurgical (e.g., strength, ductility, toughness) characteristics of the weldment. The welding process parameters and procedures control these characteristics. Complex relationships that exist between the process parameters —welding current, voltage, welding speed, shielding method — and are most often undefined. This requires the development of welding procedures that are suitable for a given range of welding parameters, and joint design to achieve a good quality joint prior to use on the production shop floor, followed by non-destructive inspection of those welds. Errors, which affect the quality of the joint, result from the complex coupling nature of the weld parameters and the performance of the human welders and machines. Such errors are detected by non-destructive inspection only after the fact, resulting in rejection, increased costs, lost productivity and delayed production. The intense heat and fumes generated by the welding processes, along with early eye fatigue caused by the brilliance of the arc and environments with restricted access, limit the human operator to short

periods of quality welding. The average industrial arc welding time — time in which the arc is struck — is approximately 35 to 40 percent[3] as a result of these limitations. To achieve quality workmanship, increased productivity, high repeatability, lower cost and on-time delivery, mechanization/automation of the welding process has become imperative.

Unfortunately, these developments have not, in general, resulted in the expected improvement in weld quality. Semi-automatic welding systems still rely on the skill of the welding operator to ensure high-integrity welds. Preset automated systems, in which the welding parameters are pre-programmed before any welding takes place, lack the ability to compensate for perturbations that arise during the welding process. Perturbations are caused due to thermally induced distortions, improper joint preparation and fit-up, changes in material and shielding gas composition, and sudden changes in plate thickness, all of which can result in torch offset, non-uniform penetration and lack of side-wall fusion.

To successfully weld in conditions where the weld parameters cannot be totally defined requires a system capable of sensing the variations and modifying some aspects of the machine behavior sufficiently, thereby allowing it to cope with these perturbations in real-time. Hence the need for systems that can monitor and control the in-process status of the welding process (i.e., systems incorporating adaptive process control). In such systems, the status of weld characteristics is continually measured and compared with the desired values, and corrective feedback action is implemented whenever a variation is detected.

Of all the welding parameters, weld-penetration depth is the most important, as it determines the mechanical properties and the life of the joint. However, control of the penetration depth is difficult since it is neither visible nor easily measurable from the topside surface of the weld joint. Measurement of penetration depth can be performed only by post-weld destructive (cross-sectioning) or non-destructive (ultrasonic and radiography) methods. Adaptive welding process control requires the development of indirect penetration depth indicators. Investigation on the use of optical sensors, ultrasonics, radiography, weld pool oscillations, acoustic emission and infrared sensors has been conducted for their suitability for detecting the penetration depth[1-39].

Temperature monitoring near the weld pool using infrared sensors is very convenient since it is simple, has responds quickly, and requires no physical contact with the surface at high temperature. The IR sensors can be used for measuring temperature of targets in motion, in hostile environments or at inaccessible locations. Earlier investigations[29-38] using infrared cameras have shown that the infrared sensing method has the capability of detecting penetration depth variations through changes in the surface temperature distribution, and could be used for adaptive process control. The infrared camera, however, has not been popular, as it is bulky, fragile, intrusive and expensive. Recent studies[39] performed at Auburn University concerning the viability of point infrared detectors for GTA welding process control have shown great promise. The performance of the sensor system was tested by controlling the temperature at a point close to the weld pool through changes in the heat input, thereby indirectly controlling the weld penetration depth.

Fabrication and refurbishment of ships involves a substantial amount of money, with a large amount of it is directly associated with welding process. Typically the submerged arc welding

(SAW) process accounts for one-third of all the welds produced in a shipyard. In the fabrication of ship-hull panels, welding from either one or both sides of the joint joins the plates. Welding from one side of the joint requires the use of backing material to hold the molten metal at the root of the joint and a consistent joint fit-up. Welding from one side without the use of backing material often results in defects such as burn-through, improper penetration, lack of side-wall fusion and slag inclusions. Difficulties in producing consistent joint fit-up over a large length of the plates and thermal distortion occurring during the welding process are two causes of variable joint gaps, which lead to weld defects. Welding from both sides requires turning the large plates over and back-gouging the root of the first weld before welding from the other side in order to assure a good-quality, full-penetration joint. The cost of the backing material, time involved and labor required for placing the backing material and for the back-gouging operation are important considerations in evaluating these two methods. A significant reduction of cost and time can be achieved if the use of the backing material and back-gouging is eliminated or minimized. But elimination of the backing material or back gouging operation requires the use of a system that is capable of adjusting the welding parameters according to the changes in the joint fit-up, specifically the root gap and the plate thickness.

1.3 Research Objective

The objective of this research work was to develop a point infrared sensor system for real-time monitoring and control of weld penetration for the submerged arc welding process. Monitoring the temperature distribution at a point adjacent to the weld pool controlled the welding process. The heat input was adjusted through the control of the welding current and arc voltage using the infrared sensor signal as the feedback variable. The infrared sensor process control system was aimed at eliminating the use of backing material and back-gouging operation to achieve a joint with complete weld penetration and without defects such as burn through, improper weld penetration, lack of side-wall fusion and slag inclusions. The performance of the infrared sensor control system was tested on joints with variable plate thickness and variable joint gap.

2.0 SENSING

Significant advances have been made in the development of automatic welding systems. An essential element of any monitoring and control system is the sensor, which observes and/or measures the performance of the process by monitoring one or more variables. This information serves as the feedback signal for the implementation of the control system. Several sensing techniques have been developed for real-time monitoring of penetration depth during the welding process. Most of the techniques do not allow direct measurement of the weld penetration depth, since it is not visible to the surface of the plate. This requires measurement of a physical weld characteristic, which is related to the penetration depth.

2.1 Ultrasonic Sensing

Ultrasonic testing has been used effectively as a non-destructive inspection technique for locating discontinuities below the surface of castings, forgings, plates and welds. It has become a standard technique for locating cracks, lack of fusion and penetration, porosity and other discontinuities in fusion welds. The ability of the ultrasonic sensing method to measure the

location and dimensions of the discontinuities has prompted researchers to investigate its use in real-time welding process control.

The weld pool constitutes a change in phase and material properties relative to the rest of the weldment, and thus, is a reflector of ultrasound. The pulse-echo method using longitudinal and shear waves utilizing normal and angle beams respectively were found to be capable of detecting reflections from the weld pool[4]. Research concentrated on the use of angle-beam technique, since it had the advantage of allowing placement of the transducer on the top side of the plate, offering better industrial viability than the normal beam. Hardt and Katz[5] examined the conditions for reflection of ultrasonic waves from a weld pool and presented a means for interpretation of such reflections. A theoretical relationship between the radius of hemisphere and time of flight was developed. Experiments conducted on cylindrical rods with machined hemispherical cavities and stationary weld pool created at the end of the rod showed good correlation with the theoretical predictions.

Researchers at the Idaho National Engineering Laboratory[6], performed feasibility studies on the detection of weld pool geometries using contacting transducers. "A-scans" were obtained using machined samples simulating the weld preparation and four typical weld pool geometries. An expert system was developed from the digitized data for the identification of the solid/liquid interface and potential weld imperfections. A system capable of discriminating side-wall penetration, incomplete root penetration and single concave radius geometries with accuracy up to 71 percent was developed.

Use of contact piezoelectric transducer and couplant presented the problem of loss of contact and weld contamination. In order to achieve industrial viability of real-time sensing of the welding process, a non-contacting type transducer was required. Carlson and Johnson investigated a non-contact ultrasonic sensing technique using a pulsed laser for sound generation and an electromagnetic acoustic transducer (EMAT) for detection[7]. The EMAT produces a magnetic field in the sample using permanent or electromagnets. The arriving sound field causes the charges in the metal to move in the magnetic field, creating a secondary field that is detected by a pick up coil. When incomplete penetration is present, the sound does not reach the EMAT and the signal of interest is absent. The system, thus, detects flaws by evaluating the presence or absence of the signal of interest in the acquired A-scans. The arrival time, propagation mode and displacement amplitude of the sound front generated by the laser spot were calculated using generalized ray theory. Calculated transit times and propagation modes of sound were compared to those acquired from a solid carbon steel sample and molten weld pool, and were found to have good agreement. The feasibility studies indicated the dependence of the signal on the weld pool geometry, particularly the weld pool depth.

The laser/EMAT, non-contacting concurrent sensor system was demonstrated on a robotic GMAW process. The laser spot was delivered to the solidified weld metal using a compact pulsed laser system mounted on the welding head and the sound waves were received using the EMAT. Recently, Hopko and Ume[8] have reported the development of a robust and flexible laser ultrasonic probe using an optical fiber delivery system and a focusing objective for real-time welding process control. The objective serves to protect the optical fiber and focus the laser spot for the purpose of surface ablation. The strong signal generated by the laser ultrasonic probe is

detected by a non-contacting EMAT. Time-of-flight techniques for determining weld penetration depth were demonstrated for simulated solidified welds and liquid weld pools. Greenberg, et al[9] monitored the diffusion-bonding process by analyzing the amplitude ratio and attenuation of the acoustic waves. The completion of the bonding process was identified by the disappearance of the reflected beam from the joint interface. The joint interface disappeared as the bonding progressed. The monitoring function was performed through M-mode display, which involved performing sequential A-scans at few-minute intervals.

Major difficulties reported with the ultrasonic sensing techniques were the effect of temperature on the speed of sound in the material. Attenuation of sound at high temperatures caused a low signal-to-noise ratio and misinterpretations, since time of flight was used for calculating the weld penetration depth. Coupling of the contact type transducers to the workpiece and accurate synchronization of movement of sensors with the welding torch is required in order to obtain true signals. The systems are also fairly complex and require costly signal analysis hardware.

2.2 Radiographic Sensing

Rokhlin and Guu[10] implemented the use of real-time radiography for on-line monitoring and control of weld penetration during submerged arc welding. X-ray penetrating radiation was used for volume observation in the weld pool and the heat affected zone during the welding process. The welding process control was developed based on information on weld quality, received from automatic recognition of real-time radiographic images. Radiographic images, acquired and processed using digital image processing software, was used for closed loop control of the welding parameters. The X-ray unit was mounted vertically above or at small angles to the welding torch, and the image intensifier was placed below the weld test piece. This configuration was found to be appropriate for studying discontinuity formation and for monitoring incomplete fusion and joint penetration. A television camera was used for observing and recording the output from the image intensifier. The television images were fed to an image processor for digitization, enhancement and extraction of quantitative information on weld quality. The digitized images were analyzed using different pattern recognition algorithms for identification of weld quality and type of weld discontinuities. Penetration depth was determined from the brightness of the radiographic image. Brightness profiles were analyzed from the image at a distance of about one-inch (25 mm) behind the welding torch to avoid the molten area, which was noisy due to pool oscillations. This distance was still considered to be small enough for a quick response on the weld quality and for corrections. The image brightness and area of cross-section were used as criteria for monitoring and control of the SAW process.

This radiographic monitoring and control system has serious drawbacks when real-time, shop-floor applications are considered. The unit is too bulky and requires the bottom of the weld to be accessible for placing the image intensifier. Since the image for controlling the process is acquired about 25 mm behind the arc, this would delay the control action, and the system would fail to achieve its objective in actual shop-floor conditions. Extensive protection is required to prevent human exposure to the harmful radiation, and the highly intrusive nature of the system make it difficult to be implemented on a regular production shop floor.

2.3 Weld Pool Oscillation

Weld pool oscillation was first recognized as an important phenomenon occurring during arc welding by Kotecki, et al[11]. Studying the weld bead ripple formation in solidified stationary welds using high-speed photography, they were able to explain this formation in terms of the oscillation of the weld pool surface. Renwick and Richardson[12] and Zackenhouse and Hardt[13] investigated the behavior of stationary weld pools triggered into oscillation by short current pulses, and determined the oscillation frequency by monitoring the arc voltage (which is linearly related to the arc length). They carried out experiments under different welding conditions and found an inverse relation between the oscillation frequency and the weld pool size. Madigan and Renwick[14] used the weld pool oscillation principle as a basis for weld penetration sensing. Sorensen and Eagar further developed this approach[15]. Deam[16] monitored the arc length variations resulting from weld pool oscillations using an optical sensing method. A glass fiber optic bundle was used to observe and measure the arc light variations due to changes in the arc length. Relationship between the arc light intensity and the amplitude of the weld pool oscillations was used for distinguishing fully and partially penetrated welds. However, the disadvantage of this method was the need for additional optical equipment. Hardt[17] performed welding experiments under different conditions and found, in the case of partial penetration, a clear relationship exists between the weld pool width and oscillation frequency.

Xiao and den Ouden[18,19] observed a distinct transition in the modes of oscillation between partially and fully penetrated welds for both stationary and traveling welds. Recently Hu and den Ouden[20] reported the use of one specific frequency to control the weld pool geometry for traveling arcs. The control frequency was selected based on the weld pool top width and eccentricity. The effect of travel speed and material properties on the oscillation frequency was studied. Penetration control was demonstrated using the GTAW process on mild-steel and stainless-steel plates. The welding current was automatically controlled in real-time using a specific frequency response of the weld pool.

The primary obstacle for using this process for real-time penetration control stems from the presence of several modes of vibrations in the weld pool. No clear demarcation of frequencies exists between a partial- and full-penetration weld, and there are other extraneous sources for arc voltage variations, resulting in false indication and improper control.

2.4 Optical Sensing

Human welders use their vision to recognize perturbations in the weld pool and make corrections to their travel speed, welding current and other parameters. To achieve on-line control of the welding parameters, optical sensing methods attempt to give the automatic welding systems the vision sensory skills similar to human welders. Most of the optical sensing methods developed have involved the use of laser/solid-state camera combination or the laser/photo-diode combination for seam tracking and weld geometry control. The effect of weld puddle size and shape on weld quality has been recognized, and mathematical models for the weld puddle have been developed in the past. But these models usually predict steady-state values and give little or no indication of the weld puddle variation in real time. Since there appears to be a correlation between the weld puddle shape and quality, the weld puddle shape has been chosen by many

researchers for control. The width measurement of the puddle represented the best specification of the puddle for control purposes since only a single linear measurement could be made using a line scan camera in the early days. Vilkas[21] implemented a penetration control system using a photocell focused on the back of the weld joint to monitor the radiation from the bottom of the weld pool. The amount of radiation at this location was a direct measure of the weld penetration. The output of the photocell was used to adjust the welding current or the travel speed and therefore obtain constant penetration. Vroman and Brandt[22] used a line scan camera with the aid of a front surface mirror to view and measure the weld puddle width. The heat input to the weld puddle was controlled through the welding speed. A train of voltage pulses was developed by the diodes in the camera due to the light intensity variations across the puddle. This filtered and scaled voltage was compared with a preset value, and the welding speed was adjusted accordingly to achieve adaptive control. Boughton, et al[23] reported monitoring and control of weld pool shape using a linear array of photo-diodes. The measured weld pool width from the light intensity was used for penetration control through simultaneous regulation of welding current and travel speed. Sugitani, et al[24] developed "Intelliarc," an intelligent arc-welding robot that could perform penetration control, weld geometry control and joint tracking. The robotic system consisted of a high-speed, rotating GMA welding head with a camera-based image-processing system. The electrode was made to rotate orbitally at a frequency of 20 to 60 Hz, and the changes in the arc voltage corresponding to the bevel joint faces were used for tracking the joint. A CCD camera was used for measuring the root gap just ahead of the weld pool. The root gap was obtained by processing the transverse brightness scans. The brightness was found to be highest from the reflection of the arc on the bevel surface while lowest in the root opening. The distance between the brightness was were used as feedback to keep the penetration and bead height at constant values by controlling the welding current, wire feed rate, arc voltage and welding. Zhang, et al[25] reported the use of a weld face vision sensor for controlling the weld joint penetration. A structured light, three-dimensional vision sensor was used for measuring the weld face geometric parameters in real time. The image of the weld pool obtained using laser stripes and camera was processed using an image-processing algorithm to obtain the weld geometries. Through experimental and statistical analysis, a linear relationship was found to exist between the root surface weld width and a new parameter called the average depression depth. A weld penetration control strategy was proposed, based on the relationship between the root surface weld width and the measured weld-face parameters. Kovacevic, et al[26] developed a vision system for real-time monitoring of joint penetration from the weld pool size and shape. The system consisted of a high-shutter-speed camera assisted with pulsed laser illumination to capture the image of the weld pool. The weld pool boundary was extracted using a real-time image-processing algorithm, and the geometrical appearance was characterized by the rear angles and length of the pool. The joint penetration information was obtained as an output of a neural network analysis using the weld pool geometries obtained by the vision system as the input.

The optical systems were affected by the arc brilliance, spatter and smoke. Since the penetration was determined indirectly from weld pool size and shape, the control system may not compensate for all variations in material thickness or composition. In addition to being fragile and expensive, the hardware requires sophisticated image processing to extract useful information. Moreover, this method cannot be applied to the SAW process since molten slag and flux cover the weld pool.

2.5 Acoustic Emission Sensing

Thermal stresses formed in the material during welding generate acoustic emissions, which travel throughout the workpiece. The amount of acoustic emission is a function of the amount of fused metal. The acoustic emission technique has been developed to monitor penetration for the laser welding process[27]. As the penetration progresses from partial to full, the frequency content and shape of the acoustic emission change and is picked up by the acoustic transducer that is in contact with the workpiece. Further work is being performed to relate the frequency spectrum and amplitude of the emissions to the weld penetration depth. Both contacting and non-contacting sensors can be applied for a variety of welding processes. But the systems are complex and costly due to the signal conditioning hardware requirements.

2.6 Infrared Sensing

All materials above 0°K emit infrared radiation (IR) due to the thermal energy. The IR part of the electromagnetic spectrum spans wavelengths from 0.7 to 1000 microns. The radiation intensity is a function of the body temperature and surface emissivity. The emissivity depends on the material, the surface finish and the wavelength of the radiation. Planck[28] derived the following theoretical relationship between the spectral emissivity, temperature and the radiant energy.

$$W_\lambda = C_1 \varepsilon_\lambda [\lambda^5 (\text{Exp} (C_2 / \lambda T) - 1)]^{-1}$$

where, W_λ = spectral radiant intensity, W/(cm^2-μm)

C_1 = 34,413 W-μm^4/cm^2

C_2 = 14,388 μm - K

ε_λ = emissivity

λ = wavelength, μm

T = temperature, K

The Stefan-Boltzmann formula, obtained by integrating Planck's formula from $\lambda = 0$ to $\lambda = \infty$, gives the total radiant emittance of a blackbody.

$$e_b = \sigma T^4$$

where, σ = Stefan-Boltzmann constant (5.669 X 10^{-8} W/m^2, K^4)

e_b = energy radiated per unit time, per unit area by the ideal radiator and

T = absolute temperature of the surface.

If the emissivity of a surface and the temperature of its surroundings are known, the radiance can be measured and the temperature of the body determined using the Stefan-Boltzmann law. This is the basis for the radiometric method of measuring temperature.

The temperature distribution around the weld pool provides important information on the status of the welding process. The pool shape, absolute temperature and temperature distribution symmetry are directly related to the welding parameters and other process variables: joint mismatch, root gap variations, thickness of the members, composition, etc. Temperature

monitoring by infrared sensors is very convenient, since contact with the surface at high temperatures is not required. The IR radiant energy is converted into electrical energy by the infrared sensor, which can be used for displaying the temperature as in infrared pyrometers, or processed and used for monitoring and controlling applications. The IR sensors can be used for measuring temperatures of targets in motion, a vacuum, hostile environments or at inaccessible regions. The IR sensors are simple, have fast response, and are easier to adapt to the shop-floor conditions.

Infrared sensing techniques have been used to study various aspects of the welding process as early as the 1960s. Infrared cameras, point sensors and other variations have been used for measuring the temperature distribution around the weld pool for seam tracking, bead width control and penetration control. In 1963, Ramsey, et al[29] investigated the feasibility of using infrared temperature-sensing systems for automatic welding. Fixed and scanning radiometers were used in this study to determine the heat flow pattern during welding, and to correlate this pattern with changes in the welding parameters. For the case of a fixed radiometer, where the point of sensing was held constant, experiments showed very high arc interference. For the case of a scanning radiometer, the point of inspection was moved along a prescribed path. It was expected that a radiometer scanning across the weld bead at constant speed would produce an output signal in the form of a pulse, with characteristics related to the bead width. The scanning radiometer was found to be promising since signals with a width related to the radiation profiles across the weld bead were obtained. The authors found the signals were not a unique function of the temperature, but they correlate well with the bead width over a wide range of welding parameters. Lukens and Morris[30] investigated the use of IR sensing equipment for real-time monitoring of the weld metal cooling rate. Cooling rates of GTAW and GMAW bead on plate welds were evaluated using the IR technique and correlated with thermocouple measurements. Hardness and microstructural correlations with the cooling rates were obtained. Brown and Bangs[31] studied the use of an infrared radiometer for sensing and recording the thermal signature of resistance spot welds. From the thermal signatures, the formation of weld nugget and the size of the nugget were obtained and correlated to the tensile shear strength of the spot weld. Boillot, et al[32] investigated the use of a fiber optic thermographic monitoring system, which allowed thermographic monitoring by discrete point thermal inspection. This system helped to avoid long and expensive image processing, as well as the requirement for bulky and fragile infrared cameras near the welding area. Temperature sensed from a fixed point was used for obtaining information on the width of the weld pool, and thus, indirectly on the depth of penetration. Mechanical scanning of the fiber optic sensor to scan the temperature of the surface in front of the weld pool was used for seam tracking purposes. The value and the position of the temperature peaks detected on the borders of the root opening were used for seam tracking. Another variation involved the use of a linear array of optical fibers located inside the gas lens of a GTAW torch. This system was used for demonstrating seam tracking of the weld joint. Bentley and Marburger[33] developed a feedback control system for GTAW weld penetration control using an IR sensor. The IR radiation measured from the backside of the weld was used as the feedback signal. A fiber optic cable was used for transmitting the radiation to the sensor. The feedback control system was demonstrated in tests with varying welding speeds and part thickness.

Extensive work involving the use of the infrared sensing technique for welding process control has been done at the Auburn University. The use of an infrared thermographic camera and point infrared sensor for process control has been investigated over the past decade. Chin, et al[34] performed a feasibility study of using infrared thermography to detect perturbations like arc misalignment, impurities, joint geometry and penetration variations. An infrared camera capable of sensing a ±0.20°K difference in temperature was used for proving the ability of the sensing method for discerning the variations in the temperature field around the weld pool introduced due to the perturbations. Groom, et al[35] and Nagarajan, et al[36,37,38,39] demonstrated seam tracking and weld penetration control. Radii measurement of the thermal profiles along both the welding torch and 45 degrees in a direction opposite to the motion of the torch yielded error signals used to identify the arc position relative to the joint. The minor axis and area of the ellipse of isotherms were found to be sensitive variables for studying changes in the weld penetration. In another method, the distinct drop in the measured temperature distribution, which was found to coincide with the joint gap was utilized for seam tracking. In the temperature gradient profile, the gap was characterized by three changes in the sign. The second change in the sign was found to correspond to the gap center, while the first and third changes in sign were found to coincide with the edges of the joint. These unique changes were used to successfully track curved contours of joints with a gap. Chen[40] proposed a control strategy based on the width and area of the thermal profile. A linear relationship was found to exist between the bead width and the thermal peak of the temperature distribution. An exponential relationship was found to exist between the depth of joint penetration and integrated area under the peak temperature profile. Banerjee, et al[41,42,43] utilized the change in the temperature gradient at the solid-liquid interface for monitoring weld geometry and penetration control. The gradient technique was used for identifying changes in the plate thickness, minor element content, shielding gas composition, bead width and joint penetration. The linescans — the thermal profile along a line on the plate transverse to the direction of torch motion — were employed for determining the thermal gradients. A control strategy based on bead width control was demonstrated on plates with varying thickness, and penetration control was demonstrated during a change in the shielding gas composition. Wikle[44] was the first to use a point infrared sensor for monitoring and controlling of the GTA welding process. The response of the process control system to step changes in variables was investigated. Welding process control was demonstrated on constant thickness plates and plates with step change in thickness.

3.0 SUBMERGED ARC WELDING PROCESS

3.1 Introduction

The birth of arc welding occurred when Sir Humphrey Davy discovered the electric arc in 1801; however, the first attempt to use the intense heat of the electric arc for welding using a carbon electrode was made by Auguste de Meritens in 1881. Shortly after, Slavianoff and Coffin developed a process in which the carbon electrode was replaced by a metal rod. This metal electrode not only supplied the heat for fusion, but also added filler metal necessary to fill the joint, resulting in the invention of consumable electrodes for welding. The use of bare metal electrodes, however, frequently led to excessive spatter and instability, not to mention the brittle deposited weld metal. The embrittlement occurred due to atmospheric contamination through the formation of oxides and nitrides. In 1907, Oscar Kjellberg from Sweden proposed the idea of

using a flux coating on metal electrodes for improving arc stability and preventing weld metal embrittlement. Improvement to this idea by several researchers over the years has led to a whole gamut of flux coatings suitable for different alloys, welding processes, welding parameter ranges, welding positions and production efficiencies.

During the 1930s, numerous attempts were made to achieve some degree of mechanization to the arc welding process. The early attempts involved the use of continuously fed bare wire, with no shielding other than a thin flux that was sometimes painted on the work-piece. In 1932, an innovation led to the use of a heavy layer of flux placed along the weld seam ahead of the electrode. The heat from the arc melted the flux, forming the slag that provided shielding to the molten weld pool. This improvement led to the development of the submerged arc welding process (SAW) in 1935. The SAW process can be defined as an arc welding process in which the arc is formed between the continuously fed bare electrode and the workpiece concealed by a thick blanket of granular and fusible flux. Another distinguishing feature of the SAW process is that the granular flux covers the weld area and prevents arc radiation, spatter and fumes. The flux, which forms the slag, deoxidizes and refines the weld pool, insulates the weld to reduce the cooling rate and helps to shape the weld contour. The flux is also of major importance in achieving the high deposition rates and high quality of weld deposit characteristic of this process. This welding process first found its use in shipbuilding and thick-section pipe fabrication. In 1946, hand-held, semi-automatic guns were developed; the voltage and current were controlled automatically, and subsequent improvements have been made mainly in the areas of fluxes and more sophisticated welding equipment and controls.

3.2 Advantages and Limitations

The SAW process is typically three to 10 times faster than the SMAW process. High current densities, which are characteristic of the SAW process, increase penetration and decrease the need for edge preparation. There is virtually no restriction on the material thickness, provided a suitable joint preparation is adopted. Higher deposition rates and welding speeds provide a substantial reduction in cost per unit length of weld joint. The shielding provided by the flux is not sensitive to wind draft as in SMAW, GMAW and GTAW. Low hydrogen weld deposits can be achieved with proper selection of consumables. Alloy ingredients can be added in the flux to enhance specific properties of the weldmetal. As the arc is completely covered by the flux layer, there is no arc flash, spatter or fume, and the heat loss is extremely low, producing a thermal efficiency as high as 60 percent.

Initial cost of a SAW system is high. Flux is subject to contamination that may cause weld discontinuities. Welds can be performed only in the flat and horizontal positions in order to prevent runoff of molten slag from the joint and to hold the flux in position. Due to the high heat input, it is commonly used to join steels more than 4.8 mm (three-sixteenths-inch) thick.

3.3 Applications

The SAW process is widely employed for welding all grades of carbon, low alloy and alloy steels. Alloys steels can be readily welded if care is taken to limit the heat input, thereby preventing damage and grain coarsening to the HAZ. Stainless steel and some nickel alloys are

also effectively welded or used as surfacing alloys with this process. SAW is also ideally suited for longitudinal and circumferential butt and fillet welds. It is primarily used for shipbuilding, pipe fabrication, pressure vessels and structural components for bridges and buildings.

3.4 Principle of Operation

In a typical SAW setup, the wire electrode is fed into the joint by mechanically powered rolls. A layer of flux is laid in front of the electrode from a hopper. The flux can also be heated in the hopper using electrical heaters. The welding current — which can be direct current with electrode positive or negative, or alternating current — is supplied to the electrode through the contact tube. The flux is the basic feature of the SAW process, making possible the special operating conditions that distinguish it. Apart from protecting and refining the molten pool, it influences the shape of the weld bead. The flux is a non-conductor of electricity in the cold condition; in the molten state, it becomes a highly conductive medium. The heat from the arc causes the surrounding flux to become molten, thus forming a conductive path. In the molten state, however, the flux provides suitable conditions for high current intensities, thus generating high quantities of heat. The insulating properties of the flux concentrate the intense heat into a relatively small welding zone. This results in deep penetration and makes increased rates of travel speed possible. As the electrode progresses along the joint, the lighter molten flux rises above the molten weld metal in the form of slag. The weld metal, which has a higher melting point, solidifies while the slag above it is still molten. The slag then freezes over the newly solidified weld metal, continuing to protect the metal from contamination and reaction with oxygen and nitrogen in the atmosphere. The unused flux and the slag are removed after the welding is completed.

The welding head contains the welding torch, flux hopper, wire feed system, and controls for adjusting the welding parameters, and for start and stop. The welding head moves on a horizontal beam or on self-propelled trackless carriage, based on the type of system. Through the regulation of current, voltage and travel speed, the operator can exercise close control over penetration depth and bead shape. While deep penetrating properties of the process could be used for eliminating edge preparation, the shallow beads can be used for cladding purposes.

3.5 Power Sources

Either a variable voltage direct current generator or rectifier; a constant voltage direct current generator or rectifier; or an alternating current transformer may provide welding power. Power sources, which provide high currents with high-duty cycles, are required for most SAW installations. Most of the welding is performed in a range from 300 to 1,200 amperes. The variable-voltage motor generator or rectifier type of power source is the type most widely used for director current welding. Heavy-duty transformers with built-in motor-controlled reactors and primary contactors are generally used for alternating current welding.

3.5.1 Volt-Ampere Characteristic

Two types of characteristic curves are available for SAW power sources — drooping and flat. In the case of a power supply with drooping characteristics, also called 'constant current,' the

voltage between the terminals of the power supply decreases sharply as the current increases. Such power supplies may provide alternating and/or direct current outputs. For the case of a power supply with flat characteristics ("constant voltage"), the voltage remains almost constant as the current is increased. Such power supplies provide only direct current output. In a situation where there is a sudden decrease in the level of the work piece, the arc voltage increases, causing the current to shift to a slightly lower value on a constant-current power supply. For the same situation in a constant-voltage power supply, there is a large decrease in the current, restoring the arc voltage to its previous value much more rapidly than the constant-current power supply. Thus, a power supply with constant voltage, which is self-regulating, has an advantage when used with a constant-speed wire feeder.

3.5.2 Wire Feed Systems

Equipment for feeding the electrode wire in SAW employs either of two types of systems for control of wire feed rate: [1] voltage sensitive system with constant-current power supply; and [2] constant speed systems with constant voltage power supply.

Voltage-sensitive systems are those in which the power supply maintains an essentially constant welding current, and the electrode wire feeder varies the feed rate to maintain a constant arc voltage. This is accomplished by monitoring the arc voltage and having the voltage control momentarily increase the wire feed rate when the voltage increases beyond a preset level, or decrease the feed rate when the voltage drops. A voltage-sensitive control system is preferred for large-diameter wire welding.

Constant-speed systems are essentially the same as voltage-sensitive systems, except for the substitution of a constant speed control for voltage control. In this system, the arc voltage is pre-selected at the power supply, which is designed to maintain this voltage regardless of current demand. The wire is fed at a predetermined rate, and the arc length is held constant through automatic adjustment of the current by the power supply. This system provides increased voltage stability, consistent scratch starting and more convenient adjustment of voltage and current.

3.6 Electrodes

Submerged arc electrodes are available in three different forms: solid wire, cored wire and strip. Solid wire is most commonly used and is available for welding of carbon steel, low-alloy steel, stainless steel, and a variety of non-ferrous alloys. Wire is normally in the form of coils, and is available in diameters varying from one-sixteenth to one-four-inch and higher. Except when welding corrosion resistant alloys, the electrodes are usually copper coated.

AWS specifications AWS A5.17 and AWS A5.23 prescribe the requirements for the classification of carbon steel and low-alloy steel electrodes and fluxes for SAW, respectively. The welding electrodes and fluxes are classified according to:

1. the mechanical properties of the weld metal obtained, with a combination of a particular flux and a particular classification of electrodes;
2. the condition of heat treatment in which those properties are obtained; and

3. the chemical composition of the electrode or the weld metal produced with a particular flux.

3.7 Fluxes

The flux provides arc stability, protects the molten pool against atmospheric contamination through the formation of slag envelope, refines the weld metal through de-oxidation and de-sulfurization, modifies the weld metal chemistry and mechanical properties through introduction of alloy ingredients into the molten pool, and influences the bead shape. The fluxes are formulated to provide the functions as described previously and to carry heavy welding currents. Fluxes used in SAW are granular, fusible mineral materials containing oxides of manganese, silicon, titanium, aluminum, calcium, zirconium and magnesium, and other compounds such as calcium fluoride. Fluxes are classified by AWS on the basis of mechanical properties of weld metal they produce with some certain classification of electrode under specific test conditions. Fluxes can be categorized depending on the method of manufacture, alloying additions to the weld metal, and basicity (oxygen content).

3.7.1 Flux Categories

3.7.1.1 Fused Fluxes

Fused fluxes are mixtures of silica and metal oxides with a small amount of halide salts, which are melted in a furnace to form metallic silicate glass. The molten mixture is then rapidly cooled, crushed to a range of particle sizes, and packaged. Due to the nature of their manufacture, fused fluxes do not contain ferroalloys and deoxidizers. Fused fluxes may be further subdivided into [1] alkaline earth metal silicates; and [2] all silicates where manganese is replaced by part or nearly all the alkaline earth metals.

3.7.1.2 Bonded Fluxes

The bonded fluxes consist of intimate mixtures of finely divided oxides of alkaline earth metals, manganese, alums, silicon, titanium or zirconium, and killing agents or deoxidizers (i.e., silica, manganese, ferromanganese, ferrosilicon or similar alloys, and small amounts of halogen salts). The powdered ingredients are dry blended, and mixed with a suitable binder (usually potassium or sodium silicate). The wet flux is then dried in an oven or kiln, sized and packaged. Because of low temperatures involved in the bonding process, metallic deoxidizers and ferroalloys can be included in the flux. The solidified slag is readily detachable after welding. A disadvantage of the bonded flux is that the binder in the flux is likely to absorb moisture, which can cause porosity and hydrogen-induced cracking; hence, these potential disadvantages require proper storage and baking.

3.7.1.3 Agglomerated Fluxes

Agglomerated fluxes are similar to the bonded fluxes, except a ceramic glass binder, cured at high temperature, is used. They may contain varying proportions of fused or bonded fluxes, or mixtures of finely divided minerals and metallic deoxidizers necessary for desired performance.

3.7.2 Classification Based on Alloying Additions to the Weld Metal

A flux can be described as active, neutral or alloy flux, depending on its ability to change the alloy content of the weld deposit.

3.7.2.1 Active Fluxes

Active fluxes contain controlled amounts of manganese and/or silicon to provide resistance to porosity and cracking caused by contaminants such as oxygen, nitrogen, and sulfur in or on the plate. Active fluxes are primarily used for single-pass welds. Due to the manganese and silicon content in the flux, the alloy content of the weld metal will change with respect to the flux-to-wire ratio, resulting in changes in the strength and impact properties of the weld metal. Since the flux-to-wire ratio is dependent on the arc voltage, tighter control of the arc voltage is necessary when using active fluxes rather than neutral fluxes.

3.7.2.2 Neutral Fluxes

Neutral fluxes contain little or no deoxidizers and do not produce any appreciable change in the weld metal composition. Since the flux contains no deoxidizers, the wire electrode is required to provide them. Welding an oxidized surface may result in cracking or porosity. Neutral fluxes are primarily used for multipass welds. Wall neutrality number (N) is used to define the active/neutral behavior of a flux. It is given as

$$N = 100\ [(\Delta\%Si) + (\Delta\%Mn)]$$

A flux electrode combination that produces a Wall neutrality number of less than 40 is considered neutral, while over 40 indicates an active flux.

3.7.2.3 Alloy Fluxes

Alloy fluxes contain ingredients to produce an alloy weld metal with a carbon-steel electrode. They are also used with alloy and stainless-steel wire, and strip electrodes. Alloy fluxes find major applications in hardfacing and cladding operations. The transfer of alloy content from the flux to the weld metal is a function of the arc voltage, hence the manufacturer's recommendations are necessary considerations while using alloy fluxes.

3.7.3 Classification Based on Basicity Index

The basicity index is defined as the ratio of strongly bonded metallic oxides (basic) to weakly bonded metallic oxides (acidic) in the flux. The Boniszewski index is given by,

$$BI = \text{Basic Oxides} / \text{Acidic Oxides}$$

The basicity index is used for estimating the oxygen content of the weld metal. Basic fluxes produce weld metal with lower oxygen content, thereby resulting in good weld metal toughness. Acidic fluxes produce higher oxygen content resulting in lower weld metal toughness.

3.7.3.1 Acidic Fluxes

Fluxes with basicity index lower than one are considered to be acidic. Acidic fluxes are preferred for single-pass welds because of their superior operating and bead-wetting characteristics. They also have more resistance to porosity caused by plate contamination by oil, rust and mill scale.

3.7.3.2 Basic Fluxes

Fluxes with basicity index more than 1.5 are considered being basic in nature. Basic fluxes produce weld metal with very good impact properties in large multipass welds. They have poorer welding characteristics than acidic fluxes on single-pass welds.

3.8 Process Variables

Many of the operating variables of the SAW have a direct and/or interaction effect on weld size, shape and quality. To obtain good and consistent quality welds, knowledge and control of the variables are essential. The variables of importance are welding current, welding voltage, welding speed, electrode stickout, electrode size, depth of flux and layer, and type of depth of flux and electrode.

3.8.1 Welding Current

Welding current is the most important variable, since it controls the penetration (arc force), rate of deposition (electrode melting), and the amount of base metal fused (dilution).

3.8.1.1 Magnitude

A high-welding current results in higher penetration with a tendency for burn-through, high dilution, excessive reinforcement and distortion, greater weld shrinkage, large HAZ and lower flux-to-wire ratio. A low-welding current results in unstable arc, shallow penetration, higher width-to-depth ratio, greater flux-to-wire ratio and greater tendency for lack-of-fusion defect.

3.8.1.2 Type

Direct current with electrode positive (DCEP) for a given set of welding conditions produces wider beads and higher penetration with lower deposition rate. Direct current with electrode negative (DCEN) results in narrower beads with less penetration, higher reinforcement, lower dilution, and higher deposition rate. DCEN is frequently used for surfacing applications, and weld joints with poor fit-up. In the case of alternating current, the bead shape, penetration and deposition rate falls between those of DCEP and DCEN polarities. Alternating current is used in applications where very high currents or multiple wires are required. Arc blow, which is caused due to the magnetic field generated around the electrode by the high currents, is minimized when alternating current is used for welding.

3.8.2 Welding Voltage

Welding voltage is the difference in the electrical potential between the tip of the welding wire and the surface of the molten weld pool. The welding voltage varies the length of the arc between the wire and the weld pool. Increasing the voltage increases the arc length, and decreasing the voltage decreases the arc length. The arc voltage primarily affects the weld bead cross section and weld metal composition, but has little influence on the deposition rate.

High arc voltage produces longer arc length resulting in a wider, flatter, shallower weld bead with an increase in flux-to-wire ratio. This affects the composition and properties of the weld metal and increases the flux consumption. Higher-than-normal operating arc voltage helps in bridging gaps when the joint fit-up is poor. With excessively high voltage, the arc breaks out from the cover of the liquid flux, causing porosity due to atmospheric contamination of the molten weld metal. High arc voltage also results in poor slag removal and undercuts.

Lowering the arc voltage produces a stiffer arc, which increases penetration and resists arc blow. When the arc voltage is excessively low, the molten globules of weld metal passing from the electrode to the work piece cause continual short circuit resulting in excessive spatter and large reinforcement.

3.8.3 Welding Speed

Welding speed (travel speed) is an important variable governing the production rate and metallurgical quality of welds. It also determines the width and depth of the weld. High welding speeds result in decreased heat input per unit length of weld, lower weld metal per unit length of weld, lower dilution, less reinforcement and lower penetration. Excessively high welding speed decreases wetting action, and increases the tendency for undercutting, arc blow, porosity and uneven bead shape. Excessively slow speed produces a hat-shaped bead that is prone to cracking, excessive melt through, and rough bead and slag inclusions from the large molten pool flows around the arc.

3.8.4 Electrode Stickout

The stickout is the length of the electrode from the end of the contact tip to the point of emergence of the arc. The current flowing through the electrode stickout causes heating of the electrode due to the I^2R resistance. This heating effectively increases the electrode-melting rate, and at the same time, introduces a voltage drop in addition to the arc voltage. The greater the stickout, the greater the resistance heating of the electrode. To compensate for the voltage drop, the voltage must be increased to obtain a properly shaped bead. Extending the electrode 20 to 40 times the diameter of the electrode can increase the deposition rate by more than 50 percent. Although higher deposition rates can be achieved, higher stickout increases the difficulty of aligning the electrode to the joint.

3.8.5 Electrode Size

The electrode size principally affects the depth of penetration for a fixed current. Because of current density, decreasing the diameter of the electrode wire increases the pressure of the arc,

thereby increasing the penetration depth and decreasing the width-to-depth ratio of the weld bead. Where poor fit-up is encountered, a larger electrode is capable of bridging the gaps better than smaller wires.

3.8.6 Depth of Flux Layer

The width and depth of the flux layer affects the penetration, appearance and quality of the welds. When the layer is too deep, the arc is too confined, resulting in a rough weld with a rope-like appearance. A greater-than-normal amount of flux is also melted, resulting in narrower beads. The gases generated cannot readily escape, causing surface imperfections. When the flux layer is shallow, the molten weld metal is not entirely submerged, thereby causing flashing and spattering. Porosity also results due to improper shielding from the atmosphere. To offset these considerations, optimum depth of flux that prevents flashes and provides easy escape of the gases should be selected for each welding condition.

3.8.7 Type of Flux and Electrode

Apart from the effect of the process parameters, the specific chemical and physical properties of the electrode, base metal and flux controls the weld metal composition, microstructure and properties. Due to the complex interactions of these factors, specific wire and flux combinations should be selected to optimize the weld metal properties.

3.9 Welding Technique

Factors other than the process variables affecting the welding technique are fixturing, backing methods, type of joint design and other physical considerations.

3.9.1 Fixturing

Tacking, clamping or jigging — or combinations of these — are required to securely hold the joint and limit joint displacement due to heat. In the case of large and heavy assemblies, tack welds are enough to keep the joint properly aligned. The self-weight of the assemblies prevent displacement during welding. For thinner sections, clamping bars can be used to maintain alignment and prevent warpage. In the case of intermediate thicknesses, a combination of clamping and tacking may be required.

3.9.2 Backing

The large volume of the weld metal created by the SAW process remains fluid for an appreciable period of time. Support and containment of the molten metal until it is solidified is essential. In joint designs where the root face is sufficient enough, the molten metal is supported by the base metal itself without the requirement of backing bars. This method is used for butt welds (square or vee-groove), fillet welds, and plug or slot welds.

The common methods of supporting the molten weld metal where the base metal is incapable of supporting it are: [1] backup bar having the same chemistry as the base metal; [2] weld metal backup; [3] copper backup bars; [4] flux backup; and [5] ceramic backup.

In the case of backup bars made of the same material as the base metal, the weld penetrates into the backup bar and becomes an integral part of the joint. The joint must be properly located so that a part of the structure forms the backing or a separate backing strip may be used. In a weld-metal-backed joint, the first weld (root) pass made by some other method (usually SMAW, FCAW, GMAW or GTAW) forms the backing for subsequent passes made either from the opposite side or the same side. The backing weld may remain as a part of the completed joint if it is of suitable quality, or it may be removed by arc gouging or mechanical means.

Copper is used as a backing material because of its high thermal conductivity. The high thermal conductivity also prevents the weld metal from fusing to it and so it is reusable. The backup bar can be grooved to obtained the desired shape and amount of reinforcement. The backing bar may be water-cooled for removing the heat, or cladded with a ceramic material. Copper backing bars are usually used in high-production welding applications.

Flux under moderate pressures is sometimes used as backing material. The loose granular flux rests in a trough on a thin piece of non-conducting material, which in turn is placed on an inflatable rubberized canvas hose. The flux is pressurized by feeding air into the canvas hose.

Ceramic blocks affixed to wide adhesive aluminum strips are used as backing material. This strip is then attached to the plate surface to form the backing. The ceramic provides a chemically inert refractory substance to be in contact with the molten pool. The temperature of the molten pool conforms to the shape of the ceramic backing, resulting in a proper weld backing contour and reinforcement.

3.9.3 Joint Fit-up

The joint fit-up affects the quality, strength and appearance of the finished weld. The deep penetrating characteristic of the SAW process makes it imperative to have close control of fit-up. Joints with close tolerances such that the edges of the parts are uniformly close together are essential to reduce the welding costs. A gap of one-thirty-seconds-inch to one-sixteenth-inch between the plate edges is sometimes required to prevent angular distortion and weld cracking. The gap can also be used for obtaining penetration without edge preparation and for controlling weld reinforcement.

3.9.4 Joint Design

The common types of welds made using the SAW process are butt welds, fillet welds, and plug welds. Butt joints are the most prevalent type of joints welded using SAW. Material thickness ranging from 18-gauge sheet metal to several inches thick can be welded. The joint design and welding procedure depends on the thickness of members being welded. Greater penetration inherent to the SAW process permits square groove joints up to five-eights-inch to be completely welded with one pass from each side. To achieve a greater thickness, beveling the edges is often required to achieve proper fusion and penetration. The common types of bevels are single-V, single-J, single-U, double-V, double-J and double-U. Double-V, double-J and double-U grooves are used when the joint is accessible from both sides and is thicker. The important considerations for groove selection are the included angle, root opening, root face, root radius

and root gap. The root gap should be increased as the included angle is decreased to allow for proper electrode access and to achieve good sidewall fusion and slag removal. For V-bevel grooves, the included angle usually varies from 20 to 60 degrees. A proper butt joint design that minimizes the amount of weld metal, provides the required accessibility and is cheaper to prepare should be selected for a particular application.

Fillets welds of three-eights-inch throat size can be made with one pass using a single electrode. Positioning the work usually makes welds larger than five-sixteenths-inch. The bead width must be maintained at least 25 percent greater than the depth since narrow beads are subject to cracking.

In the case of plug welds, the electrode is positioned in the center of the hole and remains in this position until the weld is complete. Retaining rings may be used for holding the flux in position. A weld of three-fourths-inches in diameter is normally the maximum size used for plug welding. Since it is difficult to know when the hole is filled, the plug welding operation is usually timed depending on the size and depth of the hole.

3.10 Multiple Electrode Welding

In SAW, multiple electrodes are used for increasing the deposition rates. Multiple arcs may also decrease the freezing rate and porosity in the weld metal. These systems can be differentiated on the basis of the number of electrodes, type of power connection used and the position of the electrodes (tandem or transverse) with respect to the direction of travel.

3.10.1 Number of Electrodes

Based on the system, two to four electrodes are usually in simultaneous operation. More electrodes are used for special heavy section applications.

3.10.2 Power Connection

In multi-electrodes, multi-power connections, each electrode has its own power supply, welding head, voltage-control mechanism and wire feeders. Single-phase or three-phase power, and many possible combinations of alternating and direct current, can supply the electrodes. The use of alternating current minimizes magnetic arc blow between the electrodes.

In parallel connection, two or more electrodes fed through the same welding head receive power from the same power source. This results in deposition rates more than double that of a single electrode. The ground is connected to the work piece. The current densities are low, and joint penetration is lower than with multipower connection. This technique is primarily used on welds where fill-in is a major consideration at high speeds.

In a series connection, two electrodes are connected in series, and each electrode operates independently having its own welding head, feed motor and voltage control. The power supply cable is connected to one welding head and the return power cable is connected to the second welding head instead of to the work piece. The welding current travels from one electrode to the other through the arc, instead of to the work piece. Since there is no connection to the work

piece, almost all of the power is used to melt the electrodes. Since the electrodes are of opposite polarity, the magnetic field spreads the ends of the arc away from each other and results in fanning or spread of the arc zone. High deposition rates with minimum penetration and dilution can be achieved using this technique.

3.10.3 Electrode Position

Electrodes can be arranged in tandem or transverse position with different types of power connections to produce different effects. Usually, the electrodes are arranged in the tandem position with one electrode following the other. In the transverse position, one electrode is placed alongside the other as they move in the direction of travel. The type of position used depends on the joint design and application.

4.0 INFRARED SENSOR DEVELOPMENT

To date, scanning infrared camera sensors are the sensors more commonly used to monitor welding processes. Researchers have extensively used infrared cameras for monitoring and control of the GTA welding process. The infrared cameras are costly, fragile, and require constant cooling using liquid nitrogen. The large physical size of these systems is intrusive and does not allow placement of the sensors in close proximity to the welding arc. Moreover, infrared cameras are difficult to use for monitoring SA welding process due to the presence of hot slag and excess flux covering the weld pool region. Recent advances in infrared detector technology have resulted in the development of low-cost, highly rugged, miniature-sized sensors that offer great potential for use in metal fabrication industries. One such point infrared sensor was selected for implementation of the monitoring and control of SA welding process.

The IR detector used in this work, Armtec-Ragen model 620-050201 (Figure 1), is a thin-film themopile detector with an active area of $4x10^{-2}$ cm^2 and 48 hot junctions. The detector was packaged in a T0-5 canister, backfilled with Xenon gas. The detector had a germanium window, which allowed radiation only in the eight to 14 μm wavelengths to reach the sensing element. The response time constant was approximately 50 to 100 msec, and the sensor generated 5,100 μV direct current output at 10 mW/Cm^2 IR incident radiation. The detector generated an electric potential based on the radiant energy reaching it. The electric potential was also a function of the temperature difference between the target and the detector itself. The voltage generated by the detector V_{det} can be expressed as follows:

Figure 1. Armtec-Ragen model 620-050201 IR detector

$$V_{det} = M\sigma\varepsilon(T_T^4 - T_D^4)$$

where, T_T is the target temperature (K)

T_D is the detector case temperature (K)

σ is the Stefan Boltzmann constant = 5.6686 X 10^{-12} watts/cm^2/K

ε is the emissivity of the target surface and

M is a constant, = $\frac{\sigma}{\pi}\frac{A_T A_D}{d^2}R$; which depends on the area of the target (A_T), area of the detector (A_D), distance from the detector to target (d) and the responsivity (R) of the detector.

4.1 Signal Conditioning

The raw signal obtained from the infrared detector is of very low strength and is affected by background electrical noise. To obtain a strong and noise-free signal for monitoring and control purposes, signal conditioning of the raw detector signal was required. The sensor head and the signal processor unit performed signal conditioning that involved amplification and filtration, respectively. Initial amplification of the IR signal above the background electrical noise was performed at the sensor head. The sensor head that contained minimal number of electronic components was attached to the welding torch and placed close to the infrared detector. A minimal number of electronic components were placed in the sensor head to avoid the harsh welding environment. The signal processor unit located away from the welding environment was used for filtration and further amplification of the IR signal.

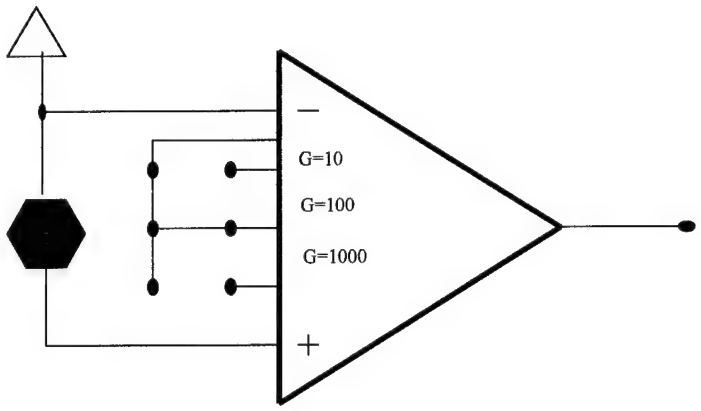

Figure 2. First stage amplification circuit

In the sensor head, the thermopile detector output signal was amplified with a single instrumentation amplifier (Analog Devices AD524) using a configuration as shown in Figure 2. The signal could be amplified 10, 100 or 1000 times by positioning a jumper on the sensor head circuit board. Amplification by 100 times was found to be adequate without saturating the amplifier output. The output of the sensor head entering the signal processor unit can be expressed as

$$V_0 = 100\ V_{det}$$

The signal processor unit consisted of three stages: [1] offset, [2] filter and [3] gain. Optimized sensor signal was obtained through combined adjustment of the offset, signal gain and filter. Each stage of the signal processor unit also contributed to the overall system gain. The electrical circuit design, shown in Figure 3, was implemented with a single quad op-amp (Analog Devices AD713). The offset stage of the signal processor unit was based on a simple addition circuit using a single op-amp. A voltage divider, built with a 10-turn potentiometer and the power supply voltage, was used to provide the second input to this stage, the first input being the signal from the sensor head. The output of this stage can be described as,

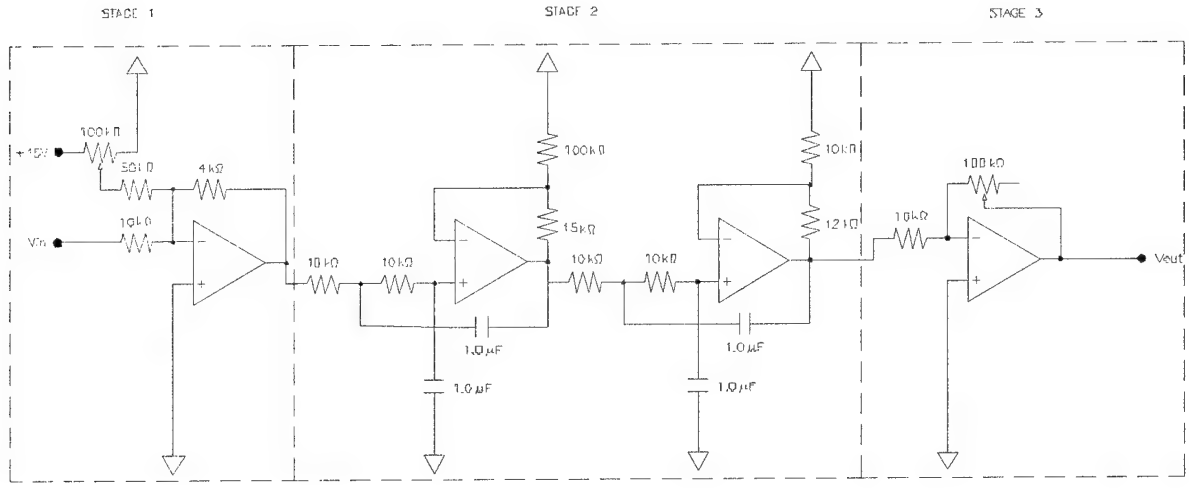

Figure 3. Single processor unit circuit

$$V_1 = -\frac{1}{25}(3n_0 + 10V_0)$$

where, V_1 is the output of the first stage of the signal processor unit

V_0 is the input from the sensor head and

n_0 is the number of turns on the external potentiometer for offset adjustment.

The second stage (filter), composed of a four-pole, low-pass Butterworth filter, was used for smoothening the signal from the sensor head. The filter stage was designed with a cutoff frequency of 15Hz, well below the AC line frequency of 60Hz. The overall gain of this stage is given by

$$V_2 = 2.5\ V_1$$

where, V_2 is the output of the second stage and

V_1 is the input from the first stage.

A 10-turn potentiometer was used to establish the gain at the third stage. For each turn of the pot, the gain increased by one as given below,

$$V_3 = -n_g\ V_2$$

where, V_3 is the output of the third stage,

V_2 is the input from the second stage and

n_g is number of turns on the external potentiometer for gain adjustment.

The overall effect of each of the stages of the signal processor unit is given by,

$$V_3 = n_g\ (0.3n_0 + 100V_{det})$$

4.2 Mechanical Design

The sensor head, which contained the initial amplification circuit, was housed in a cooling jacket made of copper tubes to shield it from the harsh welding environment, as shown in Figure 4. Compressed air was used for cooling the copper jacket. The copper tube was also electrically grounded and attached to the welding torch close to the infrared detector. The signal processor circuit was enclosed in a steel box as shown in Figure 5.

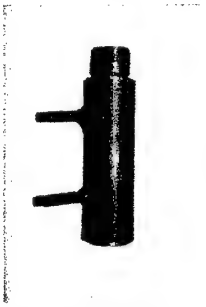

Figure 4. First stage amplification cooling tube

Figure 5. Signal processor box

As shown by the equation $V_{det} = M\sigma\varepsilon(T_T^4 - T_D^4)$, the voltage generated by the thermopile detector is sensitive not only to the target temperature, but also to its own temperature. In order to maintain the detector at a constant temperature and shield it from the harsh welding environment, the infrared detector (TO-5 container) was housed in a cooling jacket made from copper. The mechanical drawing and dimensions are shown in Figure 6.

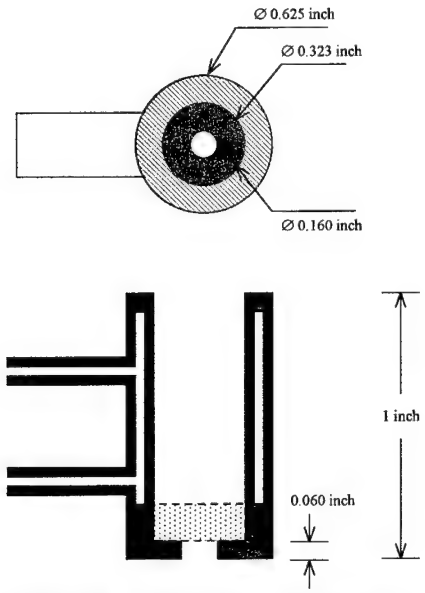

Figure 6. Schematic of IR detector copper jacket

The cooling jacket was fabricated using two concentric copper tubes as shown in Figure 7. A brass button with a counter sink to hold the TO-5 container was brazed to the bottom end of the cooling jacket. The button had an opening of dimension same as that of the germanium window of the TO-5 container. Two holes were made at the top and bottom of the jacket and smaller copper tubes were brazed to form the inlet and outlet ports. The TO-5 container was placed in tight physical contact with the copper tube. Filtered compressed air was used for cooling the copper jacket and maintaining the detector at a constant temperature. The copper jacket was further covered with a heat-resistant silicon fiber woven mat to provide insulation from the welding heat.

The signal generated by the IR detector depends on the field of view (FOV) and the spot size of the target. The FOV and distance from the object determines the size of the spot-viewed by the detector. The FOV can be determined from the geometry of the TO-5 container as follows:

$$\tan\alpha = \frac{(a-l)}{2y}$$

where, a is the window diameter and is 3.94 mm

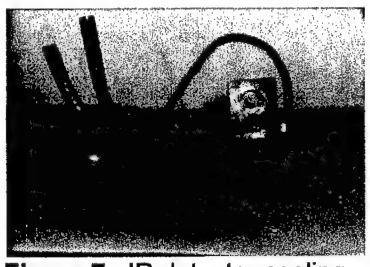

Figure 7. IR detector cooling jacket

l is the active film width and is 2 mm

y is the distance from the detector film to the germanium window and is 1.5 mm.

The spot size of the target can be determined using the equation below,

$$S = 2d \tan\alpha + l$$

where, S is the spot size and

d is the distance between the target and the detector film.

A plot of the spot-size diameter with respect to the target distance is shown in Figure 8. The spot size increases as the detector to target distance increases. Again using the equation $V_{det} =$

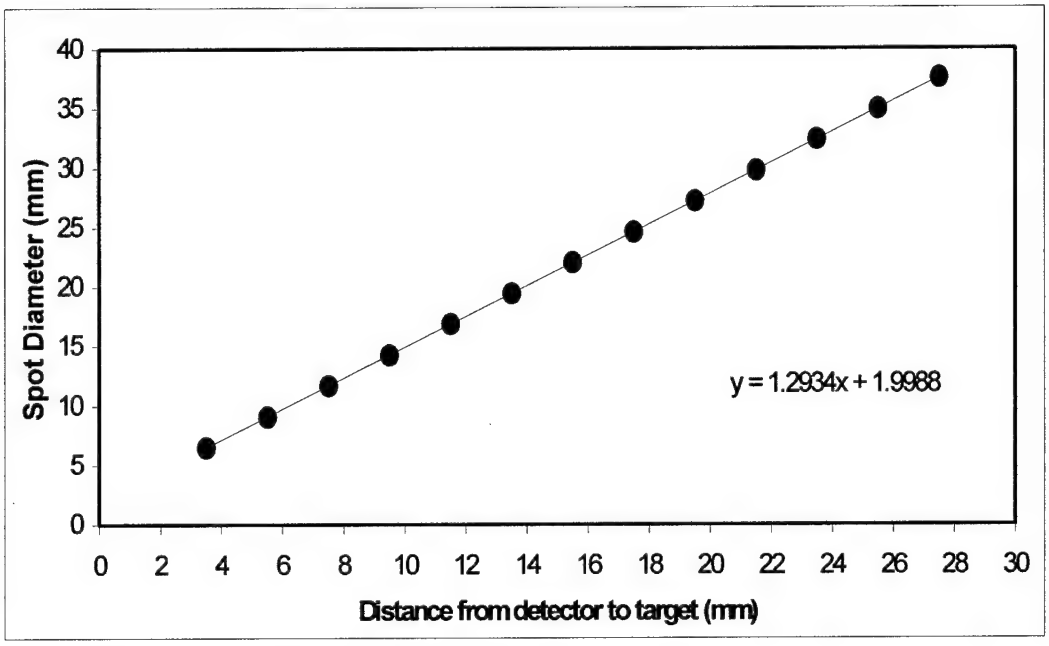

Figure 8. Spot diameter vs. target distance

$M\sigma\varepsilon(T_T^4 - T_D^4)$, the voltage generated by the IR detector can be calculated. Assuming the emissivity to be constant at one, and the detector temperature to be 298°K, the voltage generated by the IR detector for various target temperatures can be calculated. Proportionality constant (M) for different detector-to-target distance was calculated from the manufacturer's data mentioned above. The voltage generated for various target temperatures are shown in Figure 9. As the figure indicates, the voltage generated by the IR detector decreases with increase in the detector-to-target distance, even though the spot size increases. The voltage generated is inversely proportional to the square of the detector-to-target distance.

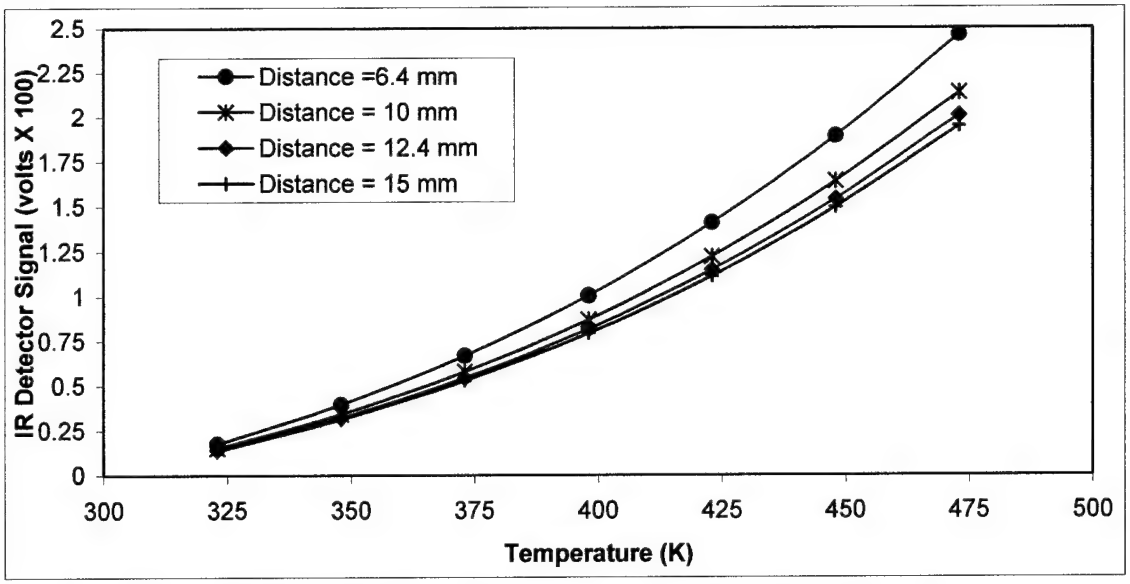

Figure 9. Voltage generated by the IR detector at various temperatures at different detector-to-target distance

4.3 Monitoring and Control

Monitoring of the SAW process was performed using a point infrared sensor. The welding head controls were modified to perform the control functions directly using a computer. Infrared radiation emanating from the plate surface was measured by the IR sensor and was used for monitoring the thermal distribution around the weld pool. Process control was achieved by using the infrared sensor signal as the feedback for adjusting the welding current. The arc voltage was also acquired and controlled. The process control system was tuned, and experiments were performed on plates with constant thickness, step change in thickness and butt joints with constant and variable joint gaps.

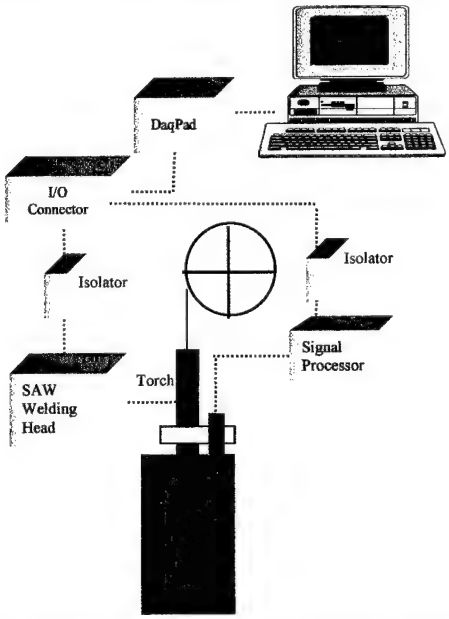

Figure 10a. Monitoring and control hardware setup

4.4 Experimental Setup

The SAW process monitoring and control system consisted of personal computer, data acquisition system, welding power supply, welding head and control and the infrared sensor system. A diagram of the system hardware is shown in Figures 10a and10b.

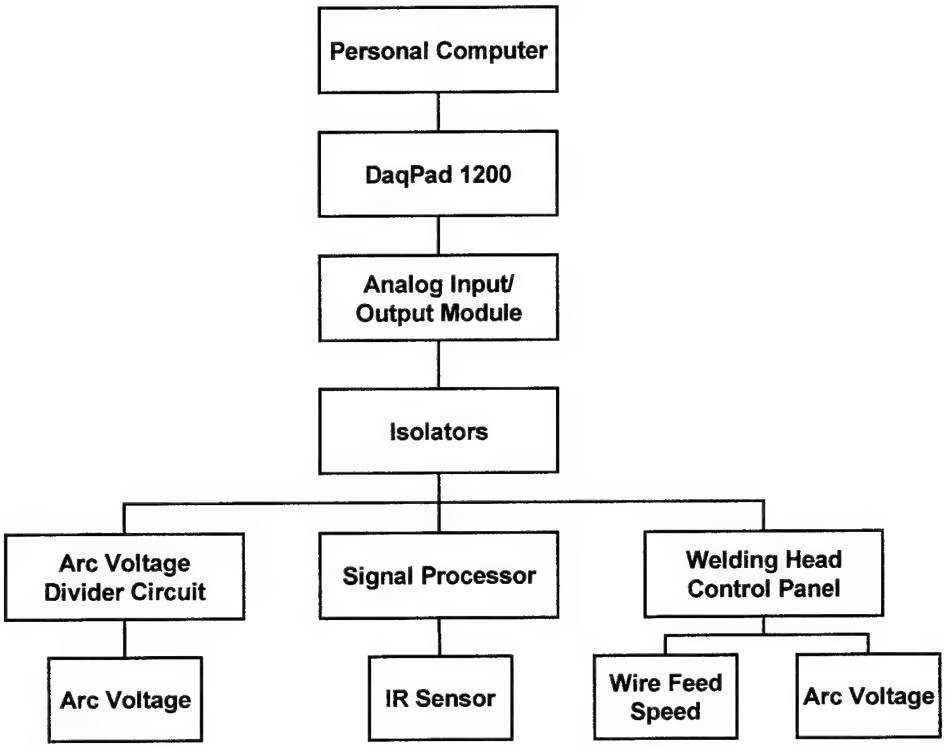

Figure 10b. Schematic diagram of weld control system hardware

4.4.1 Welding Power Supply and Welding Head

The submerged arc welds were made using an L-TEC VCR801 constant voltage power supply capable of supplying 800 amperes of current. Lincoln welding power supply was used for shop-floor welding trials at Ingalls shipyard.

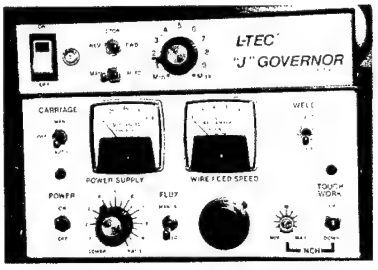

Figure 11. SAW welding head controls

Submerged arc welding power supply is of constant voltage type, and changing the wire feed speed controls the welding current. The machine electronics in the welding head were modified to facilitate direct control of the wire feed speed (welding current) and the arc voltage from the computer. The wire feed speed and arc voltage potentiometers on the control panel (Figure 11) were bypassed using double-pole/double throw-switches. The control signals for the wire feed speed and arc voltage from the computer were directly passed on to the machine electronics.

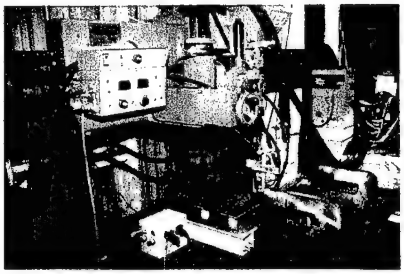

Figure 12. Welding head and table

The movable welding head was mounted on a horizontal beam (Figure 12). The welding head held the welding wire spool, flux hopper, welding torch and controls for the wire feed speed, arc voltage, weld travel speed, and switch for the

welding power. The travel speed was controlled through the control of the motion of the welding head. The plates for the welding trials were placed on table. The ground connection was made to the plate to complete the welding power circuit.

4.4.2 Torch Setup

The infrared sensor was housed in an air-cooled copper tube to shield it from the harsh welding environment. The copper tube was fastened to a support (Figure 13) made of mild steel that also had the provision for a sharp-edged steel wheel that rested on the surface of the plate to be welded. The support was used for adjusting the IR sensor tube to the plate surface distance. The support with the copper tube was attached to a stainless-steel shaft that was capable of up-down motion. The vertical motion of the shaft was achieved with the help of linear bearings. This attachment (Figure 14) ensured a constant sensor-to-plate surface distance to be maintained even in the case of distorted plates, and allowed the sensor to travel along the weld. The torch attachment also allowed easy adjustment of the position of the sensor with respect to the welding electrode. Figure 15 shows the attachment fixed to the SAW machine torch. The IR sensor was positioned at about 25 mm from the center of the torch contact tip and at a polar angle of 90 degrees. The distance between the bottom of the copper tube and the plate surface was maintained at about 3.2 mm. The excess flux in the view of the sensor was removed using a vacuum extractor.

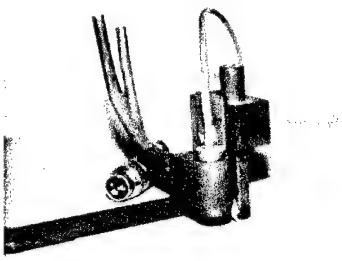

Figure 13. Copper tube attached to support

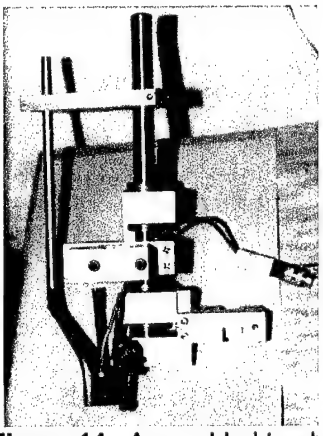

Figure 14. Assembled torch attachment

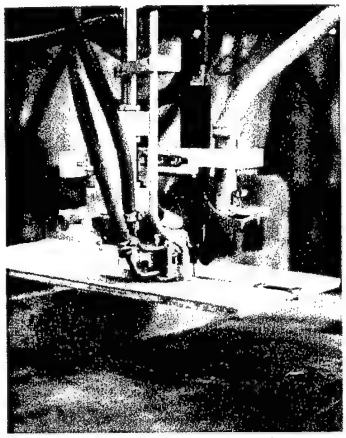

Figure 15. Torch attachment

4.4.3 Data Acquisition

The data acquisition and control system consisted of a PC desktop computer, electrical isolators/signal conditioners and the data acquisition unit (DaqPad 1200) purchased from National Instruments. The DaqPad 1200 (Figure 16) communicated with the computer through the parallel port. The DaqPad 1200, which is basically an analog-to-digital (A/D) and digital-to-analog (D/A) converter, has a 12-bit (one in 4096) resolution. It is capable of acquisition rate up to 100 KS/s with a conversion time of 8.5 μs. It has eight analog input channels and two output channels that are software configurable for unipolar or bipolar input/output. The input and the output channels were configured for a range of zero to 10+ volts. The signal gain was set at one for all

Figure 16. National Instruments DaqPad 1200

experiments. The resolution of the voltage scale is given by the equation,

$$\text{Resolution (V)} = \frac{range(V)}{gain * 2^{resolution}}$$

With the above-mentioned input and output voltage ranges, the signal resolution was 2.44 mV for both the input and the output channels. The hardware-conditioned infrared sensor signal was acquired at a rate of 60 reading per iteration.

The input signals from the infrared sensor, the arc voltage and the output signals to the welding power supply were electrically isolated using signal conditioner/isolators (Figure 17). The infrared process control system was also electrically isolated to separate the electrical grounds and to prevent damage to the data acquisition card and computer. The electrical isolation was achieved through optical isolation technique in the isolators.

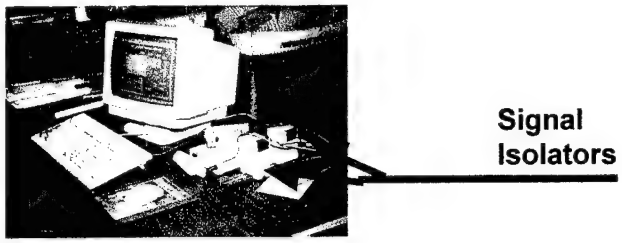

Figure 17. Signal isolators

The open circuit voltage of the SAW machine was 65 volts, and the typical arc voltage of the welding process was in the range of 24 to 30 volts. In order to acquire the arc voltage, the voltage was reduced to zero to 10+ volts range using a voltage divider circuit (as shown in Figure 18), before being acquired. The voltage divider circuit consisted of four resistors — one 4.6K and three 1K — that were connected in series with each other. The arc voltage from the SAW machine was applied to the circuit, and the output was obtained across one of the 1K resistors. For an open circuit voltage of 65V, the potential drop across the 1K resistors was 8.5V. For a typical arc voltage of 30V, the corresponding potential drop was found to be about 3.95V and was acquired by the data acquisition unit. The obtained arc voltage signal data was further smoothened by averaging method using the software.

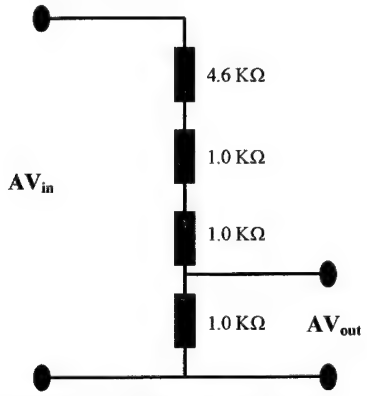

Figure 18. Schematic of an arc voltage divider circuit

4.5 Process Control

High-performance measurement and control systems, most often based on the use of digital instrumentation, play a crucial role in achieving the goals of efficient process control. Of the many control strategies available, feedback control strategy is found to be very useful for process control in many industries. In feedback control, the process variable to be controlled is measured, and the measurement is used to adjust another process variable that can be manipulated. In feedback control the objective is to reduce the error signal e(t) to zero where,

$$e(t) = R(t) - B(t)$$

and $R(t)$ = set point, $B(t)$ = measured value of the controlled variable (IR sensor signal).

Negative feedback control is utilized to perform the process control as it produces the desirable condition where the corrective action taken by the controller tends to move the controlled variable towards the set point. Feedback control strategy does not require the measurement of the disturbance variable in order to perform the process control and works even when the disturbance occurs in any process variable. No corrective action takes place until after the disturbance has upset the process. Thus, by the inherent nature, the feedback control is not capable of perfect control since the controlled variable must deviate from the set point before the corrective action is taken. This ability to handle unmeasured disturbances of unknown origin is a major reason why feedback controllers have been so widely used for process control. In the case of welding process control, the measured variable is the IR sensor signal (temperature of the plate) and the manipulated variable is the wire feed speed (welding current). The disturbance variable, for example, changes in the plate thickness or joint gap is not measured.

One of the most commonly used types of feedback control strategy is the proportional-integral-derivative (PID) control law. The ideal PID controller equation is given as

$$p(t) = \bar{p} + K_C\left[e(t) + \frac{1}{\tau_I}\int_0^t e(t^*)dt^* + \tau_D\frac{de}{dt}\right]$$

4.5.1 Proportional Control

In the case of proportional control mode, the controller output is proportional to the error signal,

$$p(t) = \bar{p} + K_C e(t)$$

where $p(t)$ = controller output

$\bar{p}$ = bias value

K_C = controller gain.

The controller gain is adjustable and is usually tuned after the controller has been installed and brought into service. Some controllers have a proportional band setting instead of controller gain. The proportional band PB (in percent) is defined as,

$$PB = \frac{100\%}{K_C}$$

An inherent disadvantage of proportional-only control is its inability to eliminate steady-state errors that occur after a set point change or a sustained load disturbance. The offset can be eliminated by manually resetting the set point R or bias p after an offset occurs, but is inconvenient. In practice, it is more convenient to use a controller that contains integral control action, which provides this automatic reset.

4.5.2 Integral Control

Integral control action is also referred to as reset or floating controls. The controller output depends on the integral of the error signal over time,

$$p(t) = \bar{p} + \frac{1}{\tau_I}\int_0^t e(t^*)dt^*$$

where τ_I is referred to as the integral time or reset time and is adjustable.

Integral control is widely used because it eliminates the offset. While the elimination of offset is an important control objective, the integral controller is seldom used by itself since little control action occurs until the error signal has persisted for some time. In contrast, proportional control action takes immediate corrective action as soon as an error is detected. Consequently, integral control action is normally employed in conjunction with proportional control as the popular proportional-integral (PI) controller:

$$p(t) = \bar{p} + K_C\left[e(t) + \frac{1}{\tau_I}\int_0^t e(t^*)dt^*\right]$$

One of the disadvantages of using integral action is that it tends to produce oscillatory responses of the controlled process, and thus reduces system stability. A limited amount of oscillation can usually be tolerated since it is often associated with a faster response. The undesirable effects of too much integral action can be avoided by proper tuning of the controller or by including derivative action, which tends to counteract the destabilizing effects. Another inherent disadvantage of the integral control action is the phenomenon known as reset windup. Reset — or integral — windup, triggered by a sustained error, results in the integral term becoming quite large, and the controller output eventually saturating. But most commercial controllers have the anti-reset-windup feature, which reduces the reset windup by temporarily halting the integral control action whenever the controller output saturates and resumes when the output is no longer saturated.

4.5.3 Derivative Control

Derivative control is also referred to as rate action, pre-act, or anticipatory control. Its function is to anticipate the future behavior of the error signal by considering it rate of change. Thus for ideal derivative action,

$$p(t) = \bar{p} + \tau_D\frac{de}{dt}$$

where τ_D, is the derivative time. The derivative action is mostly used in conjunction with proportional or proportional-integral control.

By providing anticipatory control action, the derivative mode tends to stabilize the controlled process. It is often used to counteract the destabilizing tendency of the integral mode. The derivative control also tends to improve the dynamic response of the controlled variable by decreasing the process settling time, the time taken by the process to reach steady state. When the process measurement is noisy, with high frequency random fluctuations, the derivative of the measured (controlled) variable changes very wildly, and the derivative action amplifies the noise unless the measurement is properly filtered.

4.6 Typical Responses of Feedback Control Systems

Figure 19 illustrates the typical behavior of a controlled process after a step change in load variable occurs. The controlled variable C is shown as a deviation from the initial steady-state value. If no feedback control is used, the process slowly reaches a new steady state. A proportional control speeds up the process response and reduces the offset. Addition of integral action eliminates the offset but tends to make the response more oscillatory. Adding derivative action reduces the both the degrees of oscillation and the response time. However, the controller response depends on the choice of the controller parameter settings (K_C, τ_I, and τ_D) and the particular process dynamics.

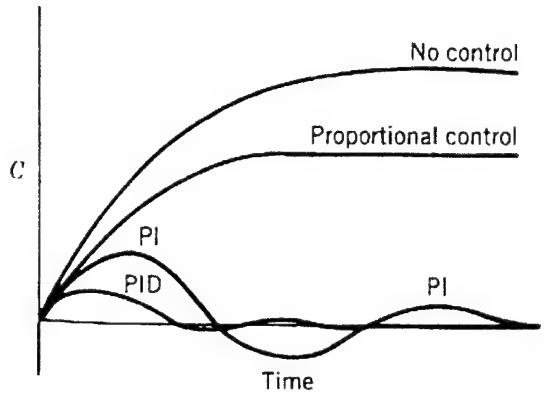

Figure 19. Typical controller response to step change

The qualitative effects of changing the individual controller settings are shown in Figures 20 through 23. In general, increasing the controller gain tends to make the process response less sluggish, but too large a gain may cause an undesirable degress of oscillation or even become unstable. Thus, an intermediate value of K_C usually results in the best control. Increasing the reset time usually makes PI and PID control more conservative (sluggish) as shown in Figure 21. For extremely large values of reset time, the controlled variables return to the set point very slowly after a load upset or set-point change occurs. For small values, increasing the derivative time tends to improve the response by reducing the maximum deviation, response time and degree of oscillation. For large values, the measurement noise tends to be amplified, and the response becomes oscillatory. Thus, an intermediate value of derivative time is desirable.

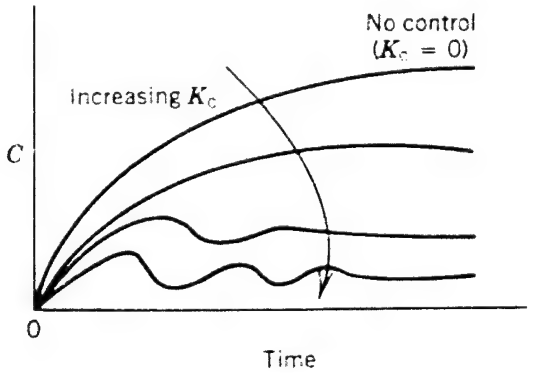

Figure 20. Proportional control: effect of controller gain

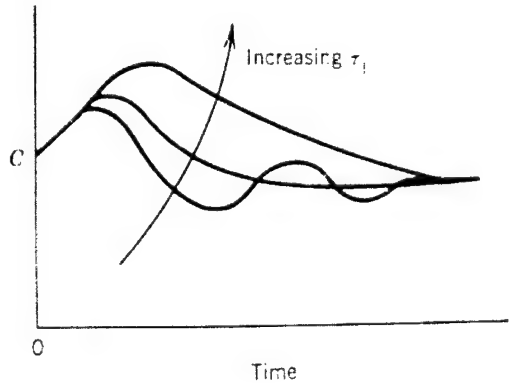

Figure 21. PI control: effect of reset time

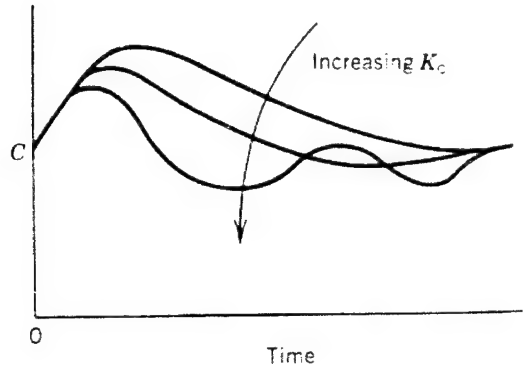

Figure 22. PI control: effect of controller gain

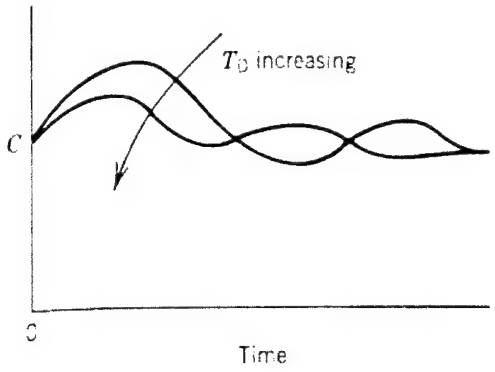

Figure 23. PID control: effect of derivative time

4.7 Tuning of Controller

The tuning parameters of the controller were adjusted to provide the best controller performance. The tuning parameters were determined using the Zeigler-Nichols tuning procedure and by performing weld trials.

The open-loop Zeigler-Nichols tuning procedure was followed for tuning the controller. In this method, a single experimental test was conducted with the controller in the manual mode and a strip-chart recorder was used for recording the process variable. When the process variable (IR signal) was completely settled, the value was noted. Then a small step change in the controller output was introduced, the process variable (IR signal) was allowed to settle, and the new value was noted. From the strip chart, T_d (dead-time in minutes), T (time constant), and

$$\text{K – process gain} = \frac{\%change\ldots in\ldots output}{\%change\ldots in\ldots PV}$$

were calculated. New tuning parameters were then found by multiplying the measured values with factors mentioned below,

$$PB = 110\frac{KT_d}{T};\ reset = 3.33T_d$$

During the weld trial, the control signal was increased from 2.4 volts to 2.9 volts. The corresponding process variable (IR signal) values were recorded to be 0.285 volts and 0.536 volts, respectively. The dead-time (T_d) measured from the chart was found to be about five seconds, and the time constant (T) was 10 seconds. The new PB and reset values were obtained by substituting the measured values in the above equations and were found to be 27.5 and 0.28, respectively.

These values were used, and weld trials were performed with automatic control. The weld trials were conducted on plates with step change in thickness and the controller tuning parameters were further tuned to provide the best results as shown in Figures 24 and 25.

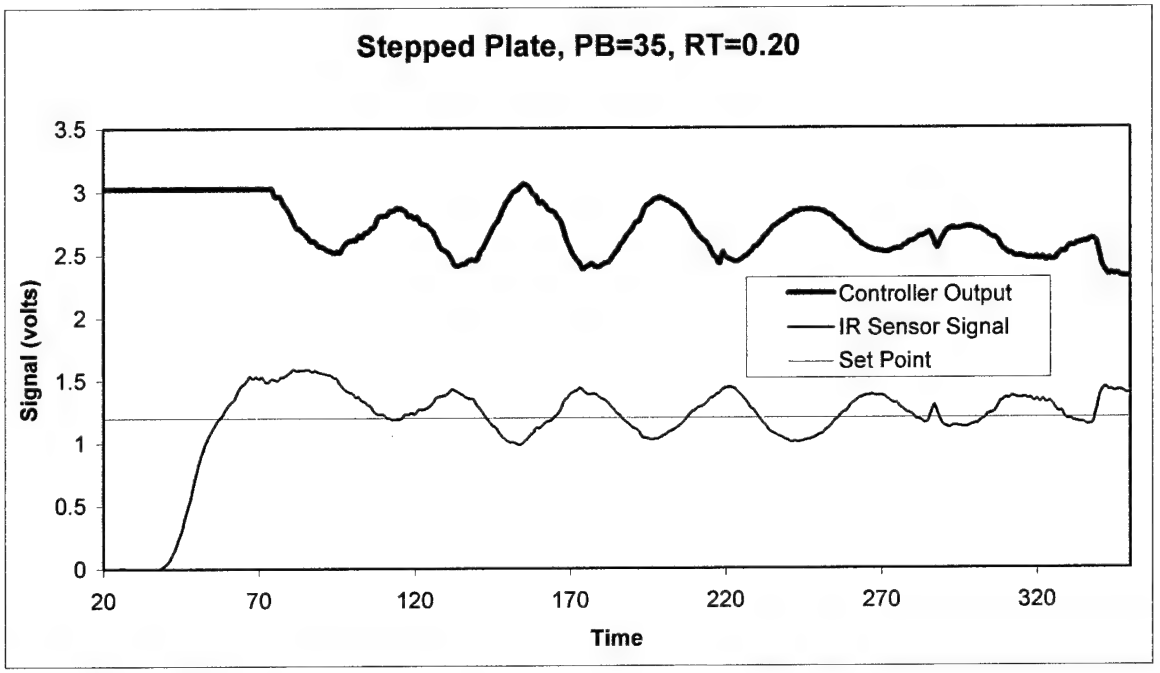

Figure 24. Oscillation of controller output

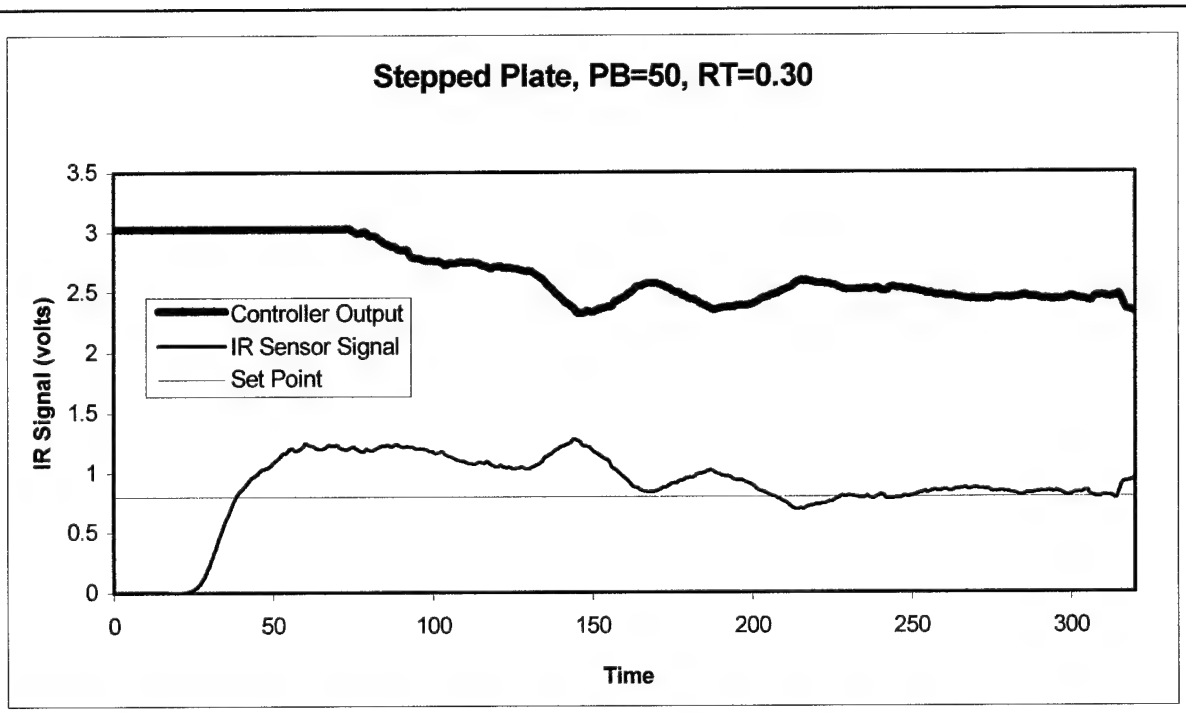

Figure 25. Graph showing smoother control due to tuning of controller parameter

4.8 Software

The welding process control system was written in a graphical language "G" using the software package LabVIEW purchased from National Instruments. LabVIEW, like any other conventional programming language, is a general-purpose programming system, but also includes extensive libraries of functions for data acquisition, GPIB and serial instrument control, data analysis, data presentation, and data storage. LabVIEW programs are also called virtual instruments (VIs) because their appearance and operation can imitate actual instruments. A VI consists of an interactive user interface called the front panel, which simulates the panel of a physical instrument and a dataflow diagram that serves as the source code. The front panel can contain knobs, push buttons, graphs, and other controls and indicators. The block diagram is constructed by wiring together objects that send or receive data, perform specific functions, and control the flow of execution. The wires are the data paths between the source and the sink. LabVIEW program execution is based on the principle of data flow, whereas the traditional programming languages are instruction driven. Any VI can be used as a sub VI in another program and all the VIs in a program can execute simultaneously, making the position of the VI on a diagram irrelevant.

A Virtual Instrument Weld Machine Controller that facilitates the control of the welding

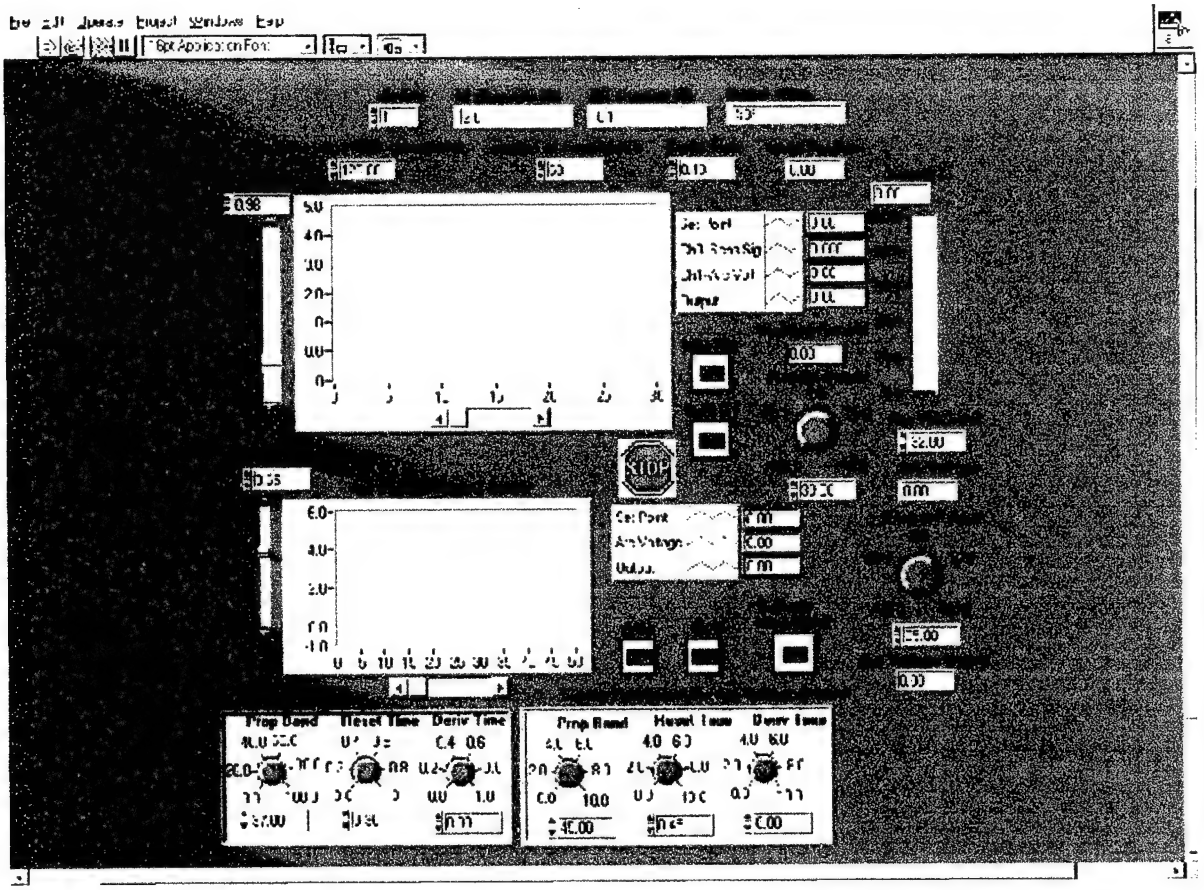

Figure 26. Virtual weld machine controller front panel

variables from the computer screen was created as shown in the Figure 26. The corresponding block diagram is shown in Figure 27. The program consisted of analog input, process controller for welding current (wire feed speed) and arc voltage, file input/output and analog output paths. Each path consisted of configuration, initialization, action, error checking and termination. The configuration and initialization operations were performed outside the loops, whereas action and

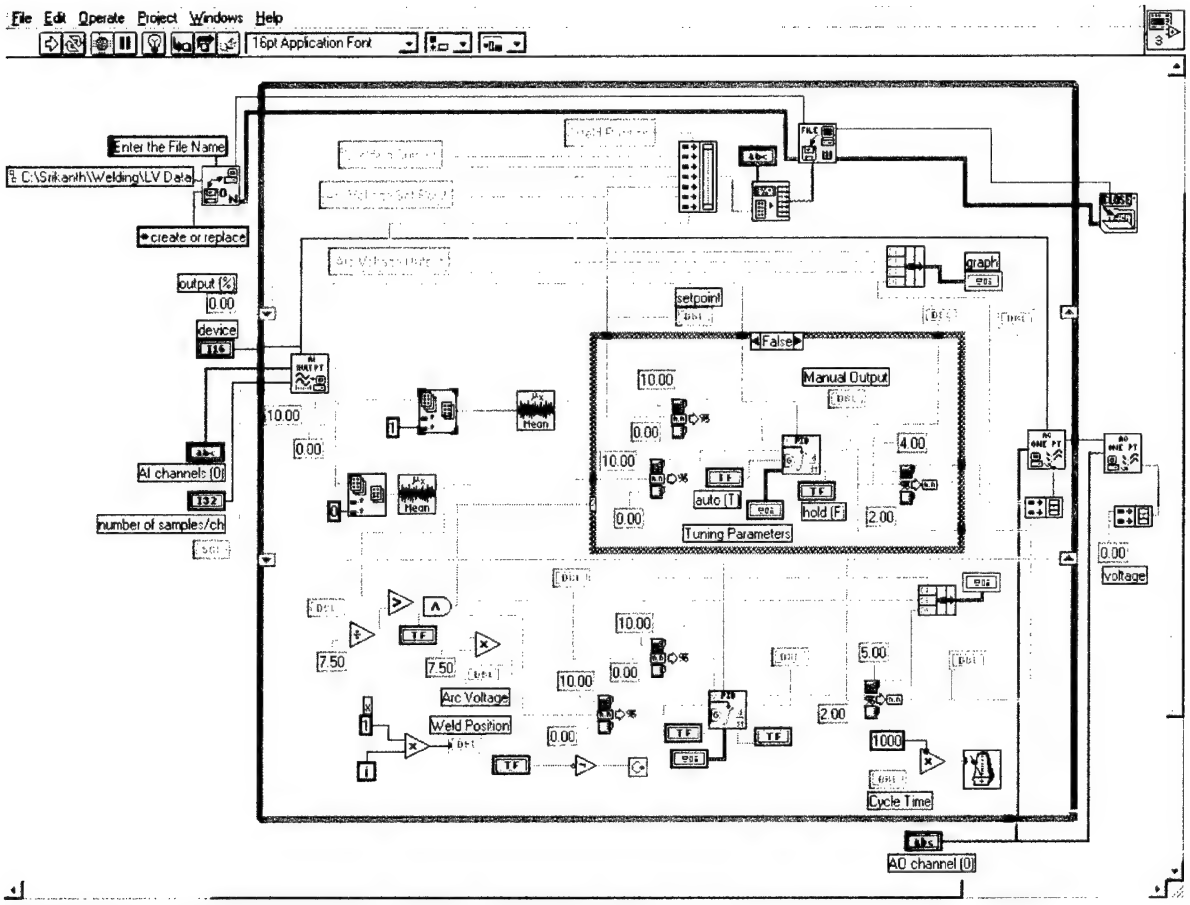

Figure 27. Virtual instrument weld machine controller diagram

error checking occurred inside the loop. The loop was iterated at a specified rate, usually one iteration per second. The loop stopped when the stop button was depressed or any error occurred. The data acquisition began at the start of the program and each channel was sampled at a high rate to avoid aliasing effects. The acquired data was smoothened using averaging methods, and the smoothed data was used for process control. A PID control technique was used for the control of welding current and the arc voltage. External Reset Feedback PID VI that calculated an analog output value with a non-linear error response based on the current value of the process variable, set point and reset feedback was used. The VI expressed the set point, process variable and output in percent. The normal action of the VI was reverse action where the output decreased if the process variable was greater than the set point. The IR sensor signal and arc voltage were the measured variables, whereas the wire feed speed and the arc voltages were the manipulated variables. The performance of the PID controller depended on the smoothness

variables from the computer screen was created as shown in the Figure 26. The corresponding block diagram is shown in Figure 27. The program consisted of analog input, process controller for welding current (wire feed speed) and arc voltage, file input/output and analog output paths. Each path consisted of configuration, initialization, action, error checking and termination. The configuration and initialization operations were performed outside the loops, whereas action and

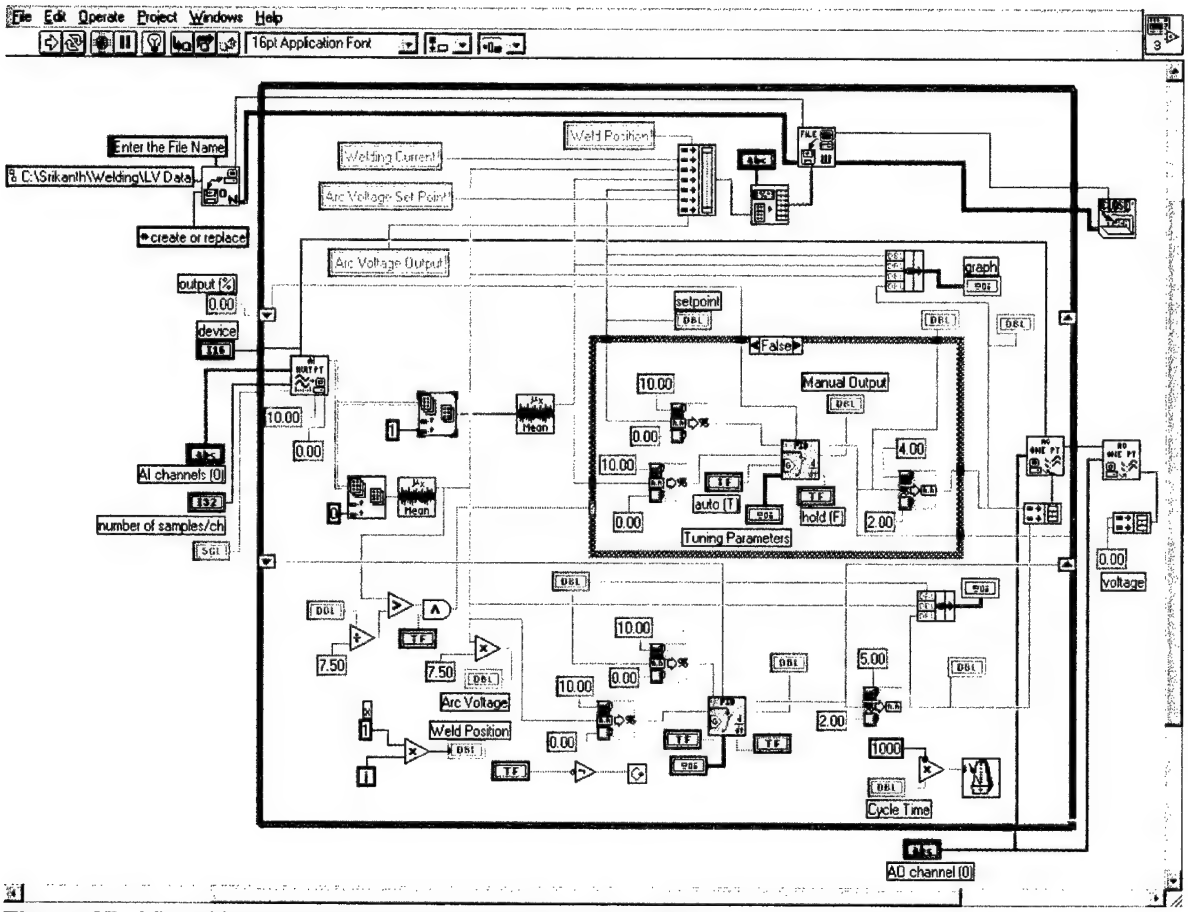

Figure 27. Virtual instrument weld machine controller diagram

error checking occurred inside the loop. The loop was iterated at a specified rate, usually one iteration per second. The loop stopped when the stop button was depressed or any error occurred. The data acquisition began at the start of the program and each channel was sampled at a high rate to avoid aliasing effects. The acquired data was smoothened using averaging methods, and the smoothed data was used for process control. A PID control technique was used for the control of welding current and the arc voltage. External Reset Feedback PID VI that calculated an analog output value with a non-linear error response based on the current value of the process variable, set point and reset feedback was used. The VI expressed the set point, process variable and output in percent. The normal action of the VI was reverse action where the output decreased if the process variable was greater than the set point. The IR sensor signal and arc voltage were the measured variables, whereas the wire feed speed and the arc voltages were the manipulated variables. The performance of the PID controller depended on the smoothness

of the acquired data and the tuning parameters. The three tuning parameters of the PID controller, which were the proportional band, reset time and the rate time, were adjusted to provide the best controller performance. The controller gain was expressed in percent as G=100/PB, whereas the reset and rate were measured in minutes by the VI. IR sensor signal and the arc voltage were both hardware- and software-filtered to eliminate the noise before feeding it to the controller.

The IR sensor signal, arc voltage, process set points and control outputs were displayed on the front panel of the VI weld process controller in real time. The acquired data were stored in ASCII format for further analysis and presentation. Initiating the automatic control caused the IR sensor signal and the arc voltage to be maintained at the respective set points through the control of the wire feed speed and arc voltage. The control system took corrective action when perturbations upset the process (i.e., when the temperature of the plate or the arc voltage changed from the set point).

5.0 THERMAL DISTRIBUTION

The temperature distribution around the weld pool provides important information on the status of the welding process. The pool shape, absolute temperature and symmetry of temperature distribution are directly related to several welding process variables such as welding current, arc voltage and welding speed, as well as geometrical variables such as joint design, root gap and plate thickness. To interpret phenomena arising during the welding operation at a given point of the assembly, it is necessary to know the thermal cycle experienced by the weld joint, particularly the temperature variation as a function of time and distance from the weld pool. The temperature at a particular point adjacent to the weld reaches a maximum value and decreases with time. The maximum temperature attained depends on the position of the point with respect to the weld centerline and the heat input as shown in Figure 28. When the welding operation is in progress with constant heat input, the maximum temperature reached for a point that is at a constant distance from the weld bead center, increases with distance covered from the beginning of the bead and becomes a constant as shown in Figure 29. Thus in the case of mobile heat sources, a quasi-stationary (steady) thermal state is established after a certain distance, and the isotherms remain unchanged and move with the heat source. The limits of the isotherms are lines parallel to the bead as shown in Figure 30. These isotherms are affected by perturbations in the welding parameters, base metal properties, and joint geometrical variables such as plate thickness, joint fit-up, etc. Prediction of changes in the isotherms could offer valuable information regarding the joint conditions, and in turn, could be used for process control.

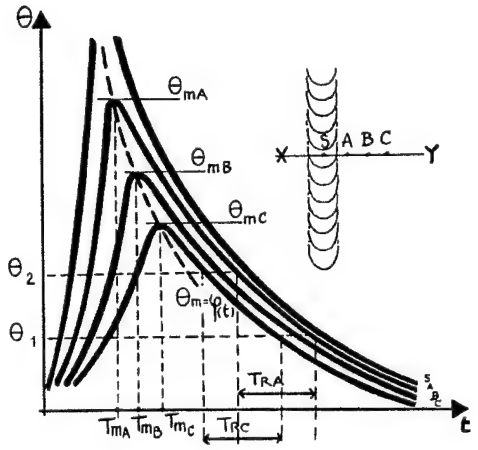

Figure 28. Temperature/time curves at different measurement points along a line perpendicular to the weld

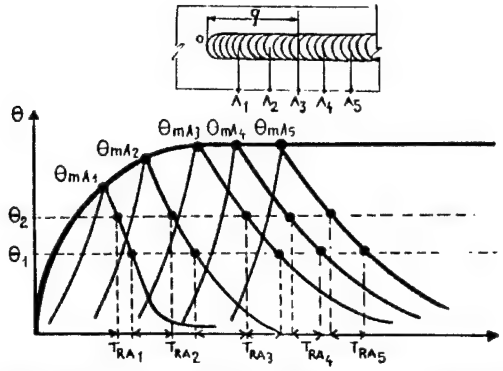

Figure 29. Temperature distribution obtained at the same distance from the weld, but at increasing distance from the start of the weld (quasi-stationary condition).

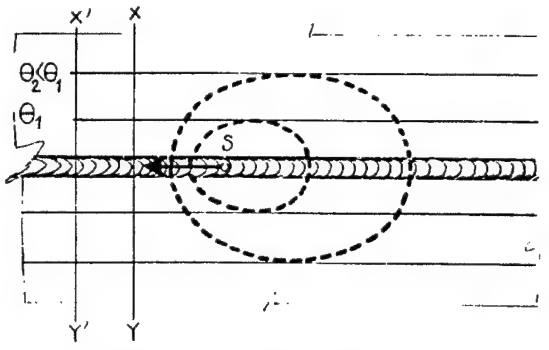

Figure 30. Position and limits of isotherms when quasi-stationary condition is achieved.

Early attempts to analyze the temperature distribution involved the use of analytical solutions to the Fourier heat conduction equation. The governing differential equation for the transient, two dimensional conduction heat transfer is given by,

$$\frac{\partial^2 T}{\partial X^2}+\frac{\partial^2 T}{\partial Y^2}+Q=\frac{\rho C}{\kappa}\left(\frac{\partial T}{\partial t}\right)$$

where, T, is the temperature at position x, y in Kelvin

t, is the time in seconds

ρ, is the density in kg/m^3

κ, is the thermal conductivity in $W/m^2.K$

C, is the specific heat in J/kg.K

Q, is the heat generation rate in W/m^3.

Rosenthal's two-dimensional analytical solution for infinite plate butt weld is given as,

$$T=T_0+\frac{Q}{2\pi\kappa g}e^{-\lambda\xi r}K_0(\lambda\nu r)$$

where, T_0, is the initial temperature

g, is the thickness of the plate

λ, is the thermal diffusivity

ν, is the welding speed

ξ, is (x-νt)

r, is $(\xi^2+y^2)^{0.5}$

K_0, is the Bessel function of the second kind and zero order.

Rosenthal's solution involves the use of many simplifications, such as infinite plate geometry, point-heat source, and temperature-independent material properties resulting in introduction of

error. Dimensionless forms of Rosenthal's solution developed[45,46] for simple geometries to generalize the predictions seem to provide a better understanding of weld-thermal distribution.

High-speed computers have made numerical methods for solving the Fourier heat equation attractive, and simplifications can be neglected to improve the accuracy. Finite element[47,48] and finite difference[49,50] have been the popular solution techniques. Finite difference methods are easy, but are often limited to simple geometries. Nagarajan[51] and Banerjee[52] adopted a numerical heat transfer model developed by Ule and Joshi[53]. Finite element methods with many software packages have become an aid in solving complex heat transfer problems. The commercial software application ALGOR was used in this study to describe the changes in the thermal distribution due to changes in the plate thickness and butt joint gaps. A very simple two-dimensional grid system was used for modeling the changes in the thermal distribution. Only conductive heat transfer and point heat source were used for the prediction of changes. The intention of this modeling effort was to show that changes to the thermal distribution in the vicinity of the weld pool take place due to perturbations. Prediction of absolute temperature changes was not undertaken due to the scope of the present work.

5.1 Step Change in Plate Thickness

The effect of step change in plate thickness on thermal distribution was investigated. The following material properties for AISI 1008 plain carbon steel were used for developing the thermal distribution,

κ, thermal conductivity	63.9 W/m.K
ρ, density	7832 kg/m^3 and
C_p, heat capacity	434 J/kg.K.

The material properties were assumed to be constant with temperature for the purposes of simplification. The following weld parameters were used:

Welding Current:	375 amps
Arc Voltage:	28 volts
Welding Speed:	9 inches/minute
Plate Thickness :	3/8 inch, decreased to ¼ inch at the region of lower thickness

As shown in Figure 31, at the region of lower plate thickness (one-fourths-inch), due to the increase in the heat input/mass ratio, the thermal distribution is distorted with an increase in temperature. The isotherms bulge at the region of lower thickness, showing that the peak temperature reached by a point in the vicinity of the weld pool is higher that at the region of higher thickness (three-eighths-inch).

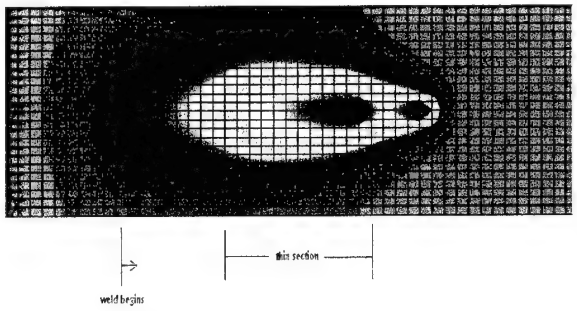

Figure 31. Thermal distribution obtained due to change in plate thickness

5.2 Butt Joint with Variable Gap

Changes in the thermal distribution in the vicinity of the weld pool due to changes in the butt joint gap were investigated for plate thickness of three-eighths-inches. The butt joint gap was increased from one-sixteenths-inch to one-eights-inch. The following weld parameters were used:

Welding Current:	400 amps
Arc Voltage:	28 volts
Welding Speed:	9 inches/minute

The mesh used for model is shown in Figure 32. As shown in Figure 33, the thermal distribution distorted at the region of wider gap. The peak temperature of the plate at a particular distance from the center of the weld bead increased at the region of wider joint gap as shown in Figure 34.

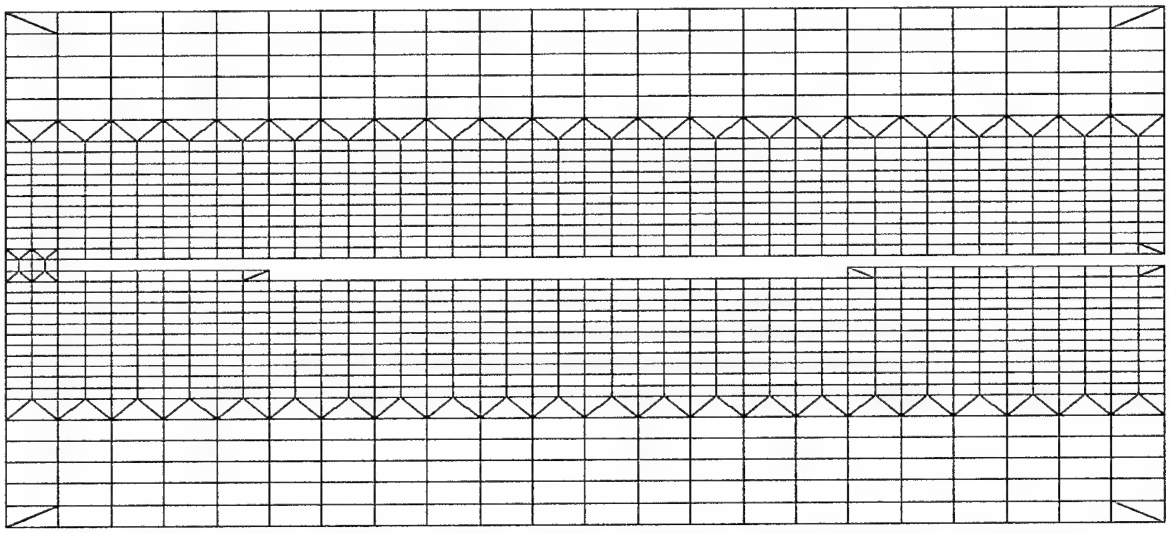

Figure 32. Mesh system used for modeling thermal distribution for butt joint with variable gap.

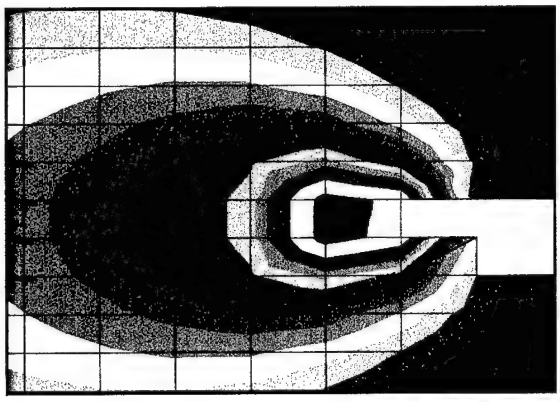

Figure 33. Close-up view of the thermal distribution at the region of the wider butt joint gap.

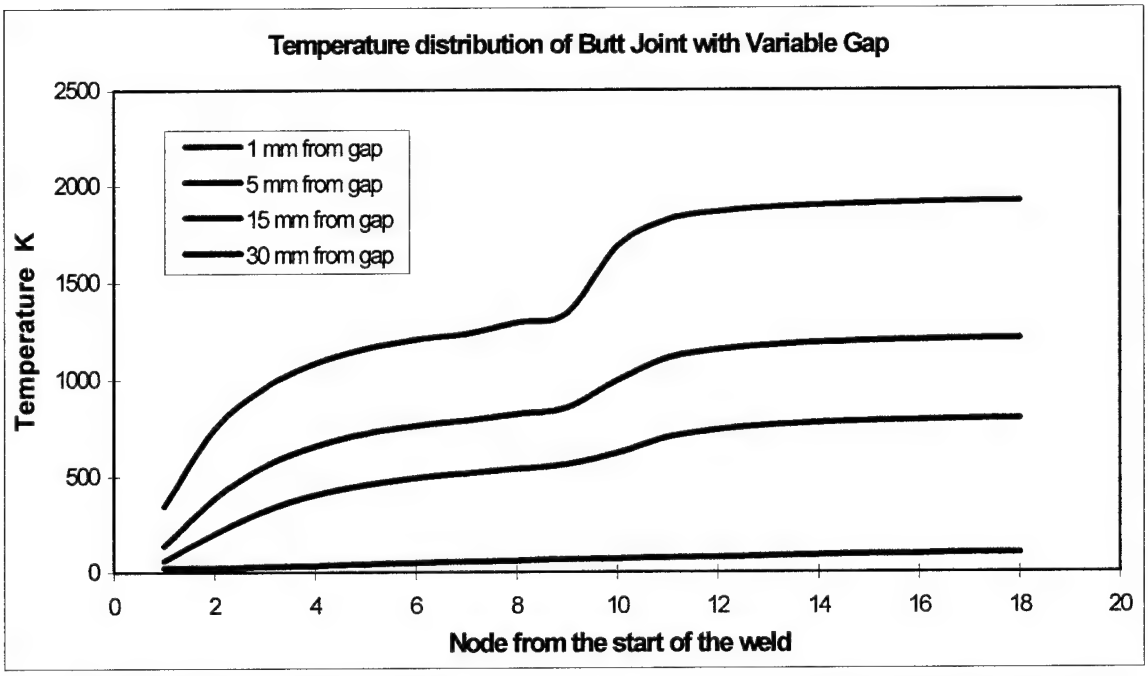

Figure 34. Graph showing the change in the temperature at the region of the wider joint gap experienced by locations at constant distance from the center of the joint gap.

6.0 EXPERIMENTS

6.1 Introduction

A simple theoretical analysis has shown that defect-producing conditions alter the temperature distribution around the weld pool. This chapter describes the various experiments performed to monitor the real-time changes in the temperature distribution and to implement feedback corrective action, thereby mitigating their deleterious effects on weld quality.

6.1.1 Consumables

All welding experiments were performed using L-12 carbon steel electrode of one-eighths-inch diameter and of chemistry 0.04 percent to 0.14 percent C, 0.25 percent to 0.60 percent Mn, 0.10 percent Si, 0.025 percent S max, and 0.025 percent P max, conforming to SFA 5.17; and Lincoln WeldFlux 780, conforming to AWS A5.7. Hot-rolled AISI 1008 carbon steel plates were used for all experiments. The plates were sandblasted or ground to remove the mill scale on the surface.

6.1.2 IR Sensor Signal, Welding Current, Wire Feed Speed and Control Signal Relationships

Precise control of the welding process depends on the relationship between the control signal, wire feed speed, welding current and the IR sensor signal. Bead-on-plate welds were performed

at different control signal values (with corresponding welding currents), keeping other weld parameters constant to analyze the relationship between the IR sensor signal, welding current, wire feed speed and controller signal.

The welds were performed on 16-by-16-by-one-fourth-inch plates with sandblasted surface. Welds were performed with control signal output ranging from 2.0 to 3.1 volts and the corresponding welding currents were measured using a tong tester. The wire feed speed was measured using a specially designed tachometer. The wire electrode passed between a pair of grooved wheels in the tachometer, and the wire feed speed was automatically read from the speed of rotation of the wheels. The IR sensor signal was obtained by averaging the values in the stable region of the weld. The relationship between all the variables were found to be linear as can be seen from Figures 35 through 39.

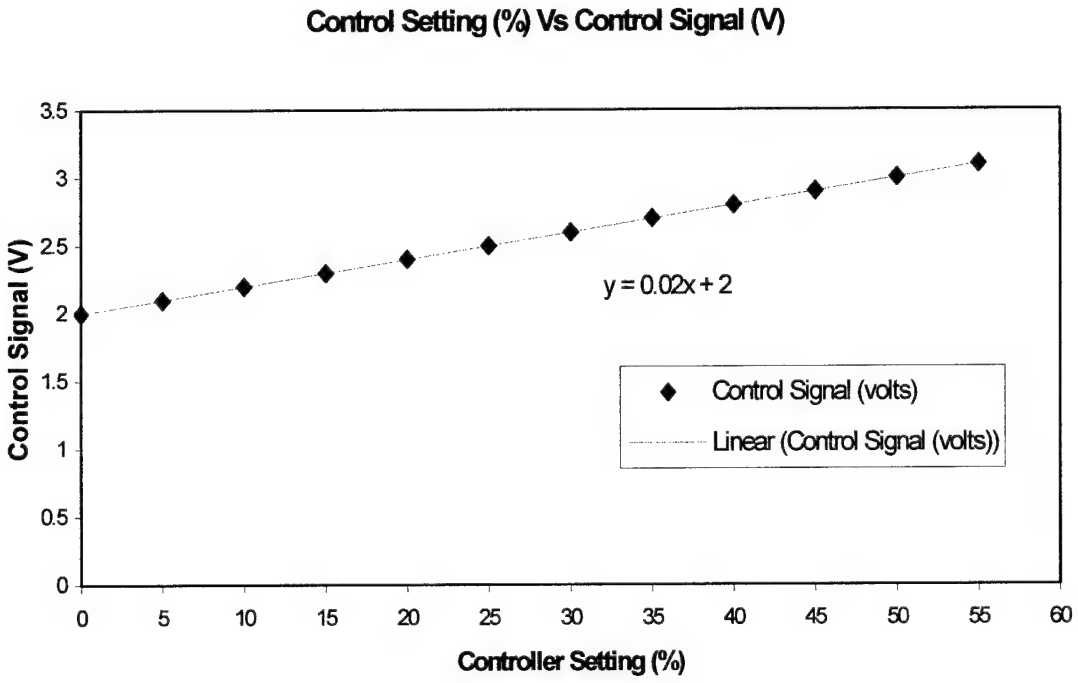

Figure 35. Control signal vs. controller setting

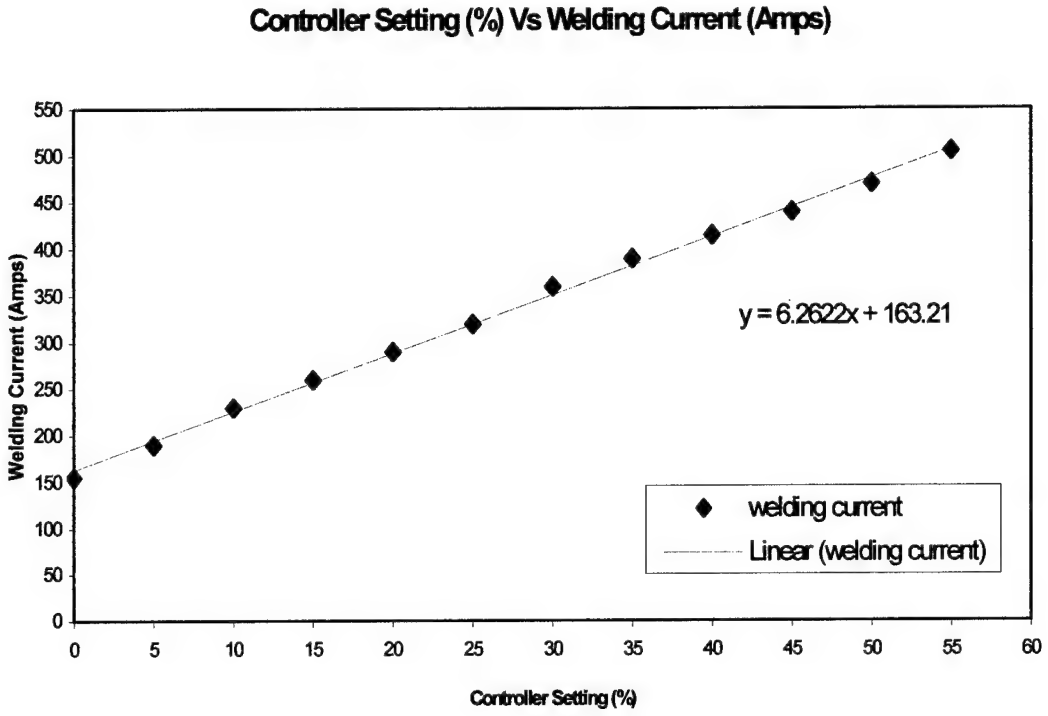

Figure 36. Controller setting vs. welding current

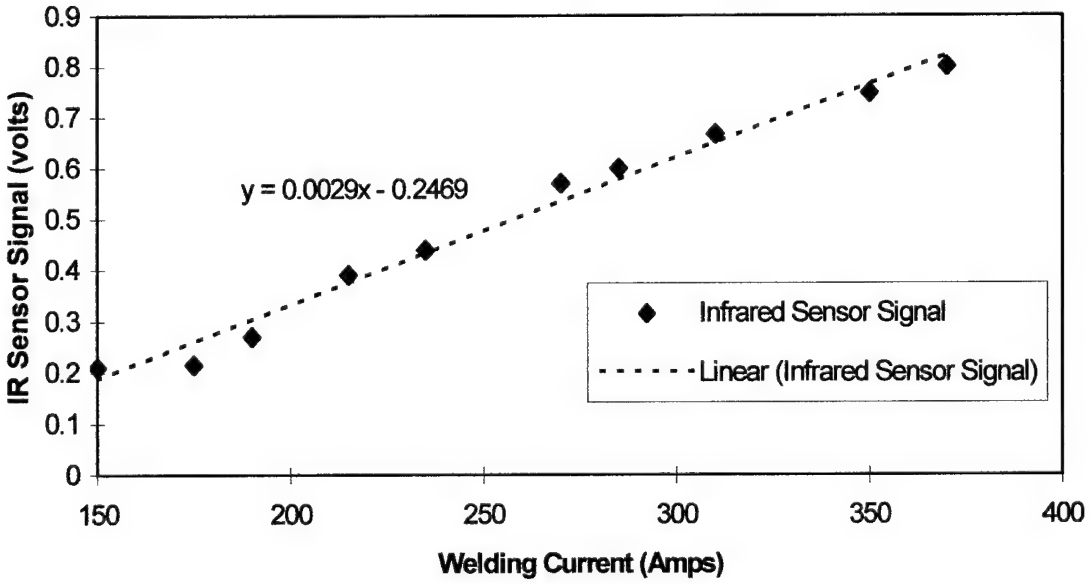

Figure 37. Control signal vs. welding current

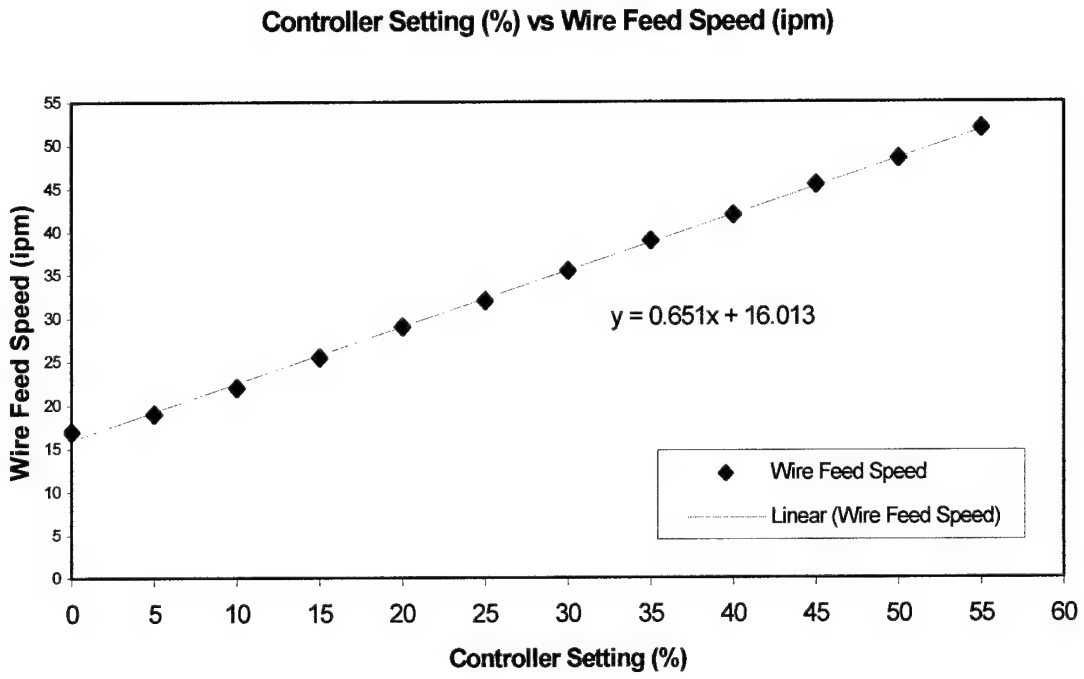

Figure 38. Controller setting vs. wire feed speed

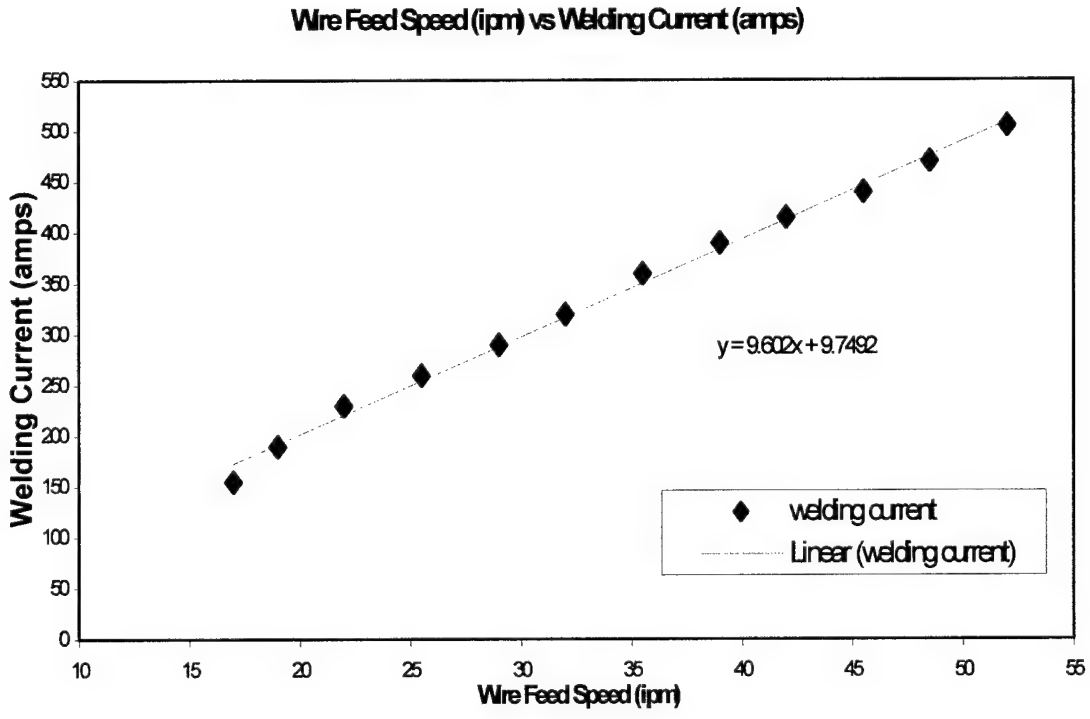

Figure 39. Wire feed speed vs. welding current

6.2 Arc Voltage Experiments

Since arc voltage is also a parameter in controlling the heat input, it is important to control not only the welding current, but also the arc voltage. The arc voltage affects the bead shape and size and, hence, the thermal distribution in the plate. Therefore it is pertinent to control the arc voltage to achieve proper weld penetration control. Although constant voltage power supplies have been developed to provide constant voltage even when the welding current is changed, true constant voltage is never achieved. Reduction in the welding current normally results in the increase of arc voltage. The magnitude of the variation of the arc voltage depends on the design of the power supply (i.e., its Volt-Ampere characteristics as shown in Figure 40.) To achieve constant voltage in scenarios were the welding current changes, it is required to change the arc voltage settings in real-time.

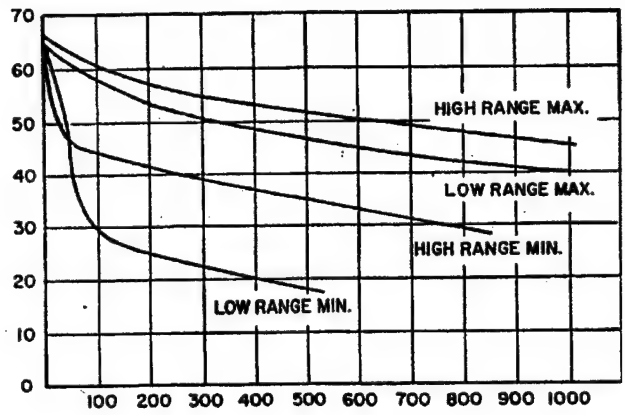

Figure 40. Volt-ampere characteristics of L-TEC Welding Power Supply

Welding trials performed with constant current showed no change in the arc voltage Figure 41.

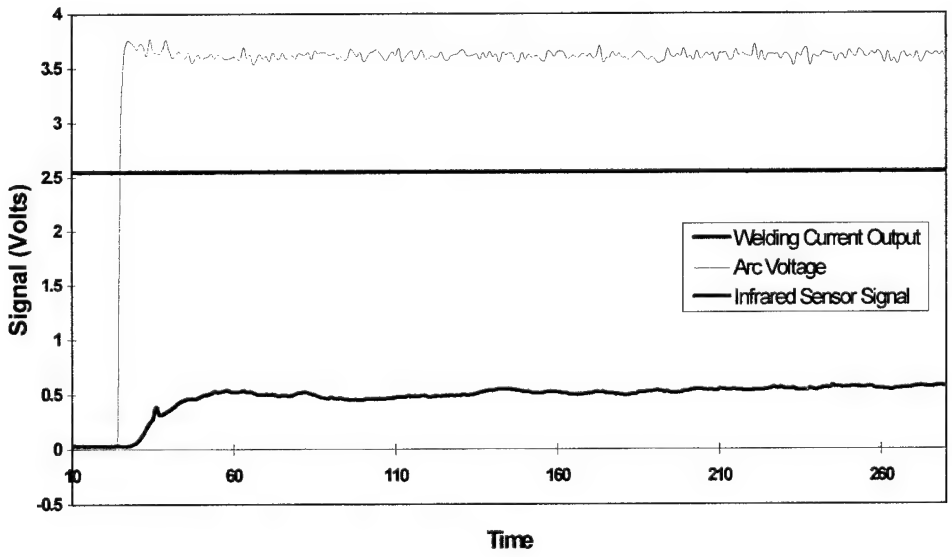

Figure 41. Graph showing constant arc voltage when the welding current is constant.

In case of welds where the welding current changed, the arc voltage also changed as shown in Figure 42. Bead-on-plate welding trials, in which the arc voltage was increased while other parameters were kept constant, showed a corresponding increase in the IR sensor signal as shown in Figure 43. The increase in the IR sensor signal was due to the direct effect of arc voltage on

the heat input. The above trials showed that control of arc voltage is necessary to achieve true control of heat input. Introduction of arc voltage control caused the arc voltage to remain constant even when the welding current changed as shown in Figure 44.

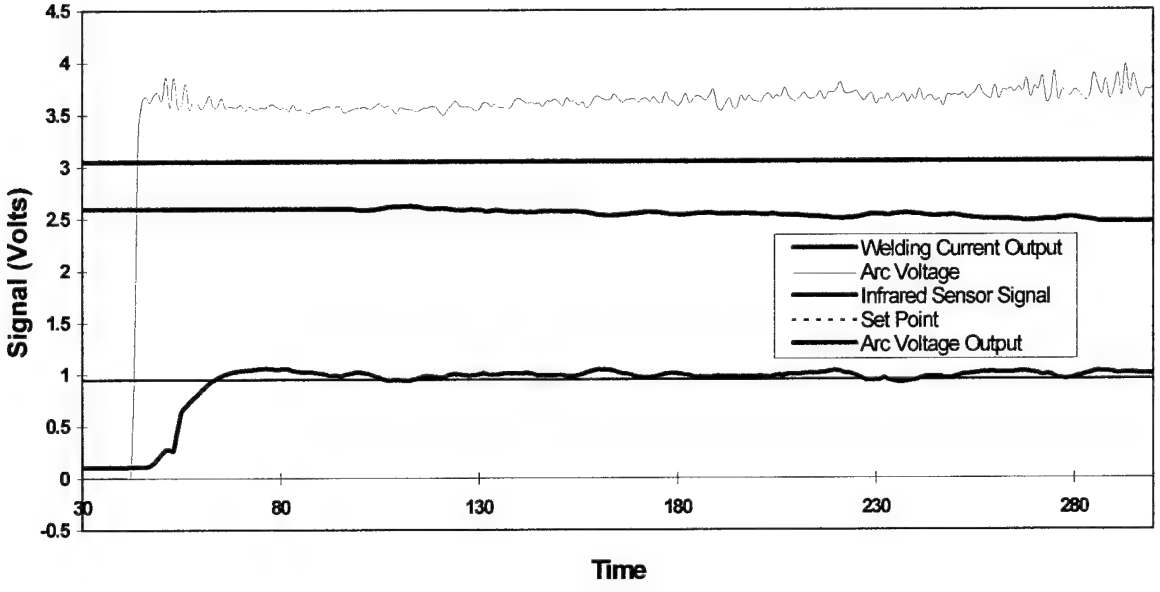

Figure 42. Graph showing increase in arc voltage when the welding current decreases.

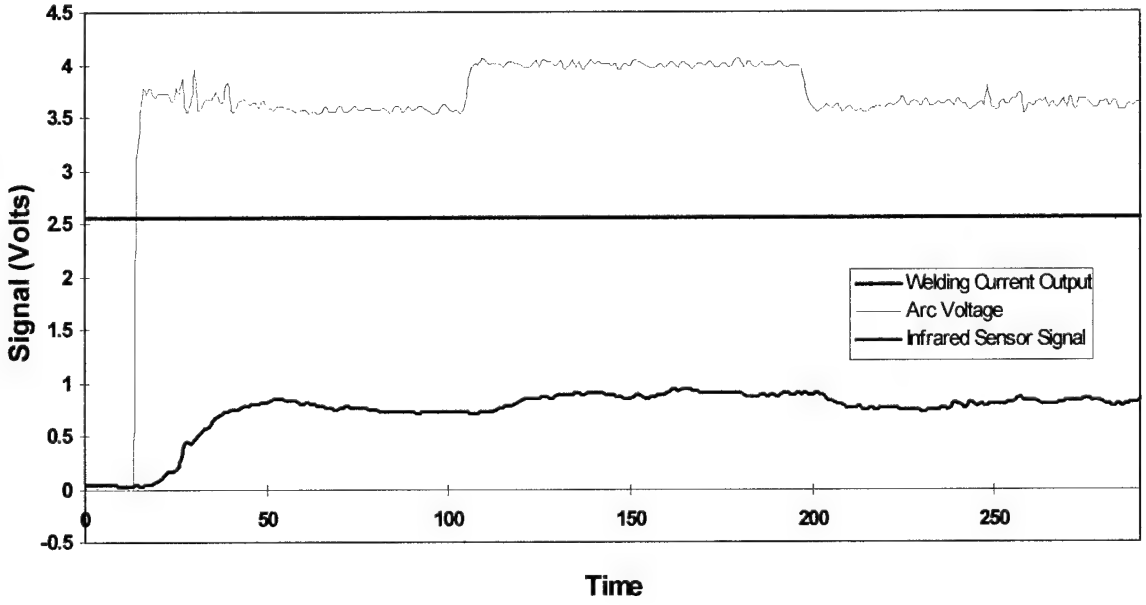

Figure 43. Graph showing change IR sensor signal due to change in arc voltage.

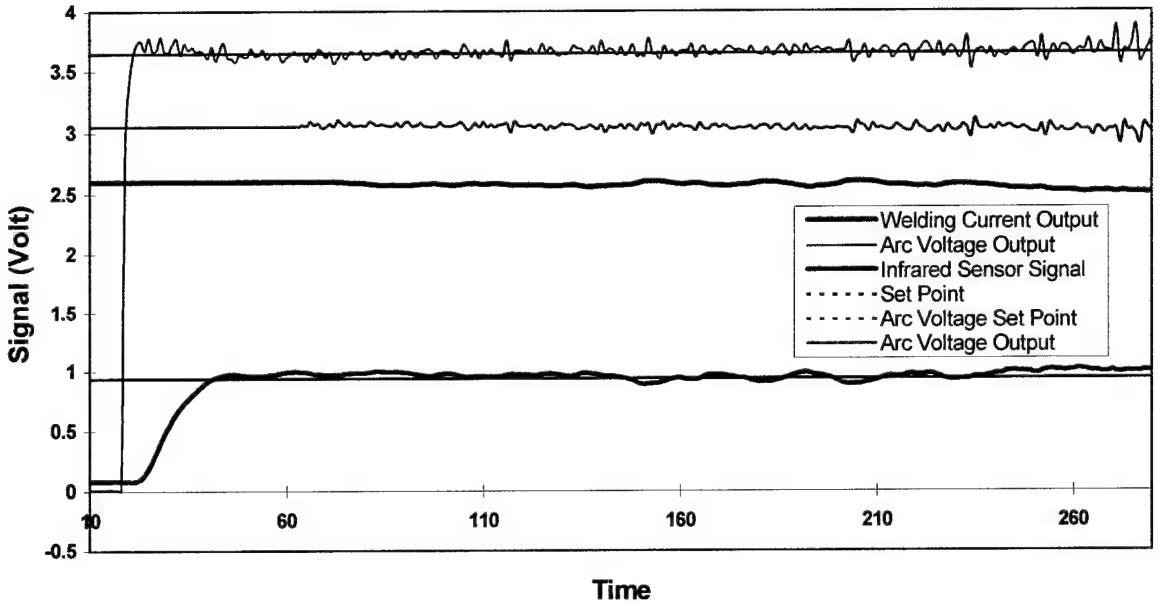

Figure 44. Graph showing arc voltage control. The arc voltage remained constant even when there was a change in the welding current.

6.3 Plate Surface Condition Experiments

The IR sensor signal depends on the emissivity of the plate surface. The surface condition of the plates determines the emissivity. Hot-rolled steel plates with surfaces in as-received (mill scale) condition, sandblasted condition and ground conditions were used to study the effect of emissivity on the IR sensor signal. Welds were performed with same welding parameters on hot-rolled plates of dimensions 24-by-four-by-three-eighths inches. As shown in Figure 45, welds performed on as-received surface condition had higher IR sensor signal magnitude than the welds performed on sandblasted and ground surfaces. This was due to the higher emissivity associated with the mill-scale surface. The IR sensor signal of welds performed on sandblasted and ground surfaces were similar in magnitude. Weld trials were performed in the manual and automatic mode on plates, which had two one-half-inch strips left in the as-received or ground condition, and the rest of the plate was sandblasted. The IR sensor signal increased at the regions of the strips where the surface was in the as-received condition, but decreased where the plate was ground. When automatic control was used, the controller changed the welding current correspondingly at the regions as shown in Figures 46 and 47. These experiments confirmed the fact that the emissivity of the plate surface must be held constant in order to avoid spurious IR sensor signal changes, leading to changes in the welding current. In future experiments, the plate surface condition under the view of the IR sensor signal was kept constant through sandblasting and grinding with scotch-brite wheels.

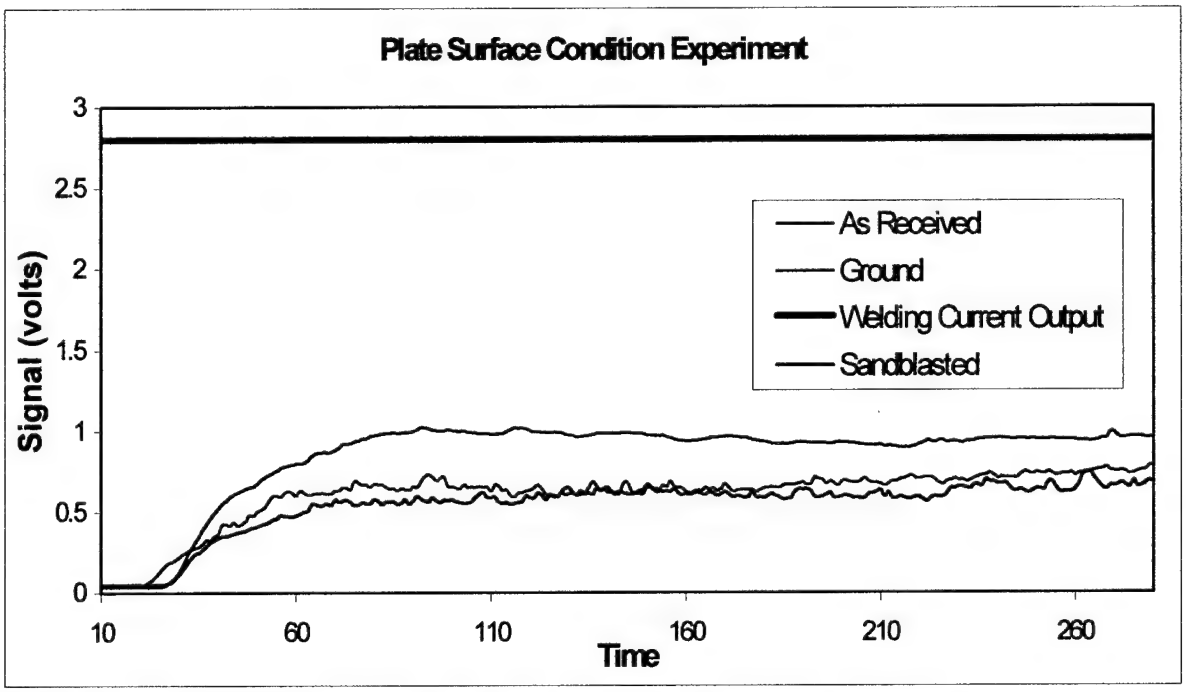

Figure 45. Graph showing the effect of surface condition on IR sensor magnitude.

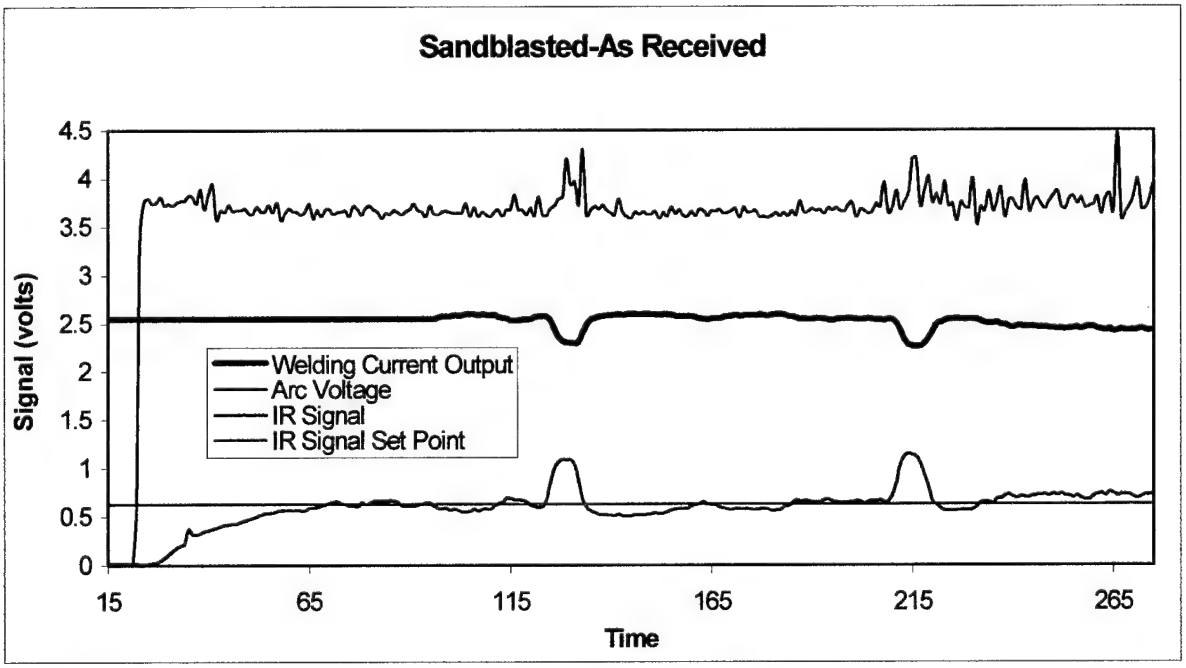

Figure 46. Graph showing the effect of the as-received (mill scale) surface condition on the weld process control.

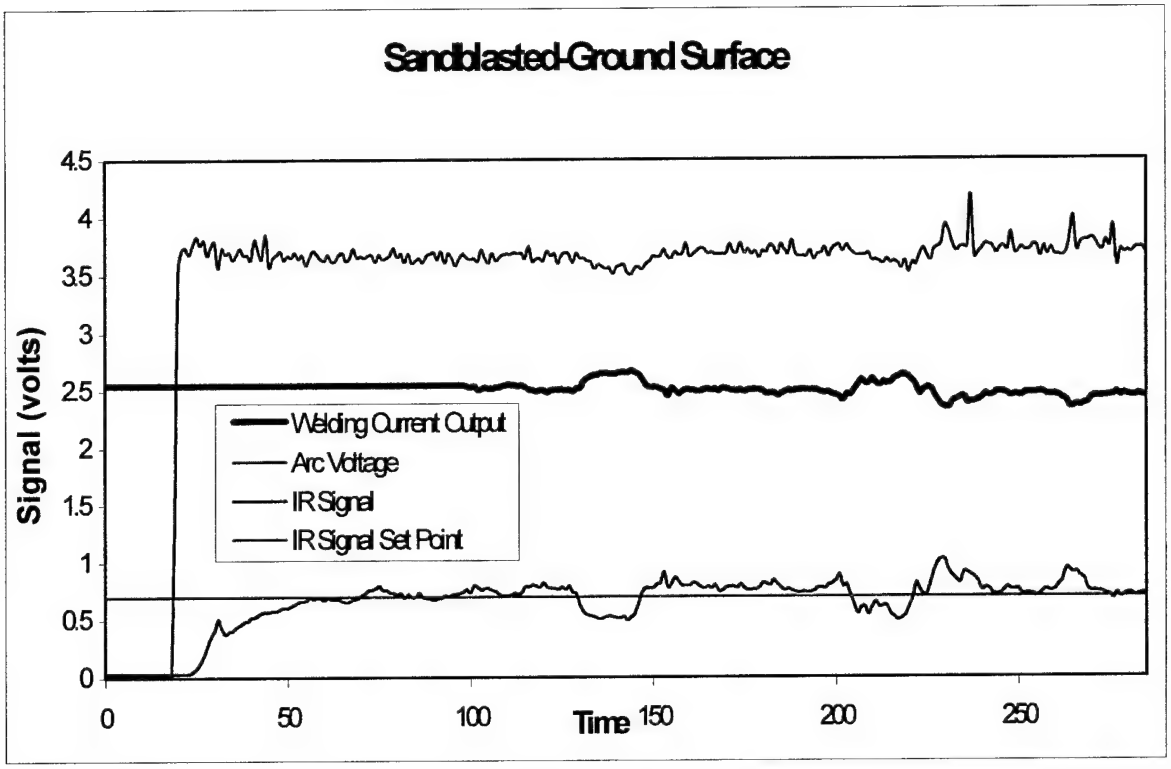

Figure 47. Graph showing the effect of ground surface condition on the weld process control.

6.4 Plate Thickness Experiments

To check for the effectiveness of the weld monitoring and control system, bead-on-plate welds were performed on plates with constant thickness and plates with step-change in thickness. Experiments were designed to investigate the effect of plate-thickness variation on the penetration indicator (IR signal). Welds were performed in both manual and automatic mode. The set point, IR signal and control signal were monitored. Automatic control of the weld process was started after the IR signal reached an initial steady-state condition.

Initially, bead-on-plate welding trials on constant thickness plates were performed to acquire the IR sensor signal. The plates were of dimensions 24-by-six-one-fourths-inch and 24-by-six-by-one-fourths-inch. The welding conditions used for the trials on three-eighths-inch-thick plates were:

Welding Current:	370 to 400 amps
Arc Voltage:	26 to 28 volts
Welding Speed:	nine inches per minute

The welding conditions used for trials on one-fourths-inch-thick plates were:

Welding Current:	270 to 290 amps
Arc Voltage:	26 to 28 volts

Welding Speed: nine inches per minute

For welds performed under manual control with a constant welding current, the IR sensor signal increased and then reached a constant value as the weld progressed as shown in Figure 48. Since there were no disturbances introduced, the IR sensor signal remained constant till the end of the

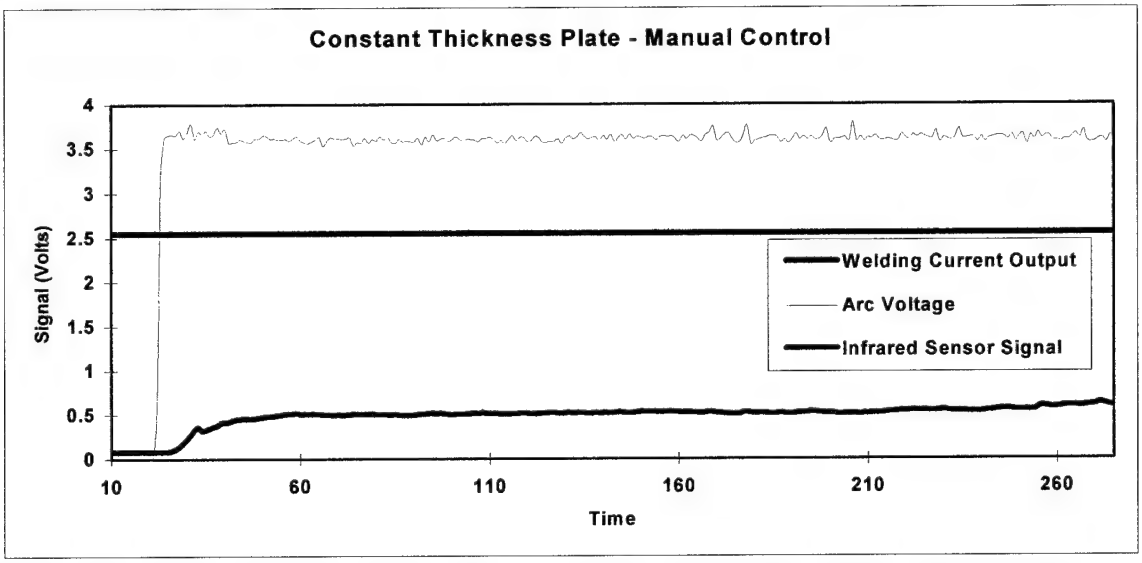

Figure 48. Graph showing IR sensor signal, arc voltage and welding current output for weld performed in manual (no-control) mode on constant plate thickness.

run. In the case of welds performed in the automatic feedback control, the IR signal was controlled at the set point by the weld process controller as shown in Figure 49. The control was

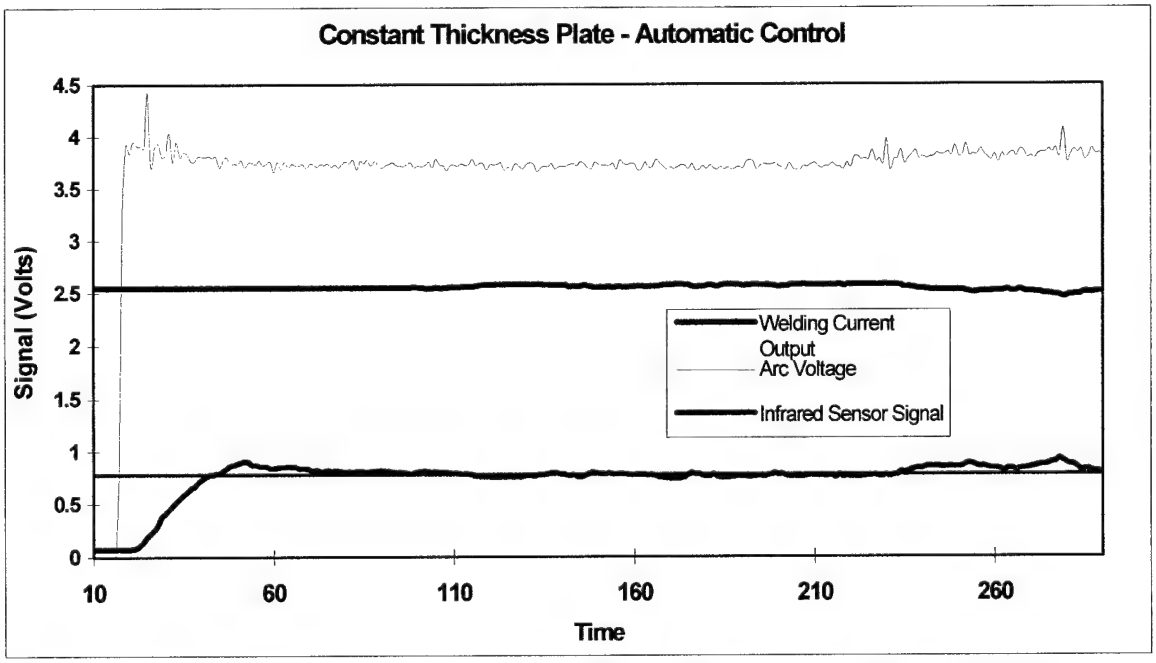

Figure 49. Graph showing IR sensor signal, arc voltage, welding current output and IR signal set point for weld performed with automatic control on constant thickness plate.

switched to the automatic mode when the IR signal reached a steady-state condition. The error between set point and the IR sensor signal was used by the controller to adjust the wire feed speed (welding current).

The weld penetration depth was measured by cross-sectioning the welds at every one-half inch. The penetration depth remained constant for welds made in manual and automatic modes as shown in Figure 50.

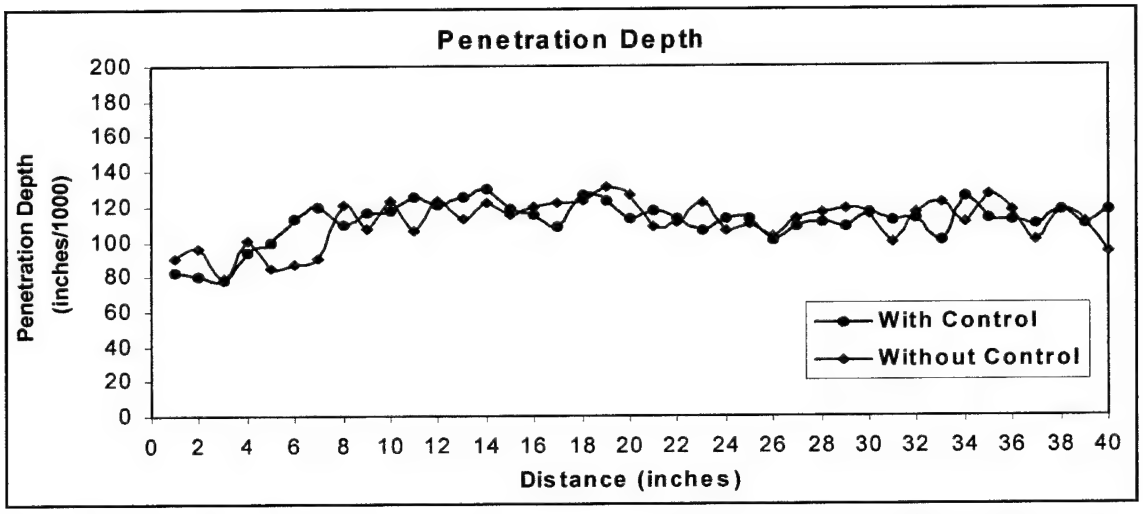

Figure 50. Graph showing the penetration depth measurements for welds performed with and without weld process control.

Step change in plate thickness was used to induce disturbances in the thermal distribution around the weld pool. The welds were performed on plates with a dimension of 24-by-six-by-three-eights-inch. The thickness was reduced to one-fourths-inch at the region of stepped thickness change for six inches in length at the center of the plate. Figure 51 shows the schematic of the stepped plate used for the welding trials. The welding conditions used were:

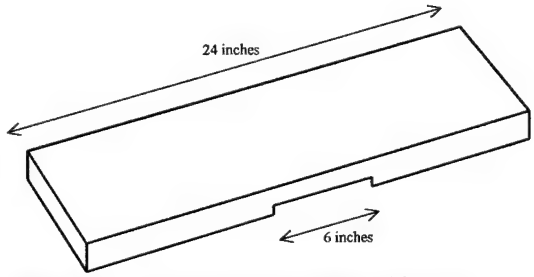

Figure 51. Schematic of plate with step change in thickness

Welding Current:	370 to 400 amps
Arc Voltage:	26 to 28 volts
Welding Speed:	nine inches per minute

Welds performed without automatic control at lower welding current showed an increase in the IR sensor signal at the region of the step change in thickness. The IR sensor signal increased due

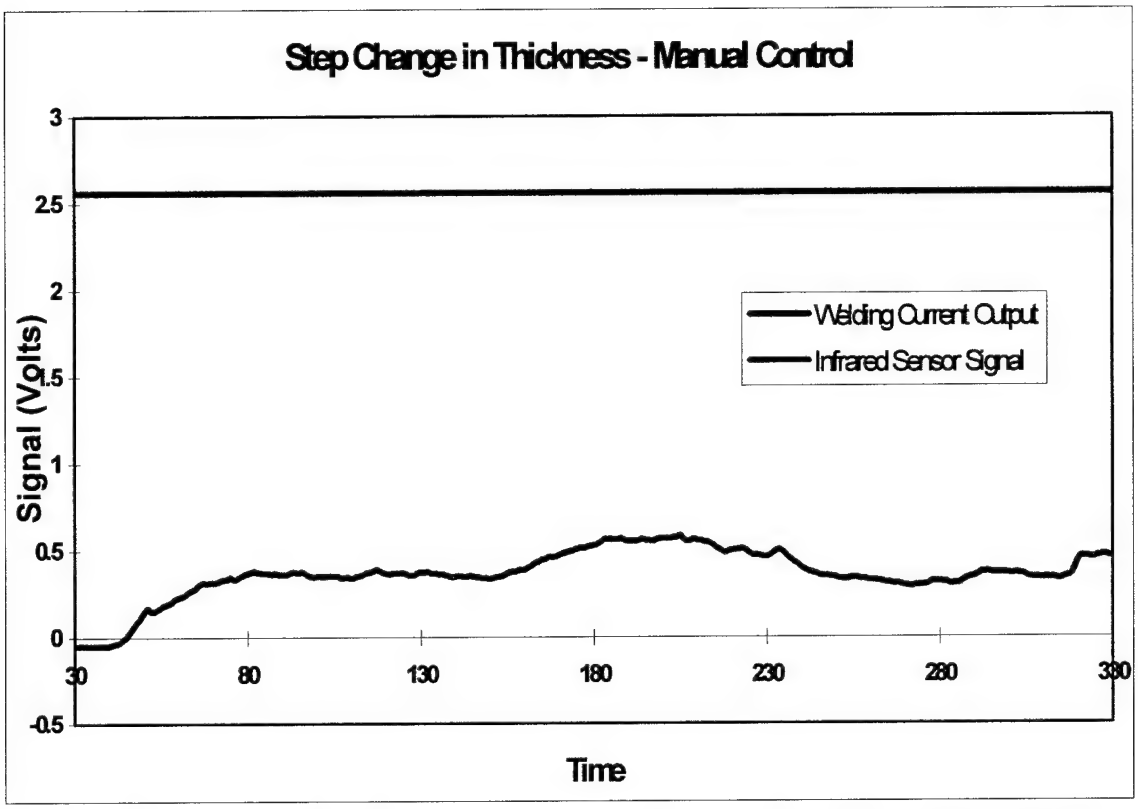

Figure 52. Graph showing the IR sensor signal and welding current output for weld performed without automatic control on a plate with step change in thickness.

to the increase in the heat-input-to-mass ratio at the region of the step as shown in Figure 52. When welds were performed without control at the above-mentioned parameters, burn-through resulted at the region of step change in thickness. When automatic control was used, the controller sensed the increase in the IR sensor signal and correspondingly reduced the wire feed speed (welding current), thereby preventing burn-through at the region of reduced thickness as shown in Figure 53. Figure 54 shows the picture of the top and bottom sides of the plates welded with and without automatic control. Penetration depth measurements were made on welds performed with automatic control. As shown in Figure 55, the penetration depth decreased at the region of decreased thickness. Figure 55 also shows the pictures of weld bead cross-sections performed at several locations along the length of the weld.

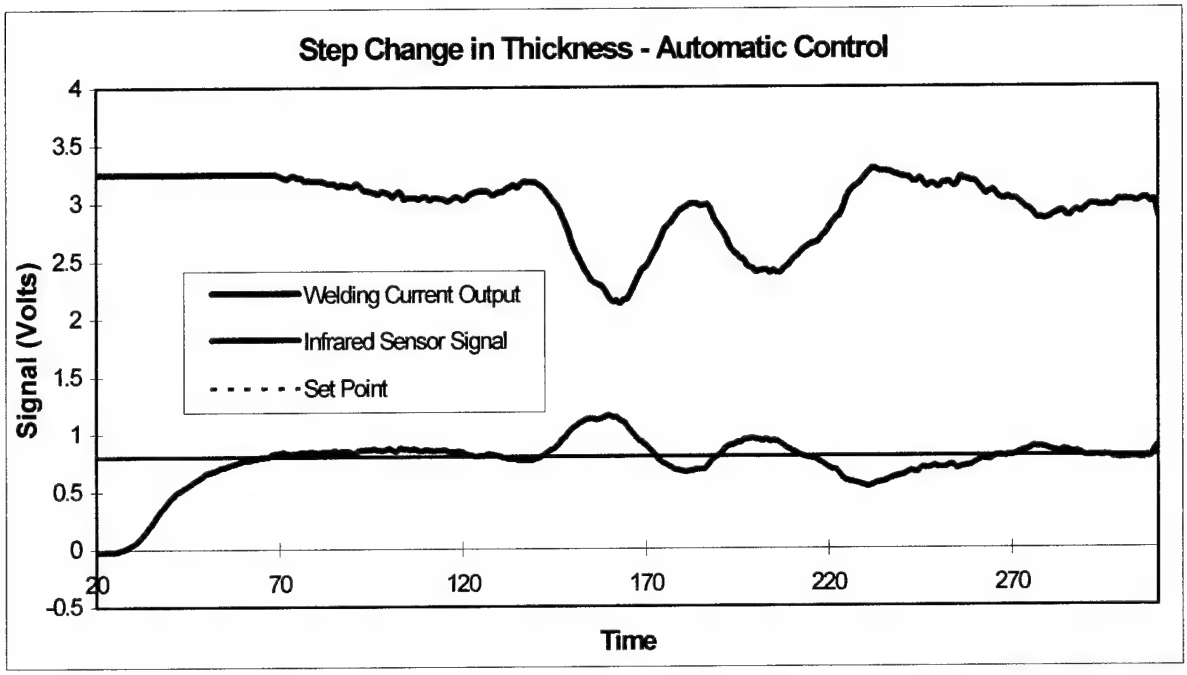

Figure 53. Graph showing the IR sensor signal, welding current output and the IR signal set-point for a weld performed with automatic control on a plate with step change in thickness.

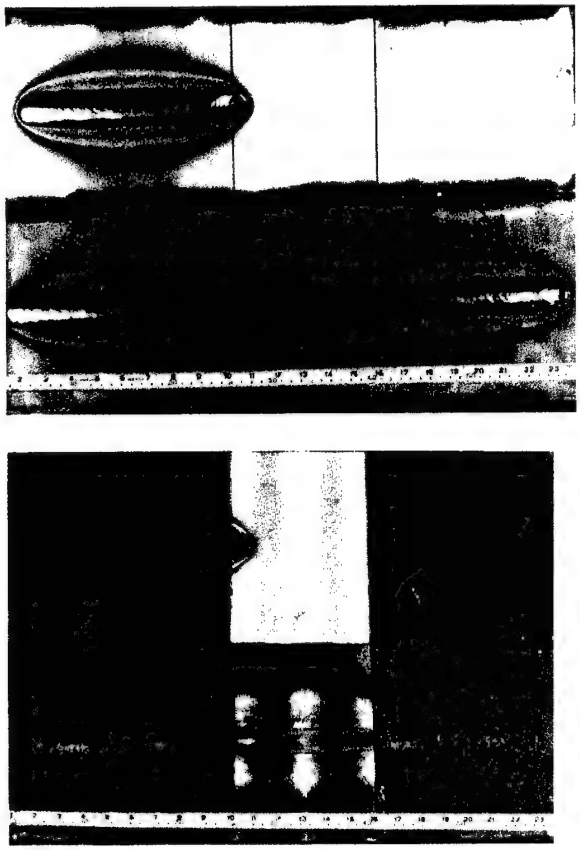

Figure 54. Pictures showing the top and bottom surfaces of plate with step change in thickness welded with and without automatic control.

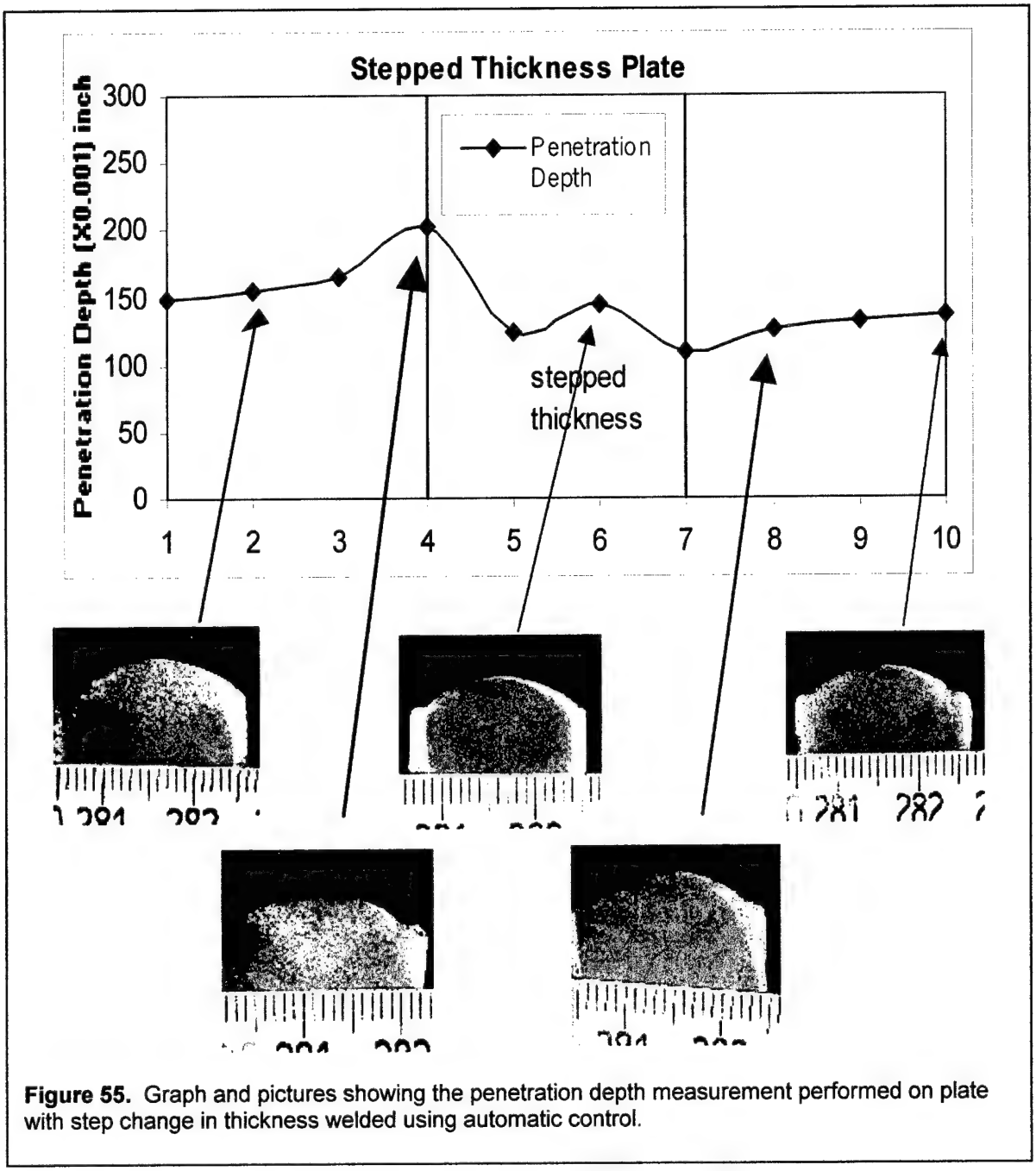

Figure 55. Graph and pictures showing the penetration depth measurement performed on plate with step change in thickness welded using automatic control.

6.5 Butt Joints

Butt joint welding trials were performed with constant and variable joint gaps. Variable joint gaps were used to simulate joint fit-up conditions that would exist in shipyard shop floors. Plates of same thickness and unequal thickness were used for making the butt joints to simulate the welding of ship hull plates. Initially, butt joint welding trials were performed using plates of dimensions 24-by-four-by-three-eights inches. Partial-penetration welds were performed with and without automatic control on both sides of the square butt joints with constant gap, to achieve penetration up to 45 to 60 percent. The joints were radiographed to check for incomplete

penetration, improper sidewall fusion and slag inclusions. The weld parameters were adjusted to achieve defect-free weld joints. Penetration depth for butt joints performed with a one-sixteenths-inch joint gap at different welding currents was measured by cross-sectioning the welds (Figure 56). These trials helped in fixing the proper welding conditions for subsequent

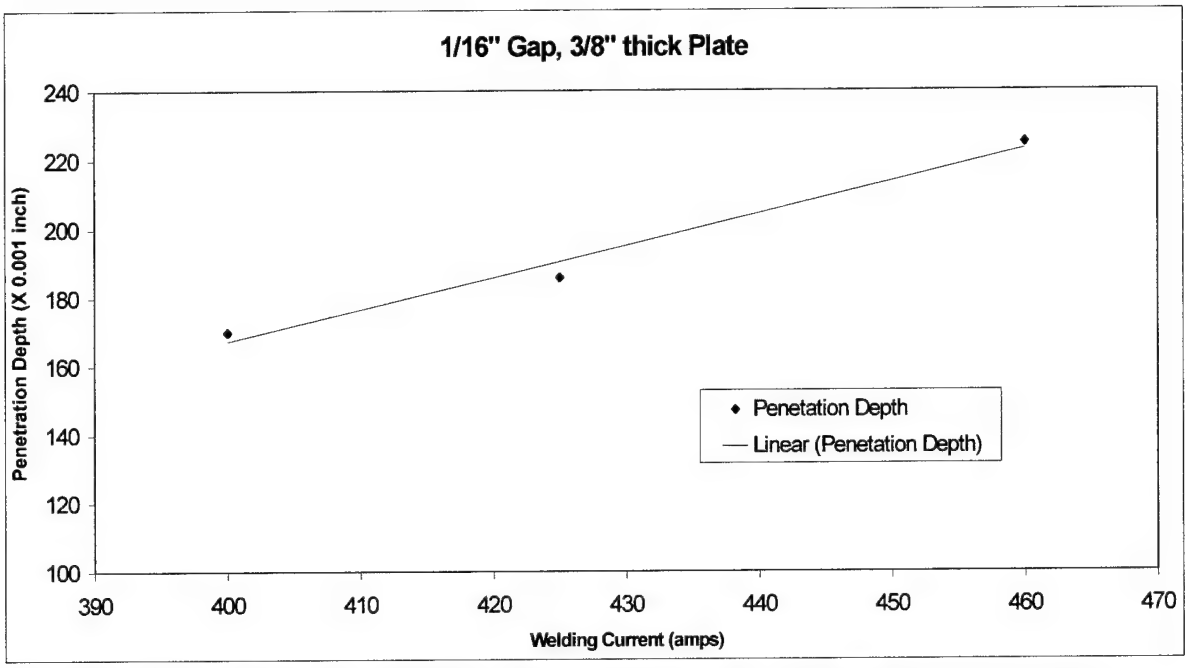

Figure 56. Graph showing the penetration depth of butt joint with one-sixteenths-inch joint gap performed at various welding currents.

butt joint trials. The welding conditions were:

Welding Current:	375 to 425 amps
Arc Voltage:	26 to 28 volts
Welding Speed:	nine inches/minute

6.5.1 Butt Joint Welding Trials Formed with Plates of Equal Thickness

Extensive butt joint welding trials were performed using plates with dimensions of 24-by-four-three-eights inches. Butt joint trials were also performed using plates with dimensions of 36-by-four-one-fourths inches and 36-by-four-one-half inches (Table 1). Butt joints with constant gap and sudden variable gap were performed to investigate the performance of the weld process controller.

	Butt Joint Combination: Plates of Equal Thickness		
Constant Gap	¼ - ¼	3/8 – 3/8	½ - ½
Variable Gap	¼ - ¼	3/8 – 3/8	½ - ½
Welding Current	320 amps	410 amps	485 amps

Table 1. Butt joint combinations for plates of equal thickness

Figure 57 shows the schematic of the joint design used for variable gap welding trials. In the region of variable gap, the joint gap was increased from one-sixteenth inch to one-eighteenth

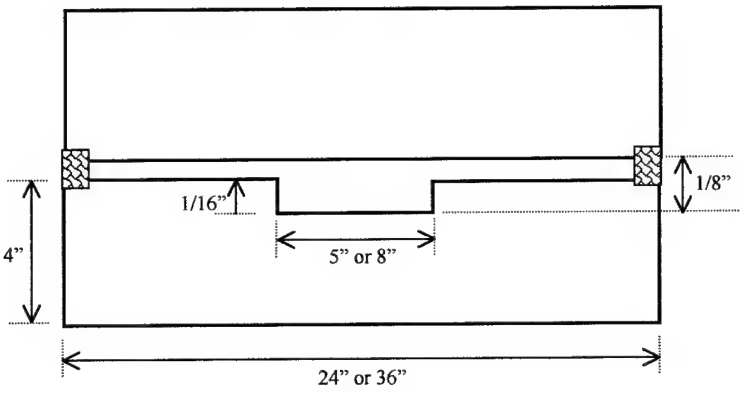

Figure 57. Schematic of butt joint design with variable gap used for welding trials

inch for five inches in length for three-eighths-inch-thick plates, and eight inches in length for one-fourths-inch-thick and one-half-inch-thick plates. Welds performed without control on joints with variable gap showed an increase in the IR sensor signal at the region of wider gap due to the higher heat input to the unit-mass ratio as shown in Figure 58. In the case of welds performed using automatic weld process control, the controller sensed the increase in the IR sensor signal corresponding to the increased gap and decreased the wire feed speed (welding current), thereby preventing burn-through shown in Figure 59. Welds performed without control but at the same initial welding current caused the weld pool to collapse leading to burn-through at the region of increased gap. Figure 60 shows the picture of butt joint weld with variable gap performed with automatic control. Penetration depth measurements were performed on butt joint with variable gap welded with and without automatic weld process control. As shown in Figure 61, in the case of weld performed with automatic control, the penetration depth decreased corresponding to the region of the wider joint gap. The corresponding location in the

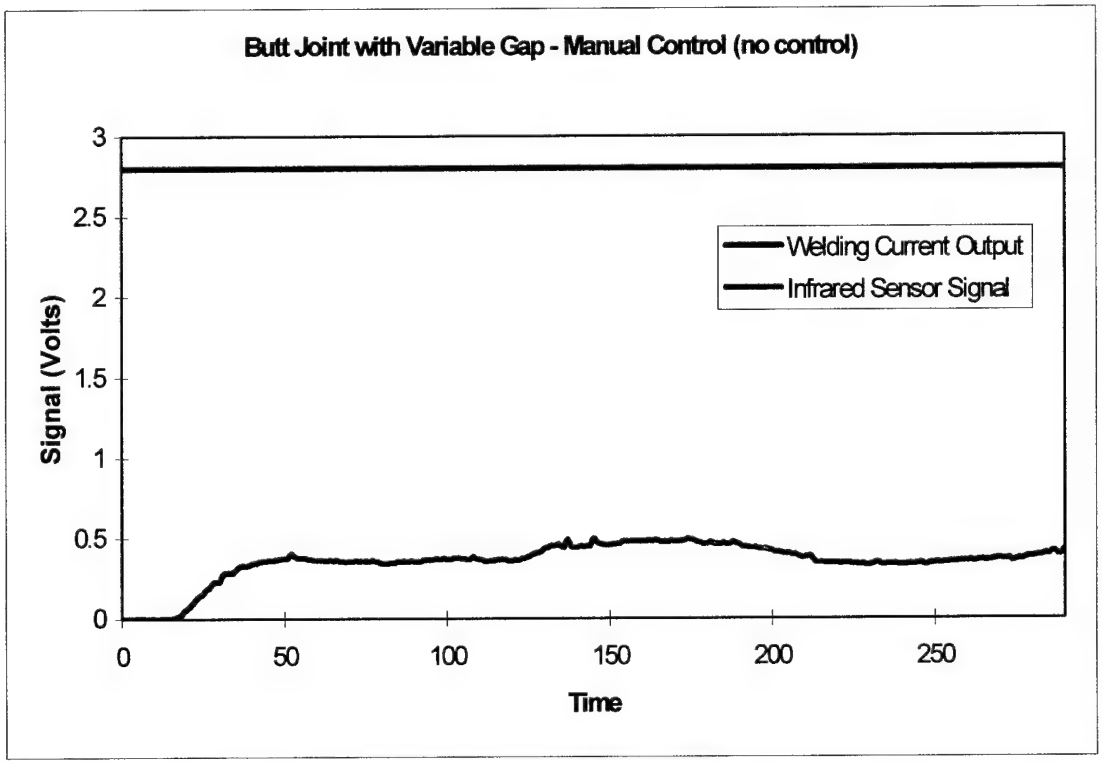

Figure 58. Graph showing IR sensor signal and the welding current output for butt joint with variable gap performed without automatic control.

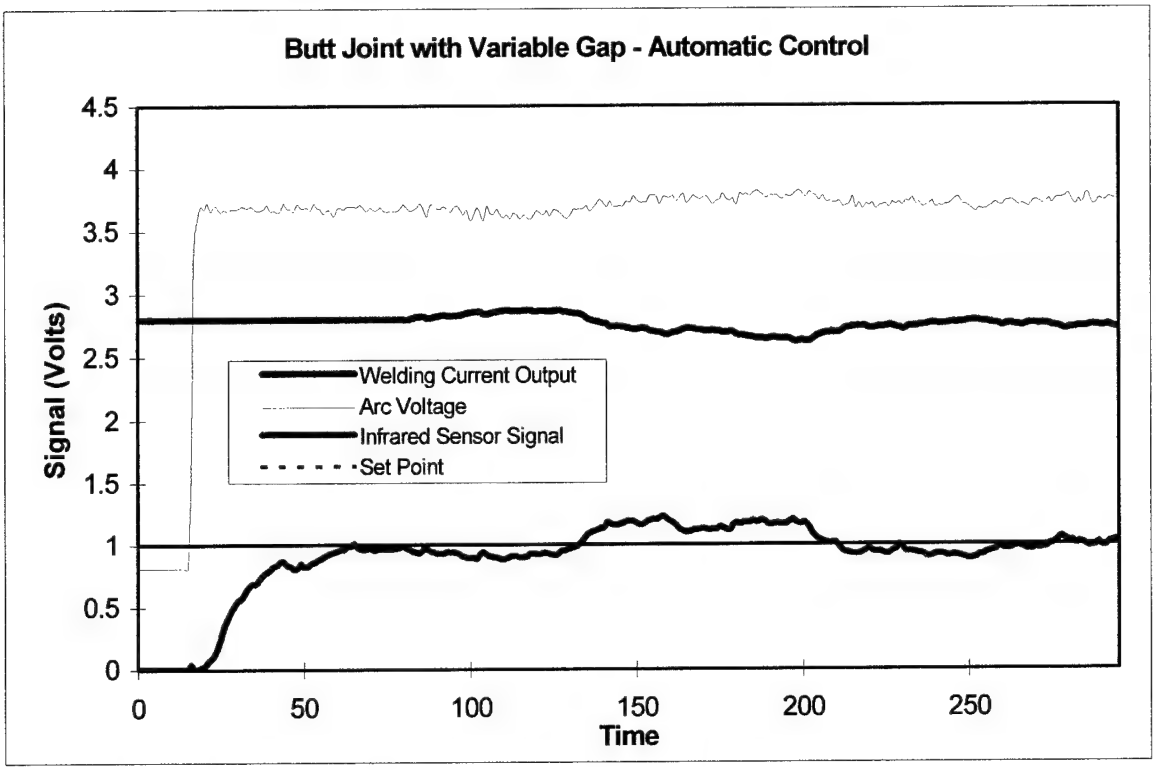

Figure 59. Graph showing the IR sensor signal, arc voltage, welding current output and IR signal set point for butt joint with variable gap performed with automatic control.

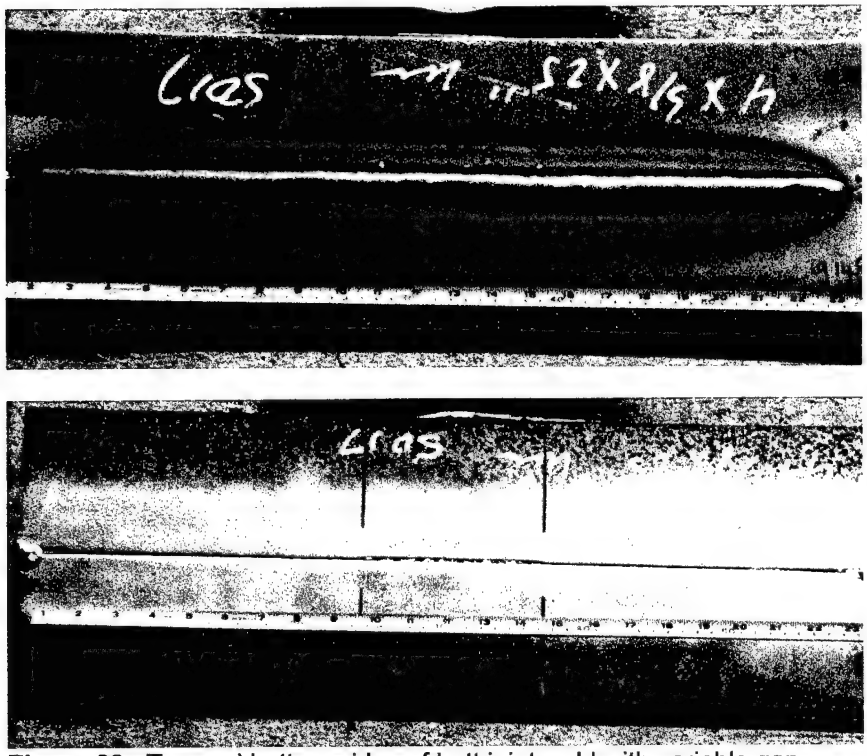

Figure 60. Top and bottom sides of butt joint weld with variable gap performed with automatic control.

weld performed without automatic control showed higher penetration depth. Figure 61 also shows the pictures of weld cross sections at various locations along the weld length. When welded from both sides, full penetration of the butt joint is achieved, as shown in Figure 62.

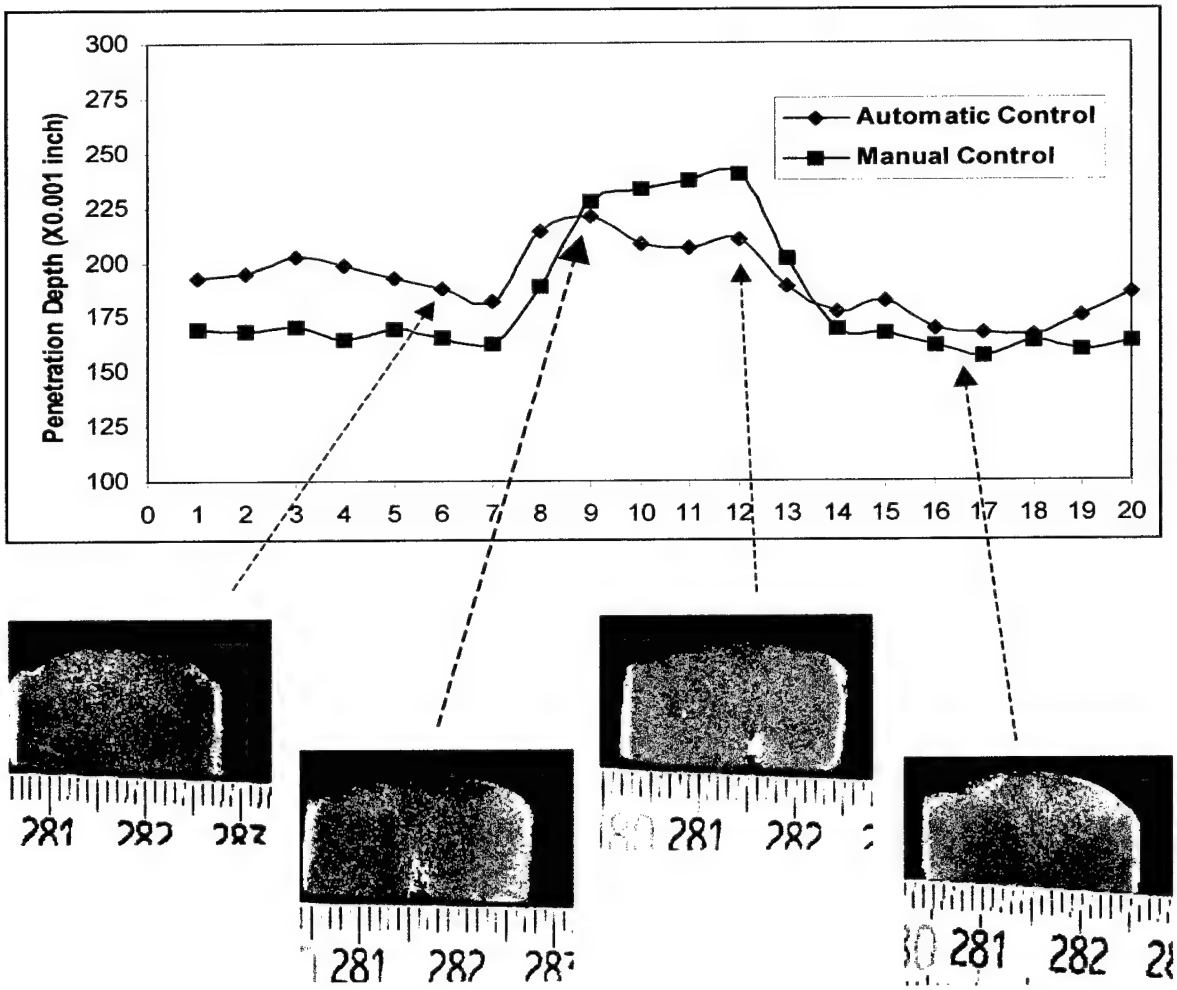

Figure 61. Graph and pictures showing penetration depth measurements for butt joints with variable gap performed with and without automatic control.

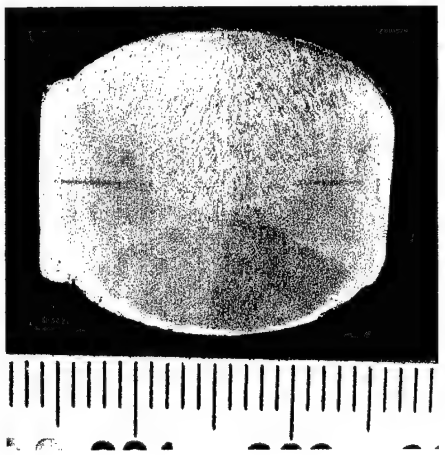

Figure 62. Weld cross-section at the region of wider gap showing complete penetration when welded from both sides. The two welds overlap to achieve full penetration.

6.5.2 Butt Joint Welding Trials Formed with Plates of Unequal Thickness

Butt joint welding trials were performed using plates of unequal thickness to simulate the welding of ship-hull plates. Butt joints were made using plates of different thickness combinations, as shown in Table 2. Both constant-gap and variable-gap butt joint trials were performed to investigate the performance of the automatic weld process control system. The variable gap was formed in the plate of smaller thickness for all combinations. The variable gap was eight inches long and about one-eighths-inch wide. The plates were 36 inches long. The IR sensor showed an increase in magnitude corresponding to the increased gap. The automatic weld process controller sensed the increase in the IR signal and correspondingly decreased the wire feed speed (welding current).

	Butt Joint Combination: Plates of Unequal Thickness		
Constant Gap	$\frac{1}{4}$-$\frac{5}{16}$	$\frac{5}{16}$-$\frac{7}{16}$	$\frac{7}{16}$- $\frac{1}{2}$
Variable Gap	$\frac{1}{4}$-$\frac{5}{16}$	$\frac{5}{16}$-$\frac{7}{16}$	$\frac{7}{16} - \frac{1}{2}$
Welding Current	360 amps	430 amps	475 amps

Table 2. Butt joint combination for plates of unequal thickness.

Figure 63 (next page) shows the graph of butt joint with variable gap performed with automatic control for one-fourth-inch through five-sixteenths-inch plate thickness combination. The IR sensor signal increased at the region of increased gap. The controller decreased the wire feed speed (welding current) correspondingly, thereby preventing burn-through at the region of increased gap. Pictures of weld cross-sections performed at various locations along the weld length are also shown. Similar results were obtained for the five-sixteenths-inch through seven-sixteenths-inch and seven-sixteenths-inch through one-half-inch combinations. The five-sixteenths-inch through seven-sixteenths-inch and seven-sixteenths-inch through one-half-inch combinations were also welded from both sides to achieve complete penetration of the butt joint. Figure 64 shows pictures of weld cross section at the region of wider gap, revealing overlapping of the welds performed from both sides.

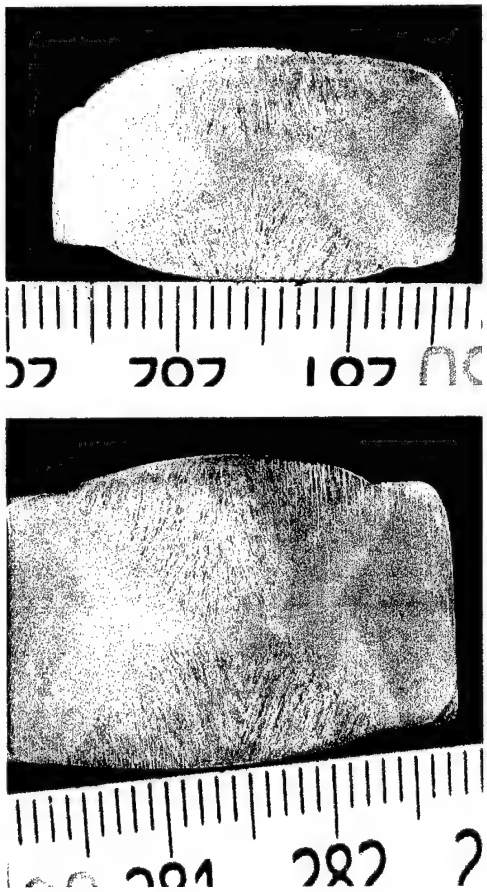

Figure 64. (Top) $\frac{5}{16}$-thickness through $\frac{7}{16}$-thickness combination. (Bottom) $\frac{7}{16}$-thickness through ½-inch thickness combination. Welds performed from both sides to reveal complete joint penetration.

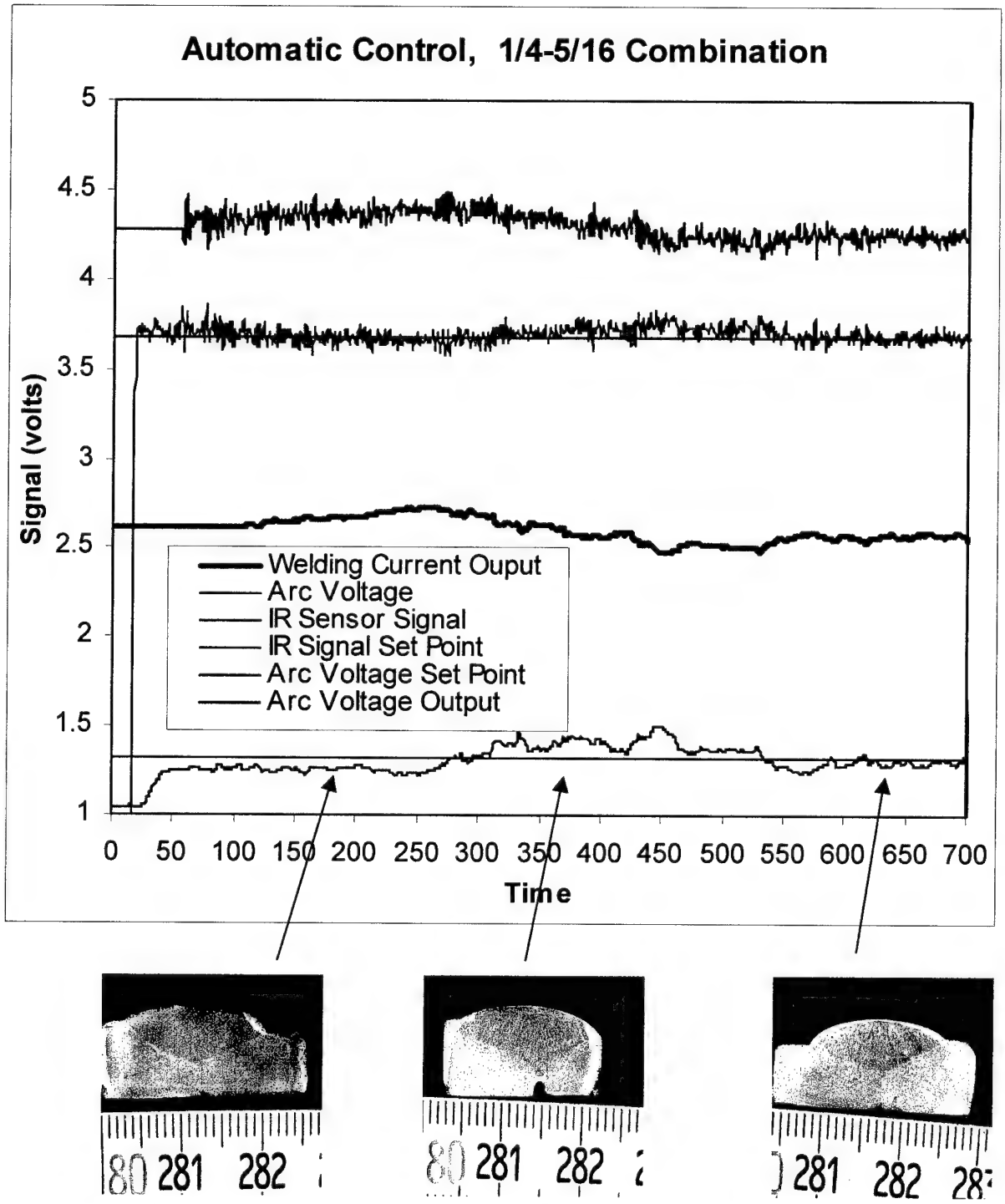

Figure 63. Graph and pictures of butt weld with variable gap performed with automoatic congrol for one-fourth through five-sixteenths-inch plate thickness combination.

5.6 Shop-floor Experiments

A shop-floor, gantry-type submerged arc welding system was modified to perform welding trials using the infrared sensor system as shown in Figure 65. The machine control was modified to achieve direct control of the wire feed speed using the computer. Initially, the sensor system was used for gathering data on production welds. The sensor signal showed variations corresponding to the tack welds and the location of the arc with respect to the joint. Welding trials using the automatic control were performed on butt joints formed between three-eighths-inch-thick plates, which were 10-feet long and four-feet wide. The plate did not have any variable gap machined along the edge. The plate was tack-welded at several locations along the length of the plate. The automatic sensor control system varied the current corresponding to the changes in the butt joint gap. The arc voltage was not controlled. Figure 66 shows the picture of the plate welded using the automatic control system. Figure 67 shows the graph of butt joint performed using the automatic control.

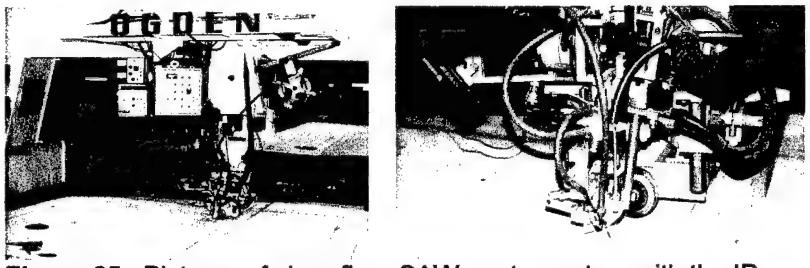

Figure 65. Pictures of shop-floor SAW gantry system with the IR sensor torch attachment

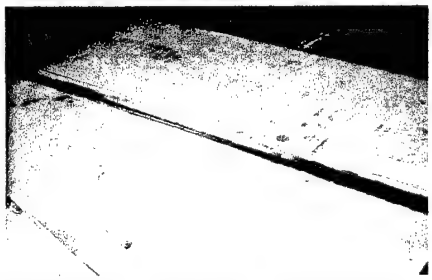

Figure 66. Picture of 10-foot-long plate welded using modified shop-floor gantry welding system

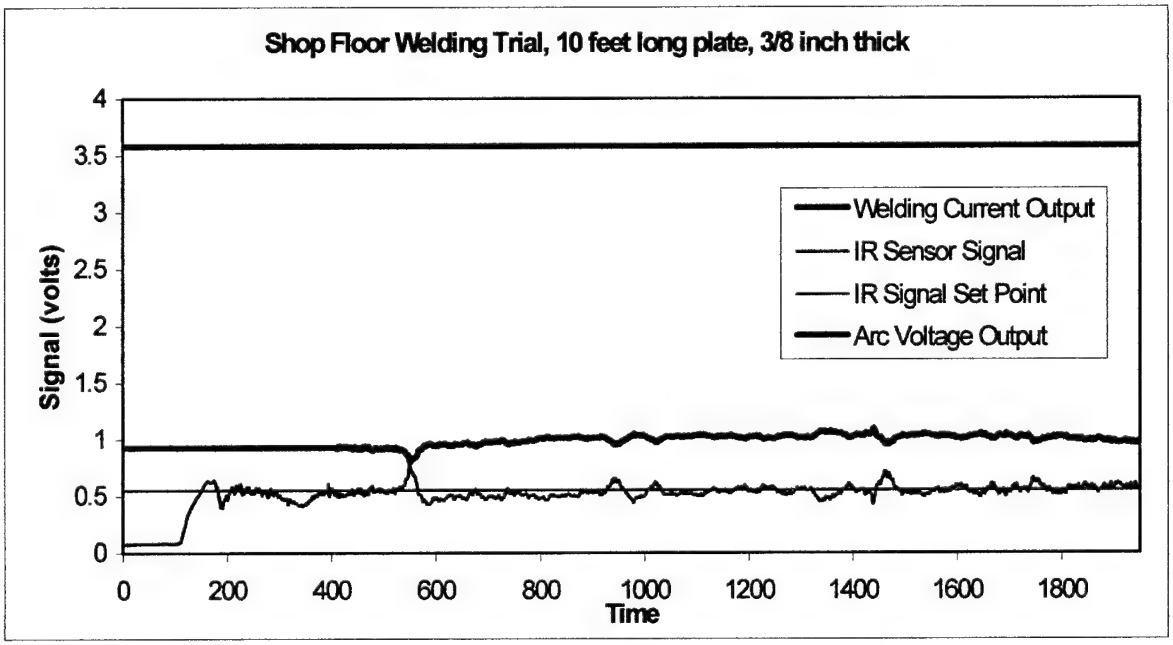

Figure 67. Graph of butt joint performed using the shop-floor gantry system with automatic control

REFERENCES

1 *AWS A3.0 Standard Welding Terms and Definitions*, American Welding Society. Miami.

2 "Welding, Brazing and Soldering," *ASM Handbook.* Vol. 6. Metals Park, Ohio: ASM International.

3 *The Procedure Handbook of Arc Welding.* 13th ed. Cleveland, Ohio: Lincoln Electric Company.

4 Fenn, R. "Ultrasonic monitoring and control during arc welding." *Welding Journal* 64.9 (1985): 18-22.

5 Hardt, D. E., and J.M. Katz "Ultrasonic Measurement of Weld Penetration." *Welding Journal* 63.9 (1984): 273-s—281-s.

6 Carlson, N.M., and J.A. Johnson. "Ultrasonic Sensing of Weld Pool Penetration." *Welding Journal* 67.11 (1988): 239-s—246-s.

7 Carlson, N.M., J.A. Johnson, L.A. Lott, L.A., D.C. Kunerth. "Ultrasonic NDT Methods for Weld Sensing." *Materials Evaluation* (November 1992): 1338-1343.

8 Hopko, S.N., I.C. Ume, I.C. "Ultrasonic Fiber Tool for Real Time Weld Monitoring and Quality Control." *Trends in Welding Research* (1988): 1169-1174.

9 Greenberg, Y., D. Itzhak, D., G. and Kohn, G. "Ultrasonic monitoring of a low temperature diffusion bonding process." *Journal of Testing and Evaluation* 28.2 (2000): 88-95.

10 Rokhlin, S.I., and A.C. Guu. "Computerized Radiographic Sensing and Control of an Arc Welding Process." *Welding Journal* 69.3 (1990): 83-s—97-s.

11 Kotecki, D.J., D.L. Cheever, and D.G. Howden. "Mechanism of ripple formation during weld solidification." *Welding Journal* 51.8 (1972): 386-s—391-s.

12 Renwick, R.J., and R.W. Richardson. "Experimental investigation of GTA weld pool oscillation." *Welding Journal* 62.2 (1983): 29-s—35-s.

13 Zackenhouse, M., and D.E. Hardt. "Weld pool impedance identification for size measurement and control." *Journal of Dynamic System, Measurement and Control* 105 (1983): 179-184.

14 Madigan, R.B., and R.J. Renwick. "Computer based control of full penetration GTA welds using pool oscillation sensing." *Proc. 1st International Conference on Computer Technology in Welding.* London, U.K. (1983): 165-174.

15 Sorenson, C.D., and T.W. Eagar. "Digital signal processing as a diagnostic tool for gas tungsten arc welding." *Proc. 1st International Conference on Trend in Welding Research.* Gatlinburg, Tennessee (1986): 467-472.

16 Deam, R. T. "Weldpool Frequency: A new way to define a Weld Procedure." *Recent Trends in Welding Science and Technology.* Ed. S.A. David and J.M. Vitek. Metals Park, Ohio: ASM International, 1989.

17 Hardt, D.E. "Measuring weld pool geometry from pool dynamics." *Proc. 3rd Conference on Modeling of Casting and Welding Process.* (1988): 3-17.

18 Xiao, Y.H., and G. den Ouden. "A study of weldpool oscillations." *Welding Journal* 69.8 (1990): 289-s—293-s.

19 Xiao, Y.H. and G. den Ouden. "Weldpool oscillations during GTA welding of mild steel." *Welding Journal* 72.8 (1993): 428-s—434-s.

20 Hu, B., and G. den Ouden. "Weld Penetration Sensing and Control during GTA Welding using Weld Pool Oscillation." *Trends in Welding Research.* Metals Park, Ohio: ASM International, 1998.

21 Vilkas, E.P. "Automation of gas tungsten arc welding process." *Welding Journal* 45.5 (1966): 410-416.

22 Vroman, A.R., and H. Brandt. "Feedback control of GTA Welding using Puddle Width Measurement. *Welding Journal* 55.9 (1976): 742—749.

23 Boughton, P., G. Rider, and C.J. Smith "Feedback control of Weld Penetration." *Proc. 4th International Conference on Advances in Welding Processes.* Harrogate, TWI, 1978.

24 Sugitani, Y., Y. Nishi, and T. Sato. "Intelligent Robot Controls Penetration and Bead Height." *Welding Journal* 69.12 (1990): 31—38.

25 Zhang, Y.M., L. Wu, B.L. Walcott, and D.H. Chen. "Determining Joint Penetration in GTAW with Vision Sensing of Weld Face Geometry." *Welding Journal* 72.10 (1993): 463-s—469-s.

26 Kovacevic, R., Y.M. Zhang, and L. Li. "Monitoring of Weld Joint Penetration Based on Weld Pool Geometrical Appearance." *Welding Journal* 75.10 (1996): 317-s—329-s.

27 Jon, M.C. "Noncontact acoustic emission monitoring of laser beam welding. *Welding Journal* 64.9 (1985): 43-48.

28 Doeblin, E.O. Measurement Systems, Application and Design. New York: McGraw Hill, 1975. 165-174.

29 Ramsey, P.W., J.J. Chyle, J.N. Kuhr, P.S. Myers, M. Weiss, M., and W. Groth. "Infrared Temperature Sensing Systems for Automatic Fusion Welding." *Welding Journal* 42.8 (1963): 337-s—346-s.

30 Lukens, W.E., and R.A. Morris. "Infrared Temperature Sensing of Cooling Rates for Arc Welding Control." *Welding Journal* 61.1 (1982): 27-33.

31 Brown, B., and E. Bangs. "The measurement and monitoring of resistance spot welds using infrared thermography." International Conference on Thermal Infrared Sensing for Diagnostics and Control, Proc., of SPIE. 1986.

32 Boillot, J.P., P. Cielo, G. Begin, C. Michel, M. Lessard, P. Fafard, and D. Villemure. "Adaptive welding by fiber optic thermographic sensing: An analysis of thermal and instrumental considerations." *Welding Journal* 64.7 (1985) :209-s—217-s.

33 Bentley, A.E., and S.J. Marburger. "Arc welding penetration control using quantitative feedback theory." *Welding Journal* 71.11 (1992): 397-s—405-s.

34 Chin, B.A., N.H. Madsen, and J.S. Goodling. "Infrared Thermography for Sensing the Arc Welding Process." *Welding Journal* 62.9 (1983): 227-s—234-s.

35 Groom, K.N., S. Nagarajan, and B.A. Chin. "Automatic Single V-groove Welding Utilizing Infrared Images for Error Detection and Correction." *Welding Journal* 69.12 (1990): 441-s—445-s.

36 Nagarajan, S., W.H. Chen, and B.A. Chin. "Infrared sensing for adaptive arc welding." *Welding Journal* 68.11 (1989): 462-s—466-s.

37 Nagarajan, S., and B.A. Chin. "Infrared Image Analysis for On-Line Monitoring of Arc Misalignment in Gas Tungsten Arc Welding Process." *Material Evaluation* 48.12 (1990): 1469-1472.

38 Nagarajan, S., P. Banerjee, W.H. Chen, and B.A. Chin. "Control of the welding process using infrared sensors." *IEEE Transactions on Robotics and Automation* 8.1 (1992): 86-93.

39 Nagarajan, S., H.C. Wikle, and B.A. Chin. "On-line weld position control for fusion reactor welding." *Journal of Nuclear Materials* (1992): 1060-1064.

40 Chen, W., and B.A. Chin. "Monitoring Joint Penetration Using Infrared Sensing Techniques." *Welding Journal* 69.4 (1990): 181-s—185-s.

41 Banerjee, P. "Gradient Technique for On-Line Weld Bead Width Control." *Welding in the World* 31.6 (1993): 17-24.

42 Banerjee, P., S. Govardhan, H.C. Wikle, J.Y. Liu, and B.A. Chin. "Infrared Sensing for On-Line Weld Geometry Monitoring and Control." *Journal for Engineering for Industry, Transactions of ASME* 117 (1995): 323-330.

43 Banerjee, P. "On-Line Weld Penetration Detection and Control in Automated Gas Tungsten Arc Welding." Ph.D. Diss. Auburn University, 1994.

44 Wikle, H. C. "Modeling, Sensing and Control of Gas Tungsten Arc Welding." Ph.D. Diss. Auburn University, 1998.

45 Christensen, N., L. Davies, and K. Gjermundsen. "The distribution of temperature in arc welding." *British Welding Journal* 12 (1965): 54-75.

46 Myhr, O.R., and Grong. "Dimensionless maps for heat flow analyses in fusion welding." *Acta Met.* 38.3 (1990): 449-460.

47 Friedman, E., and S.S. Glickstein. "An investigation of the thermal response of stationary gas tungsten arc welds." *Welding Journal* 55.12 (1976): 408s-420s.

48 Goldak, J., A. Chakravarti, and M. Bibby. "A new finite element model for welding heat sources." *Metallurgical Transactions* B.15B (1984): 299-305.

49 Pavelic, V., R. Tanbakuchi, O.A. Uyehara, and P.S. Myers. "Experimental and computed temperature histories in gas tungsten arc welding of thin plates." *Welding Journal* 48.7 (1969): 295s-305s.

50 Kou, S. "Simulation of heat flow during the welding of thin plates." *Metallurgical Transactions* A.12A: 2025-2030.

51 Ule, R., and Y. Joshi. "Three dimensional transient heat transfer computation of autogeneous arc welding." *Heat transfer in Manufacturing and Materials Processing.* Ed. Shah, R. K., *ASME, HTD* 113 (1989): 131-142.

52 Nagarajan, S. "Modeling and sensing of thermal phenomena in arc welding processes." Ph.D. Diss. Auburn University, 1991.

53 Banerjee, P. "On-line weld penetration detection and control in automated gas tungsten arc welding." Ph.D. Diss. Auburn University, 1994.